DETERMINATION OF THE STRUCTURAL DYNAMIC CHARACTERISTICS OF ROTOR BLADES AND THE EFFECT OF PHASE ANGLE ON MULTIBLADED ROTOR FLUTTER

A THESIS

Presented to

The Faculty of the Division of Graduate

Studies and Research

By

Vadrevu Ramachandra Murthy

In Partial Fulfillment

of the Requirements for the Degree

Doctor of Philosophy

in the School of Aerospace Engineering

Georgia Institute of Technology

February, 1975

DETERMINATION OF THE STRUCTURAL DYNAMIC CHARACTERISTICS OF ROTOR BLADES AND THE EFFECT OF PHASE ANGLE ON MULTIBLADED ROTOR FLUTTER

Approved:

G. Alvin Pierce, Chairman

Robert L. Carlson

Virgil Smith

Date approved by Chairman: 4-22-75

ACKNOWLEDGMENTS

I wish to express my sincere gratitude to Dr. G. A. Pierce for his guidance and assistance during this study.

Grateful appreciation is extended to Dr. C. V. Smith for his valuable suggestions for improvement. I would like to thank other members of my reading committee, Dr. R. L. Carlson, Dr. M. C. Bernard and Dr. D. J. McGill, for their contributions.

I wish to thank Dr. K. S. S. Nagaraja and Mr. S. P. Viswanathan for their helpful suggestions. Discussions with them provided more insight into problems of academic interest. My sincere thanks are extended to Mrs. Maxine Bogue for her patience and skill in typing the thesis, and to Mrs. Linda Emmerson for preparing the drawings. I owe many thanks to the staff of the Rich Electronic Computer Center for their cooperation.

My brother, V. S. Murthy, contributed significantly to my career in science and engineering during the early stages of my college education and has been a source of constant encouragement during set-backs. I owe my entire career to my mother, the late Seetha Rama Lakshmi, for her many sacrifices. I wish to extend my thanks to Mrs. Padmaja Pragada and Mr. Ray Pragada for providing me with an occasional homey atmosphere.

TABLE OF CONTENTS

LIST OF TABLES

Table Page

Table | Page

LIST OF FIGURES

NOMENCLATURE

a_∞	free stream speed of sound
B_1, B_2	section constants
b	semi-chord
b_o	semi-chord at the root
[D]	differentiating matrix
E	Young's modulus of elasticity
e	distance between mass and elastic axis, positive when mass axis lies ahead of elastic center
e_A	distance between area centroid of tensile member and elastic axis, positive for centroid forward
e_o	distance at root between elastic axis and axis about which blade is rotating, positive when elastic axis lies ahead
G	shear modulus of elasticity
h	vertical spacing between adjacent wake layers, $\frac{2\pi u}{Q\Omega}$, unless otherwise specified
[I]	integrating matrix
I_1, I_2	bending moments of inertia about major and minor neutral axes, respectively (both pass through centroid of cross-sectional area effective in carrying tensions)
i	$\sqrt{-1}$
J	torsional stiffness constant
k	reduced frequency, $\frac{b\omega}{U}$
k_A	polar radius of gyration of cross-sectional area effective in carrying tensile stresses about elastic axis

k_m polar radius of gyration of cross-sectional mass about elastic axis, $k_m^2 = k_{m_1}^2 + k_{m_2}^2$

k_{m_1}, k_{m_2} mass radii of gyration about major neutral axis and about an axis perpendicular to chord through the elastic axis respectively

L aerodynamic lift, positive up

$M_{c/2}$ aerodynamic pitching moment about mid-chord, positive nose up

M_e aerodynamic pitching moment about elastic axis, positive nose up

M_x resultant cross-sectional moment in x-direction (Part I), or resultant cross-sectional moment about major principal axis (Part II)

M_y resultant cross-sectional moment in y-direction (Part I), or resultant cross-sectional moment about elastic axis (Part II)

M_z resultant cross-sectional moment in z-direction

M_∞ section mach number, $\frac{\Omega r}{a_\infty}$

m mass per unit length along rotor span

n rotor revolution index, unless otherwise specified

Q total number of blades in rotor

q blade index for multibladed rotor

R span of the rotor

r radial distance along rotor from the center of rotation

T tension in the blade

$[\searrow T \swarrow]$ tension matrix

$[T]$ transmission matrix

t	time, or thickness of cross-section at any chordwise position
U	relative free stream velocity at radial location r
u	inflow velocity through rotor disk
V_y, V_z	shear in y and z directions
v	amplitude of simple harmonic lateral displacement in plane of rotation, positive towards leading edge
W	lateral displacement of rotor normal to plane of rotation, positive down
w	amplitude of simple harmonic lateral displacement normal to plane of rotation, positive upwards (Part I), positive downwards (Part II)
x,y,z	coordinate system which rotates with blade such that x-axis falls along initial or undeformed position of elastic axis, y positive towards leading edge, z positive upwards (Part I), or co-ordinate system which rotates with blade such that x-axis is positive towards downstream, y out board along initial position of elastic axis, z positive upwards (Part II)
$\{z\}$	state vector
β	blade angle of station x prior to any deformation, positive when leading edge is upward
η	cross-sectional axis, lies along major axis
η_{te}, η_{le}	values of η for trailing edge and leading edge of cross section
ν	slope of deflection curve in the plane of rotation
ρ_∞	free-stream density
Φ	angle of torsional deformation positive when leading edge is upward
ϕ	amplitude of simple harmonic torsional deformation
ψ	slope of deflection curve normal to plane of rotation

ψ_q phase lead of q-th blade

Ω angular velocity of rotation

ω frequency of vibration

Superscripts

/ differentiation with respect to argument

. time derivatives

- non-dimensional quantities, unless otherwise specified

* amplitude of simple harmonically varying quantities

Subscripts

o quantities at the root

SUMMARY

Frequency response concepts are reviewed. A transmission matrix, which is one form of frequency response matrix, is used to obtain the dynamic characteristics of rotating blades for combined flapwise bending, chordwise bending and torsion and five of its subcases. The orthogonality relation that exists between the natural modes of coupled flapwise bending, chordwise bending and torsion is derived. Rubin's method is used to obtain the transmission matrix.

An integrating matrix method is used to obtain the dynamic characteristics of rotating systems for flapwise bending and for coupled flapwise bending and torsion. Some aspects of this approach, viz., the orthogonality among the natural modes and applicability to semi-definite systems, are investigated. Comparisons are made between the transmission matrix approach and the integrating matrix method.

The effect of phase angle on flutter speed for a two bladed rotor is determined. For this purpose a uniform and untwisted rotor blade with coupled flapwise bending and torsional degrees of freedom is considered. The transmission matrix method is used for obtaining the natural vibration characteristics of the system. An unsteady aerodynamic theory is used to obtain the compressible aerodynamic loading.

PART I

DETERMINATION OF THE STRUCTURAL DYNAMIC CHARACTERISTICS OF ROTOR BLADES

CHAPTER I

INTRODUCTION

Structural dynamic problems are becoming more and more important in aeronautical engineering. Propellers have become larger and thinner particularly for vertical take-off and landing and short take-off and landing aircraft. As a result the propellers are more susceptible to vibration and flutter problems. Helicopter rotor blades operate in a severe vibration environment and are subject to divergence and flutter problems. Turbine and compressor blades frequently fail due to some vibration phenomena. The determination of the dynamic characteristics (natural frequencies and mode shapes) of these systems is of great and fundamental importance in structural dynamic analyses. It is necessary that they be determined accurately. They are required to exclude the resonant conditions of the systems and also they are widely used in series solutions of response problems. Furthermore the natural modes of vibration are of extreme importance in flutter problems and are the basis of nearly all practical flutter analyses.

The dynamic characteristics of a system are generally determined by solving the governing differential equations of motion. This approach is suitable for uniform

systems and systems for which the governing differential equations of motion are of lower order. However, for most practical configurations, the mass distribution etc., are nonuniform for which such exact solutions are not possible. Therefore, other techniques, which give approximate solutions to continuous systems have been developed. One method which has been extensively used since the advent of high speed digital computers is the lumped parameter approximation where the continuum is replaced by a finite n-degree-of-freedom system composed of lumped elements, i.e., massless springs and point masses. This technique was first applied by Lagrange [1] and Rayleigh [2] in studying the vibrating string. The Myklestad technique [3] belongs to this class of methods. In contrast to such lumped parameter approximations the following two methods, which can also deal with higher order continuous systems, are used to determine the dynamic characteristics of rotor blades etc.,

1) Frequency response methods

2) Integrating and differentiating matrix methods

Frequency Response Methods

A large class of systems occurring in engineering practice consist of a single element or a number of elements linked together end to end in the form of a chain. Well known examples are rotor blades, propeller blades,

continuous beams, fuselage bulkheads, turbine-generator shafts etc. The transmission matrix which is one form of frequency response matrix, is ideally suited to treat such systems. Intermediate conditions and the number of degrees of freedom present no difficulty since they have no effect on the order of the transmission matrices required; in fact their size is dependent only on the order of the differential equations governing the behavior of the elements of the system. Frequency response methods provide a useful alternate approach for exact or approximate analysis of continuous systems. These methods provide a direct means of calculating the natural frequencies and mode shapes of complex dynamical systems. They are also used to analyze forced vibrations whether they are transient or steady state character, either for discrete or continuous damped or undamped systems. In random vibration analyses this approach is particularly suitable and is called the frequency domain approach. Apart from the demand that the systems are linearly elastic no other restrictions are required for frequency response methods.

The earliest application of the transmission matrix method was the steady state description of four terminal electrical net works in which case the method is commonly designated as "four pole parameters". Molloy [4] was one of the first to systematically apply four pole parameters

to acoustical, mechanical, and electromechanical vibration problems. Pestel and Leckie [5] have catalogued transmission matrices for uniform elasto-mechanical elements upto twelfth-order. Rubin [6] has extended the application through a completely general treatment. Murthy and Nigam [7] successfully applied the transmission matrix to stiffened ring problems.

A transmission matrix is one form of frequency response matrix and the others are admittance, impedance and receptance matrices. They all contain identical information but in different arrangements, and they are all interrelated. There are certain circumstances in which one form results in simpler relationships than others. So each form has a rightfull place. In the present study the transmission matrix is used to obtain the dynamic characteristics of rotor blades. In Reference 5 several methods were discussed to derive transmission matrices. These methods have proved satisfactory for simple lumped parameter or lower order uniform continuous systems, but become cumbersome when used for nonuniform and higher order continuous systems because of the required algebraic manipulations. Recently, however Rubin [8] has formulated a systematic approach which eliminates much of the algebra and results directly in differential equations for the elements of the transmission matrix.

Integrating and Differentiating Matrix Method

The integrating matrix is a means of numerically integrating a function that is expressed in terms of the values of the function at equal increments of the independent variable. Similarly a differentiating matrix is a means of numerically differentiating a function that is expressed in terms of the values of the function at equal increments of independent variable. They can be derived by expressing the function as a polynomial in the form of a Newton's forward difference interpolation formula. The integrating matrix has been applied to obtain the natural vibration characteristics of propeller blades for combined bending in two directions [9]. This is the only reference available to the knowledge of the author and only the integrating matrix is required to analyze the problem considered in Reference 9. In the present study this technique is applied to obtain the dynamic characteristics of rotor blades for coupled flapwise bending and torsion. Unlike the problem of coupled flapwise bending and chord wise bending, coupled flapwise bending and torsion needs the introduction of a differentiating matrix in addition to the integrating matrix. Some aspects of this technique which were not brought out in Reference 9 are investigated in the present study, for example, orthogonality of the eigenvectors and applicability to semi-definite systems.

The solution to the governing differential equations of motion for combined flapwise bending and torsion is developed in matrix notation. The coupled differential equations of motion are linear homogeneous equations with variable coefficients. The boundary conditions of the problem are homogeneous. The differential equations are expressed in matrix notation and in this case (coupled flapwise bending and torsion) two matrix differential equations are obtained. These equations are integrated separately using the integrating and differentiating matrices as operators. The constants of integration are evaluated by applying the boundary conditions. The resulting two matrix equations are combined to yield a standard form of eigenvalue problem. The method of solution [10] which has been utilized for this eigenvalue problem is described. The solutions describe the natural frequencies and the associated modal displacements. The dominant eigenvalues correspond to the lower natural frequencies.

Using the integrating and differentiating matrix technique, a continuous problem can be treated instead of a discrete model of the continuous system. The method is based on the fact that the solutions of differential equations can be approximated by polynomials very accurately. In addition to the advantage of directly treating the continuous system, the method is appealing because of its simplicity for programming for digital computer calculations.

Also, the inputs are generated very easily since they are merely the coefficients of the differential equations.

The review of frequency response concepts is presented in Chapter II. The application of the transmission matrix to obtain the structural dynamic characteristics of rotating blades is discussed with the pertinent equations in Chapter III. In Chapter IV the application of the integrating and differentiating matrix method to obtain the structural dynamic characteristics of rotating blades for combined flapwise and torsion is discussed. Also, the adjoint aspects and method of solution is discussed. Finally the discussion of results and conclusions and recommendations are presented in Chapter V and VI respectively.

CHAPTER II

FREQUENCY RESPONSE CONCEPTS

Linear dynamic systems can be analyzed using a black box concept similar to the approach used in electrical circuit theory. The system may consist of many black boxes, and each black box is characterized by its input and output relations for simple harmonic excitation conditions. This approach is conducive to orderly, concise, highly general formulations of analysis and synthesis problems in the frequency domain. The linear system can be schematically represented by a block diagram consisting of black boxes. Each box can be described by its admittance, impedance or transmission properties. This approach can be applied to discrete or continuous linear systems from any technical field. The systems may be structural, electrical, acoustical etc., or may be mixed type (electro-mechanical, electro acoustical).

Fundamentals of Matrix Forms

Frequency Response

At the frequency ω, the harmonic response of a linear structure at the ith terminal, $r_i(\omega)$, is related to the harmonic force at the jth terminal, $f_j(\omega)$, by the

relation

$$r_i(\omega) = h_{ij}(\omega) f_j(\omega) \tag{1}$$

where $h_{ij}(\omega)$ is called a frequency response. If a number of forces act, the response at i is composed of the summation of responses to the individual forces by the principle of superposition

$$r_i(\omega) = \sum_j h_{ij}(\omega)\ f_j(\omega) \tag{2}$$

If p distinct responses comprise the vector $R = \{r_i\}$ and n distinct forces comprise the vector $F = \{f_i\}$, the following matrix equation can be written.

$$\underset{pxl}{\{R(\omega)\}} = \underset{pxn}{[H(\omega)]}\underset{nxl}{\{F(\omega)\}} \tag{3}$$

where $[H(\omega)] = [h_{ij}(\omega)]$ is the frequency response matrix.

Admittance

In the special case where the responses are velocities, $V(\omega)$, which correspond to application of the forces $f(\omega)$, the frequency response matrix $[H(\omega)]$ is specially designated the admittance matrix, $Y(\omega)$.

$$\{V(\omega)\} = [Y(\omega)]\{F(\omega)\} \tag{4}$$

The elements of $[Y(\omega)]$ are designated $y_{ij}(\omega)$. "Correspondence" implies that the ith velocity has the same

location and direction as the ith force for all i. Since the number of velocities equals the number of forces n, $[Y(\omega)]$ is a square matrix of order n. Because the structures to be considered are either linearly elastic or dissipative, the admittance matrix $[Y(\omega)]$ is symmetric, owing to the principle of reciprocity

$$[Y(\omega)] = [Y(\omega)]^T \text{ or } y_{ij}(\omega) = y_{ji}(\omega) \tag{5}$$

where the superscript T denotes the matrix transpose. Reciprocity holds as long as the product of each force like variable and the corresponding displacement gives the total work performed during that displacement. The diagonal elements, $y_{ii}(\omega)$, are called driving point, direct or self admittances, and the off diagonal elements, $y_{ij}(\omega)$, are called transfer, cross, or mutual admittances. If a structure is free of constraint and massless, a single applied force will produce an infinite motion. Therefore, the admittance matrix of such a structure will not exist.

Impedance

The inverse of the admittance matrix, $[Y(\omega)]$, is called the impedance matrix, $[Z(\omega)]$.

$$\{F(\omega)\} = [Z(\omega)]\{V(\omega)\} \tag{6}$$

where the elements of $[Z(\omega)]$ are designated $z_{ij}(\omega)$. By definition, then $[Z(\omega)] = [Y(\omega)]^{-1}$, assuming that $[Y(\omega)]$ is

nonsingular. Since the inverse of a symmetric matrix is also symmetric

$$[Z(\omega)] = [Z(\omega)]^T \text{ or } z_{ij}(\omega) = z_{ji}(\omega) \qquad (7)$$

The admittance matrix will be singular (the impedance matrix will not exist) if the terminal velocities are not independent. This could be the case, for, example with a rigid body. The transmission matrix is another form of frequency response matrix, and since the present study involves the transmission matrix approach it is discussed in greater detail.

Transmission Matrix

Description

A transmission matrix is one which relates input forces and velocities to those at the output terminals. This manner of description is eminently well suited to describe the performance of a series of structures connected in tandem; that is, the output of the first equals the input to the second, and so on.

The beam shown schematically in Figure 1a is an example of a transmission structure. The "State vector" at the input end, z_1, contains forces applied to the input and corresponding velocities.

Figure 1a. A Transmission Component

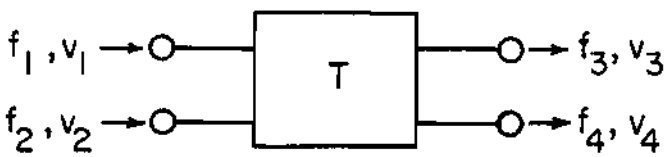

Figure 1b. Four Terminal Representation

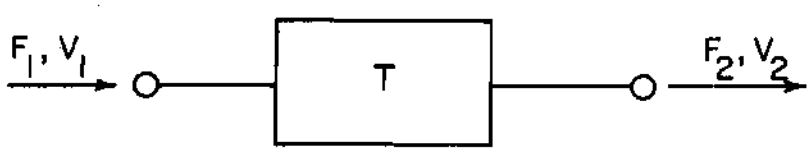

Figure 1c. Generalized Two Terminal Representation

$$\{z_1\} = \begin{Bmatrix} f_1 \\ f_2 \\ v_1 \\ v_2 \end{Bmatrix} \tag{8}$$

The "state vector" at the output end, z_2, contains forces applied by the output and corresponding velocities.

$$\{z_2\} = \begin{Bmatrix} f_3 \\ f_4 \\ v_3 \\ v_4 \end{Bmatrix} \tag{9}$$

In Figure 1b, the beam is represented as a multiterminal device. In Figure 1c it is shown as a generalized two terminal representation with state vectors

$$\{z_1\} = \begin{Bmatrix} F_1 \\ V_1 \end{Bmatrix} \text{ and } \{z_2\} = \begin{Bmatrix} F_2 \\ V_2 \end{Bmatrix} \tag{10}$$

The transmission matrix [T] is defined by

$$\{z_2\} = [T]\{z_1\} \tag{11}$$

and is a square matrix. This definition of the transmission matrix is known as the rearward form. The forward form $\bar{T}$ is defined so that

$$\{z_1\} = [\bar{T}]\{z_2\} \tag{12}$$

For brevity, the concept of a rectangular transmission matrix resulting from an unequal number of input and output forces is not covered here [6]. The forward transmission matrix is the inverse of the backward transmission matrix

$$[\bar{T}] = [T]^{-1} \tag{13}$$

The impedance, admittance and transmission matrices contain identical information, and their interrelationships are given in Reference 11. There are certain circumstances in which each form results in simpler relationships than do the other forms. Consequently, each form has a rightful place, and no form should be given preferential status. The admittance matrix form is most convenient for experimental measurement on structures and for analyzing tandem arrangements of free massless structures. The admittance form can also be quite useful for determining natural frequencies of joined structures and for treating systems containing mechanical sources. The impedance form yields simple matrix additions when structures are joined, and external forces are applied to the joints. The order of the resulting impedance matrix rises as the number of joints in the system increases. The transmission form is the most convenient for relating the input and output states at the two ends of a tandem array of structures

through simple matrix multiplication of the transmission matrices of the constituent structures. The order of the resulting transmission matrix is independent of the number of joints and is governed only by the number of elements in the state vector.

Properties of Transmission Matrices

The state vector and transmission matrix can be written in a partitioned form where the state vector becomes

$$\{z\} = \left\{\begin{array}{c} F \\ \hline V \end{array}\right\} \tag{14}$$

and the transmission matrix is

$$[T] = \left[\begin{array}{c|c} A & B \\ \hline C & D \end{array}\right] \tag{15}$$

The elements of the transmission matrix are not independent and as a consequence of reciprocity it has been shown [6] that the square submatrices of Equation (15) must satisfy

$$[A]^T[D] - [C]^T[B] = [\,1\,] \tag{16a}$$

$$[D][A]^T - [C][B]^T = [\,1\,] \tag{16b}$$

Equation (16) provides an excellent means of checking the validity of derivations of transmission matrices. It can be shown that the inverse of the backward transmission matrix is given by

$$[T]^{-1} = \begin{bmatrix} D^T & -B^T \\ -C^T & A^T \end{bmatrix} \tag{17}$$

This result can be verified by premultiplying the transmission matrix by its inverse, and utilizing Equation (16a) and symmetry of $[D]^T[B]$ and $[C]^T[A]$. Again the same result can also be verified by postmultiplying the transmission matrix by its inverse, and utilizing Equation (16b) and symmetry of $[A][B]^T$ and $[C][D]^T$. The symmetry of the matrices $[D]^T[B]$, $[C]^T[A]$, $[A][B]^T$ and $[C][D]^T$ can be established by interrelationships among the transmission, admittance, and impedance matrices. By virtue of Equations (13) and (17) the forward transmission matrix $[\vec{T}]$ can be written as

$$[\vec{T}] = \begin{bmatrix} D^T & -B^T \\ -C^T & A^T \end{bmatrix} \tag{18}$$

By interchanging rows and columns and performing successive multiplications of rows and columns by -1, it can be shown that the following two determinants are equal.

$$\begin{vmatrix} D^T & -B^T \\ -C^T & A^T \end{vmatrix} = \begin{vmatrix} A & B \\ C & D \end{vmatrix} \tag{19}$$

Clearly the above equality taken together with Equations (17) and (18) indicates that the determinant of a square transmission matrix equals one.

$$|[T]| = |[\bar{T}]| = 1 \tag{20}$$

This is a generalization of the well known result in four-pole parameter theory, namely that the determinant of the four-pole matrix is unity [4]. Many transmission structures are symmetrical in that a reversal of input and output is inconsequential to their behavior. Consequently Equations (13), (15) and (18) require that the transmission matrix of a symmetrical structure satisfies

$$A = D^T, \quad B = B^T, \quad C = C^T \tag{21}$$

(signs ignored)

Derivation of Transmission Matrices

It is often possible to find the transmission matrix by using simple statics. Such techniques are described in Chapter III of Reference 5. Sometimes the required transmission matrix can not be derived by simple statics or it is not readily available in any catalogue of transmission matrices. In such a situation the following methods can be used for the calculation of transmission matrices.

Derivation of the Transmission Matrix From an nth-order Differential Equation

The usual method of solving problems of one independent variable is to eliminate n-1 of the dependent variables to give an nth-order ordinary differential equation in the remaining dependent variable. If it is possible to find n closed solutions of this equation, it is then a straight forward matter to develop the transmission matrix. The n constants associated with the nth-order differential equation are determined by the boundary conditions of the problem. This technique will be illustrated by means of an example.

The transmission matrix is obtained for a uniform elastic shaft with mass per unit length 'm' which is undergoing torsional vibrations of circular frequency ω. From the equilibrium condition

$$\frac{dQ}{dx} + m\, i_x^2\, \omega^2\, \phi = 0 \tag{22}$$

and from elastic properties

$$\frac{d\phi}{dx} = \frac{Q}{GJ} \tag{23}$$

where i_x = radius of gyration

Q = torque

The elimination Q from Equations (22) and (23) gives the second-order differential equation

$$\frac{d^2\phi}{dx^2} + \frac{mi_x^2\omega^2}{GJ}\,\phi = 0 \qquad (24)$$

The solution for a shaft portion of length ℓ is

$$\phi = A \sin\left(\frac{\lambda x}{\ell}\right) + B \cos\left(\frac{\lambda x}{\ell}\right) \qquad (25)$$

where $\lambda^2 = mi_x^2\ell^2\omega^2/GJ$

At x = 0, coinciding with point i-1 on the shaft, the boundary conditions are $\phi = \phi_{i-1}$ and $Q = Q_{i-1}$, from which we obtain

$$B = \phi_{i-1} \quad \text{and} \quad A = \frac{Q_{i-1}\ell}{\lambda GJ}$$

The solution of Equation (24) is then

$$\phi = \phi_{i-1} \cos\left(\frac{\lambda x}{\ell}\right) + Q_{i-1}\frac{\ell}{\lambda GJ} \sin\left(\frac{\lambda x}{\ell}\right) \qquad (26)$$

and the expression for Q is

$$Q = -\phi_{i-1}\frac{\lambda GJ}{\ell} \sin\left(\frac{\lambda x}{\ell}\right) + Q_{i-1} \cos\left(\frac{\lambda x}{\ell}\right) \qquad (27)$$

At $x = \ell$, coinciding with point i of the shaft,

$$\phi_i = \phi_{i-1} \cos\lambda + Q_{i-1}\frac{\ell}{\lambda GJ} \sin\lambda \qquad (28)$$

$$Q_i = -\phi_{i-1}\frac{\lambda GJ}{\ell} \sin\lambda + Q_{i-1} \cos\lambda \qquad (29)$$

Expressing Equations (28) and (29) in matrix form

$$\begin{Bmatrix} \phi \\ Q \end{Bmatrix}_i = \begin{bmatrix} \cos \lambda & \frac{\ell}{GJ\lambda} \sin \lambda \\ -\frac{\lambda GJ}{\ell} \sin \lambda & \cos \lambda \end{bmatrix} \begin{Bmatrix} \phi \\ Q \end{Bmatrix}_{i-1} \tag{30}$$

or

$$\{z\}_i = [T]\{z\}_{i-1} \tag{31}$$

where [T] is the transmission matrix and {z} is the state vector.

Method of Finding the Transmission Matrix Using the Cayley-Hamilton Theorem

In the previous method the set of first order differential equations is reduced to one of second order. It is possible, and in many cases it is advantageous, to find the transmission matrix from the set of first-order differential equations with constant coefficients.

In general, the state vector is usually known to satisfy a differential equation of the form [12]

$$\frac{d}{dx}\{z\} = [A]\{z\} \tag{32}$$

The [A] matrix is entirely determined by the differential equations which govern a dx increment of the system.

The solution of Equation (32) is

$$\{z(x)\} = e^{[A]x} \{z(o)\}$$

or $$\{z(x)\} = [T]\{z(o)\} \tag{33}$$

where $$[T] = e^{[A]x} \tag{34}$$

is the transmission matrix of the system. $e^{[A]x}$ can be evaluated by employing the Cayley-Hamilton theorem which states that any square matrix [A] of order n satisfies its own characteristic equation. A direct result of this is that any function of A for which the Taylor's series exists, namely f(A), can be replaced by a polynomial p(A) in A of order (n-1)

$$f(A) = p(A) = C_o\, I + C_1\, A + C_2\, A^2 + \ldots + C_n\, A^{n-1} \tag{35}$$

The constants C_o, $C_1, \ldots C_{n-1}$ can be determined by using the fact that the eigenvalues, λ_i, of A also satisfy Equation (35).

If there are n distinct eigenvalues, λ_i, of A, then there are n equations which can be solved for the constants C_i. When λ_j is a multiple eigenvalue, that is, $\lambda_j = \lambda_{j+1} = \ldots = \lambda_{j+m}$ $(m < n)$, we lack m equations of the type obtained by substituting an eigenvalue in Equation (35). The missing m equations are found by satisfying the requirement that f(A) and the polynomial p(A) possess the same first m derivatives for the eigenvalue $\lambda = \lambda_j$.

Rubin's Method

The methods so far discussed proved satisfactory for simple lumped parameter or lower order uniform continuous systems, but become cumbersome when used for nonuniform and higher order systems because of the required algebraic manipulations. Recently, however, Rubin [8] has formulated a systematic approach which eliminates much of the algebra and results directly in differential equations for the elements of the transmission matrix.

It was mentioned already while discussing the method of finding the transmission matrix using the Cayley-Hamilton theorem that the state vector usually satisfies the differential equation

$$\frac{d}{dx}\{z(x)\} = [A(x)]\{z(x)\} \tag{36}$$

By definition of the backward transmission matrix

$$\{z(x)\} = [T(x)]\{z(o)\} \tag{37}$$

Differentiating Equation (37) with respect to x gives

$$\frac{d}{dx}\{z(x)\} = \frac{d}{dx}[T(x)\{z(o)\} \tag{38}$$

From Equation (37) it is obvious that

$$\{z(o)\} = [T(x)]^{-1}\{z(x)\} \tag{39}$$

Substituting this equation into Equation (38) the following equation can be obtained

$$\frac{d}{dx}\{z(x)\} = \frac{d}{dx}[T(x)][T(x)]^{-1}\{z(x)\} \tag{40}$$

Equating Equations (36) and (40) gives

$$[A(x)]\{z(x)\} = \frac{d}{dx}[T(x)][T(x)]^{-1}\{z(x)\}$$

or $$\left[[A(x)] - \frac{d}{dx}[T(x)][T(x)]^{-1}\right]\{z(x)\} = \{0\} \tag{41}$$

Since Equation (41) must be satisfied for all values of x and all values of z it follows that $[A(x)] = \frac{d}{dx}[T(x)][T(x)]^{-1}$. Then postmultiplying both sides by $[T(x)]$ yields

$$\frac{d}{dx}[T(x)] = [A(x)][T(x)] \tag{42}$$

Therefore, the transmission matrix is given directly by the solution to Equation (42). By letting x go to zero in Equation (37) the first initial condition becomes

$$[T(o)] = \text{the identity matrix} \tag{43}$$

If Equation (42) is solved as a coupled set of first-order differential equations, then Equation (43) provides sufficient number of initial conditions. However, if the elements of the transmission matrix are determined from higher order differential equations, then additional initial conditions

are required. These additional conditions can be obtained as follows. Substituting Equation (43) into Equation (42) yields

$$[T'(o) = [A(o)] \tag{44}$$

Differentiating Equation (42) with respect to x and using Equations (43) and 44) results in [T"(o)]. This process can be continued to obtain as many initial conditions as required to evaluate constants which arise in solving Equation (42).

Frequency Equation and Mode Shapes

The transmission matrix, by definition, is independent of the boundary conditions and is a function of frequency, ω. Upon substituting appropriate boundary conditions for a system into the input and output state vectors of Equation (11), a frequency determinant can be obtained. A simply supported beam, for example with the boundary conditions included in the state vectors is described by

$$\begin{Bmatrix} 0 \\ \psi \\ 0 \\ V_z \end{Bmatrix}_2 = \begin{bmatrix} \\ T_{ij} \\ \\ \end{bmatrix} \begin{Bmatrix} 0 \\ \psi \\ 0 \\ V_z \end{Bmatrix}_1 \tag{45}$$

or

$$0 = T_{12}\,\psi_1 + T_{14}\,V_{z_1} \tag{46}$$

$$0 = T_{32}\,\psi_1 + T_{34}\,V_{z_2} \tag{47}$$

For a non-trivial solution of Equations (46) and (47) the determinant of the coefficients, T_{ij}, must be zero, that is

$$\begin{vmatrix} T_{12} & T_{14} \\ T_{32} & T_{34} \end{vmatrix} = 0 \tag{48}$$

Other boundary conditions give similar second-order determinants which define the natural frequencies. The systems discussed are open systems in the sense that there have been two sets of boundary conditions. If the system is closed, however. The boundary conditions are not so obvious and such problems are treated in Reference 13.

Having determined the natural frequencies, the corresponding mode shapes can also be obtained. This is accomplished by relating the non-zero components of the input state vector to one reference component. Then the state vectors are determined at other points through the system in terms of the reference component by applying the transmission matrix which relates the input to the output at the point in question.

Forced Vibrations

It has been shown how transmission matrices may be used to find the natural frequencies and mode shapes of an elastic system. Once they are known it is possible to solve the most general cases of forced undamped vibrations, whether they are transient or steady-state in character, either for discrete or continuous systems, through the normal mode approach. On the other hand, for discrete systems, the steady state response caused by a harmonic excitation is more readily solved with the aid of a particular integral of the non-homogeneous differential equation without making use of the normal modes and natural frequencies [5].

The procedure adopted here for the steady-state response of forced vibrations with harmonic excitation has to be brought into line with that used to find the natural frequencies and normal modes. This is usually called the extended transmission matrix approach for undamped systems and the complex extended transmission matrix approach for damped systems. This procedure is valid for any arbitrary damping since normal modes are not brought into the picture. The restrictions are that the responses are steady and excitations are harmonic. With the knowledge of the system's response to harmonic inputs, the response to any arbitrary inputs can be computed by synthesizing the arbitrary forcing functions from an aggregate of infinitesimal harmonic forces

[14]. For continuous systems for which the normal mode approach is clearly unjustified or, at least questionable the transmission matrix approach can be used in the following fashion.

Consider the equation of a nonuniform beam with arbitrary damping for transverse bending

$$\frac{\partial^2}{\partial x^2}\left(EI\ \frac{\partial^2 W}{\partial x^2}\right) + C\ \dot{W} + m\ \ddot{W} = P(x,t) \tag{49}$$

Take the Fourier transforms of both sides of Equation (49). Then the Fourier transform of W

$$\bar{W} = \frac{1}{2\pi}\int_{-\infty}^{\infty} W\ \exp(-i\omega t)\ dt$$

satisfies

$$\frac{d^2}{dx^2}\left(EI\ \frac{d^2\bar{W}}{dx^2}\right) + (i\omega c - \omega^2 m)\bar{W} = \bar{P} \tag{50}$$

where $\bar{p}$ is the Fourier transform of P. Replace Equation (50) by the following first-order matrix equation for the state vector.

$$\{\bar{z}\}^T = \lfloor \bar{W},\ \bar{W}',\ EI\bar{W}'',\ (EI\bar{W}'')' \rfloor = \lfloor \bar{W},\ \bar{\theta},\ \bar{M},\ \bar{V} \rfloor$$

$$\frac{d}{dx}\{\bar{z}\} = [A]\{\bar{z}\} + \{\bar{B}\} \tag{51}$$

with

$$[A] = \begin{bmatrix} 0 & 1 & 0 & 0 \\ 0 & 0 & 1/EI & 0 \\ 0 & 0 & 0 & 1 \\ \omega^2 m - i\omega c & 0 & 0 & 0 \end{bmatrix} \tag{52}$$

$$\{\bar{B}\} = \begin{Bmatrix} 0 \\ 0 \\ 0 \\ \bar{P} \end{Bmatrix}$$

Let [T(x,s)] denote a transmission matrix which transforms the state vector at x = s into the state vector at an arbitrary x. Then the complete solution for Equation (51) may be written as follows.

$$\{\bar{z}(x)\} = [T(x,0)]\{\bar{z}(0)\} + \int_0^x [T(x,s)]\{\bar{B}(s)\}ds \tag{53}$$

It is clear that matrix [T(x,0)] is a transmission matrix which relates the state vectors at x = 0 and at an arbitrary x when the beam is unloaded. Similarly, the matrix [T(x,s)] in the integrand of Equation (53) transfers a jump in the value of the state vector equal to $\{\bar{B}(s)\}$ ds from s to x. Thus the solution for the forced vibration problem can be obtained from a knowledge of the transmission matrix.

To illustrate the application of boundary conditions let the beam be simply supported at one end and elastically supported at the other, as shown in Figure 2. The elastic support also allows for structural damping, which may be accounted for by introducing an imaginary part to each of the two spring constants. The boundary conditions require that

$$\{\bar{z}(0)\} = \begin{Bmatrix} 0 \\ \bar{\theta}(0) \\ 0 \\ \bar{V}(0) \end{Bmatrix} \quad ; \quad \{z(\ell+)\} = \begin{Bmatrix} \bar{w}(\ell) \\ \bar{\theta}(\ell) \\ 0 \\ 0 \end{Bmatrix} \tag{54}$$

These boundary conditions correspond to location $x = \ell +$ (immediate right of the elastic support). Hence the boundary conditions shown in Equation (54) correspond to free end condition. The presence of elastic supports at $x = \ell$ can be taken care of by the introduction of point transmission matrices. These point transmission matrices account for the discontinuities in transferring the state vector across the elastic supports

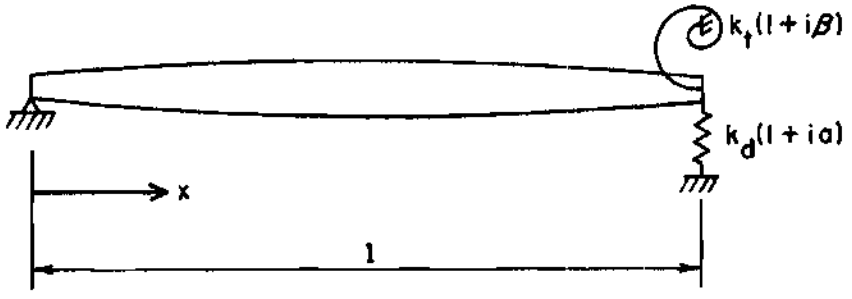

Figure 2. Boundary Conditions for Forced Response Problem

Letting $x = \ell+$ in Equation (53)

$$\begin{Bmatrix} \bar{w}(\ell) \\ \bar{\theta}(\ell) \\ 0 \\ 0 \end{Bmatrix} = [T(\ell+,0)] \begin{Bmatrix} 0 \\ \bar{\theta}(0) \\ 0 \\ \bar{V}(0) \end{Bmatrix} + \int_0^{\ell+} [T(\ell+,s)]\{\bar{B}(s)\}ds \qquad (55)$$

Extracting the third and fourth rows from Equation (55)

$$\begin{Bmatrix} 0 \\ 0 \end{Bmatrix} = {}_{\ell+}\begin{bmatrix} T_{32} & T_{34} \\ T_{42} & T_{44} \end{bmatrix}_0 \begin{Bmatrix} \bar{\theta}(0) \\ \bar{V}(0) \end{Bmatrix} + \int_0^{\ell+} \begin{Bmatrix} T_{34} \\ T_{44} \end{Bmatrix} \bar{p}(s,\omega)ds \qquad (56)$$

where each T_{jk} is the (j,k) element of the transmission matrix [T] whose arguments are indicated at the corners of the matrix symbol.

For the present boundary conditions at x = 0, Equation (53) can also be written as

$$\{\bar{z}(x)\} = {}_{x}\begin{bmatrix} T_{12} & T_{14} \\ T_{22} & T_{24} \\ T_{32} & T_{34} \\ T_{44} & T_{44} \end{bmatrix}_0 \begin{Bmatrix} \bar{\theta}(0) \\ \bar{V}(0) \end{Bmatrix} + \int_0^x \begin{Bmatrix} T_{14} \\ T_{24} \\ T_{34} \\ T_{44} \end{Bmatrix} \bar{p}(s,\omega)ds \qquad (57)$$

Elimination of the vector $\{\bar{\theta}(0), \bar{V}(0)\}$ from Equations (56) and (57) yields

$$\{\bar{z}(x)\} = -\begin{bmatrix} T_{12} & T_{14} \\ T_{22} & T_{24} \\ T_{32} & T_{34} \\ T_{42} & T_{44} \end{bmatrix}_{x} \Bigg\langle \begin{bmatrix} T_{32} & T_{34} \\ T_{42} & T_{44} \end{bmatrix}_{\ell+}^{-1}{}_{0} \int_{0}^{\ell} \begin{Bmatrix} T_{34} \\ T_{44} \end{Bmatrix}_{\ell+s} \bar{p}(s,\omega)\,ds \Bigg\rangle + \int_{0}^{x} \begin{Bmatrix} T_{14} \\ T_{24} \\ T_{34} \\ T_{44} \end{Bmatrix}_{xs} \bar{p}(s,\omega)\,ds \tag{58}$$

Taking the inverse Fourier transform of both sides of Equation (58) yields $\{z(x,t)\}$, which is the required solution.

General Discussion

The foregoing formulation has been based on a particular set of boundary conditions. Other boundary conditions can be treated analogously. Furthermore, if intermediate elastic supports and/or concentrated masses are present along the beam, then additional point transmission matrices must be introduced to account for the discontinuities in transferring the state vector across the stations with such supports and/or concentrated masses. The variations of the transmission matrix method viz.,

delta matrix, modified transmission matrix, and reduced transmission matrix methods are discussed in Reference 5 and the complementary transmission matrix approach in Reference [15].

CHAPTER III

DYNAMIC CHARACTERISTICS OF ROTOR BLADES: TRANSMISSION MATRIX APPROACH

In this chapter the application of the transmission matrix to obtain the dynamic characteristics of non-uniform pretwisted, rotating rotor blades for combined flapwise bending, chord wise bending and torsion and five subcases is discussed. The pertinent equations for obtaining the natural frequencies and mode shapes are given.

Basic Equations

The differential equations of motion for combined flap wise bending, chord wise bending, and torsion of a twisted, nonuniform, rotating blade are derived in Reference 16. They are given below for simple harmonic free vibration with frequency, ω.

$$- \{[GJ + T k_A^2 + EB_1(\beta')^2]\phi' - E B_2 \beta'(v'' \cos \beta + w'' \sin \beta)\}' + T e_A(v'' \sin \beta - w'' \cos \beta) + \Omega^2 m x e(-v' \sin \beta + w' \cos \beta) + \Omega^2 me \sin \beta v + \Omega^2 m[(k_{m_2}^2 - k_{m_1}^2) \cos 2 \beta$$

$$+ e\, e_o \cos\beta]\phi - \omega^2 m k_m^2 \phi +$$

$$\omega^2 m e(v \sin\beta - w \cos\beta) = 0 \qquad (59)$$

$$[(EI_1 \cos^2\beta + EI_2 \sin^2\beta)\, w'' + (EI_2 - EI_1)\sin\beta \cos\beta\, v''$$

$$- T e_A \phi \cos\beta - E B_2 \beta' \phi' \sin\beta]'' - (Tw')'$$

$$-(\Omega^2 m x e \phi \cos\beta)' - \omega^2 m(w + e \phi \cos\beta) = 0 \qquad (60)$$

$$[(EI_2 - EI_1) \sin\beta \cos\beta\, w'' + (EI_1 \sin^2\beta + EI_2 \cos^2\beta)v''$$

$$+ T e_A \phi \sin\beta - E B_2 \beta' \phi' \cos\beta]'' - (Tv')'$$

$$+ (\Omega^2 m x e \phi \sin\beta)' + \Omega^2 me \phi \sin\beta$$

$$- \omega^2 m(v - e \phi \sin\beta) - \Omega^2 m v = 0 \qquad (61)$$

$$T' + \Omega^2 mx = 0 \qquad (62)$$

where $$B_1 = \int_{\eta_{te}}^{\eta_{\ell e}} t\, \eta^2(\eta^2 + t^2/6 - k_A^2)\, d\eta$$

$$B_2 = \int_{\eta_{te}}^{\eta_{\ell e}} t\, \eta\, (\eta^2 + \frac{t^2}{12} - k_A^2)\, d\eta$$

The derivation of these equations is based on the principles of engineering beam theory. Secondary effects such as shear deformation and rotary inertia are not

included. Many coupling terms largely associated with the centrifugal forces, which were neglected in earlier deformation theories, have been included in these equations.

In actual applications subcases of the above equations are often encountered. Since the solutions to subcases can not be obtained from the combined formulation using the transmission matrix approach the following subcases are considered separately.

Case I: Bending in two directions, $e = e_A = B_2 = 0$; $\phi = 0$

Case II: Coupled flapwise bending and torsion, $\beta = 0$; $v = 0$

Case III: Pure flapwise bending, $e = e_A = \beta = 0$; $v = \phi = 0$

Case IV: Pure chordwise bending, $e = e_A = \beta = 0$; $w = \phi = 0$

Case V: Pure torsion, $e = e_A = B_1 = B_2 = \beta = 0$; $v = w = 0$

The differential equations of motion for the subcases are as follows

Case I, $e = e_A = B_2 = 0$

$$[(EI_1 \cos^2 \beta + EI_2 \sin^2 \beta)w'' + (EI_2 - EI_1)\sin \beta \cos \beta\, v'']''$$

$$- (Tw')' - \omega^2 mw = 0 \qquad (63)$$

$$[(EI_2 - EI_1)\sin \beta \cos \beta\, w'' + (EI_1 \sin^2 \beta + EI_2 \cos^2 \beta)v'']''$$

$$- (Tv')' - \Omega^2 mv - \omega^2 mv = 0 \qquad (64)$$

Case II, $\beta = 0$

$$- [(GJ + T k_A^2)\phi']' - T e_A w'' + \Omega^2 m x e w'$$

$$+ \Omega^2 m(k_{m_2}^2 - k_{m_1}^2 + e e_o)\phi - \omega^2 m k_m^2 \phi - \omega^2 me w = 0 \qquad (65)$$

$$(EI_1 w'' - T e_A \phi)'' - (Tw')' - (\Omega^2 m x e\phi)' - \omega^2 m(w + e\phi) = 0 \qquad (66)$$

Case III: $e = e_A = \beta = 0$

$$(EI_1 w'')'' - (Tw')' - \omega^2 m w = 0 \qquad (67)$$

Case IV: $e = e_A = \beta = 0$

$$(EI_1 v'')'' - (Tv')' - \omega^2 m v = 0 \qquad (68)$$

Case V: $\beta = e = B_1 = B_2 = e_A = 0$

$$- [(GJ + Tk_A^2)\phi']' + \Omega^2 m(k_{m_2}^2 - k_{m_1}^2)\phi - \omega^2 m k_m^2 \phi = 0 \qquad (69)$$

Equation (62) governing the tension T in the blade is a part of all the five cases described above.

Frequency Determinants

It is advantageous to use Rubin's method [8] to obtain the transmission matrices for the above systems. The state vectors are chosen as shown below for the general case and the five subcases.

General case:

$$\{z\}^T = \lfloor w,\ v,\ \psi,\ \nu,\ \phi,\ M_x,\ M_z,\ M_y,\ -V_y,\ -V_z \rfloor$$

Case I:

$$\{z\}^T = \lfloor w,\ v,\ \psi,\ \nu,\ \ M_z,\ M_y,\ -V_y,\ -V_z \rfloor$$

Case II:

$$\{z\}^T = \lfloor w,\ \psi,\ \phi,\ M_x,\ M_y,\ -V_z \rfloor$$

Case III:

$$\{z\}^T = \lfloor w,\ \psi,\ M_y,\ -V_z \rfloor$$

Case IV:

$$\{z\}^T = \lfloor v,\ \nu,\ M_z,\ -V_y \rfloor$$

Case V:

$$\{z\}^T = \lfloor \phi,\ M_x \rfloor$$

The components of the state vector, $\{z\}$, can be chosen several ways, but they are chosen here such that they represent the physical quantities of deflections, slopes, moments and shears. This is not absolutely required but highly preferable for the application of the transmission matrix to obtain the natural vibration characteristics.

Further, considerable simplication can be achieved by non-dimensionalizing the governing equations of motion and using the transmission matrices in dimensionless form. The elements of the state vectors are non-dimensionalized as shown below.

General Case and Cases I to III:

$$\bar{w} = w/b_o \ , \quad \bar{v} = v/b_o \ , \quad \bar{\psi} = \psi R/b_o \ , \quad \bar{\phi} = \phi$$

$$\bar{\nu} = \nu R/b_o \ , \quad \bar{M}_x = M_x R^3/EI_{10} b_o^2 \ , \quad \bar{M}_y = M_y R^2/EI_{10} b_o$$

$$\bar{M}_z = M_z R^2/EI_{10} b_o \ , \quad \bar{V}_y = V_y R^3/EI_{10} b_o, \quad \bar{V}_z = V_z R^3/EI_{10} b_o$$

$$\bar{\Omega}^2 = \Omega^2 \, m_o R^4/EI_{10} \ , \quad \bar{\omega}^2 = \omega^2 \, m_o R^4/EI_{10}$$

Case IV:

$$\bar{v} = v/b_o \ , \quad \bar{\nu} = \nu R/b_o \ , \quad \bar{M}_z = M_z R^2/EI_{20} b_o \ ,$$

$$\bar{V}_y = V_y R^3/EI_{20} b_o \ , \quad \bar{\Omega}^2 = \Omega^2 \, m_o R^4/EI_{20}, \quad \bar{\omega}^2 = \omega^2 \, m_o \, R^4/EI_{20}$$

Case V:

$$\phi = \phi, \quad \bar{M}_x = M_x R^2/GJ_o b_o \ , \quad \bar{\Omega}^2 = \Omega^2 \, m_o R^4/GJ_o$$

$$\bar{\omega}^2 = \omega^2 \, m_o \, R^4/GJ_o$$

The other quantities appearing in the differential equations of motion are non-dimensionalized in the following fashion.

$$\bar{x} = \frac{x}{R} , \quad \bar{k}_A^2 = \frac{k_A^2}{b_o^2} , \quad \bar{\beta} = \beta, \quad \bar{e} = \frac{e}{b_o} ,$$

$$\bar{e}_A = \frac{e_A}{b_o} , \quad \bar{e}_o = \frac{e_o}{b_o} , \quad \bar{k}_{m_1}^2 = \frac{k_{m_1}^2}{b_o^2} ,$$

$$\bar{k}_{m_2}^2 = \frac{k_{m_2}^2}{b_o^2} , \quad \bar{k}_m^2 = \frac{k_m^2}{b_o^2}$$

Equations (63) to (69) are non-dimensionalized and reduced to first order equations in terms of the appropriate non-dimensional state vectors. These sets of non-dimensionalized first order differential equations are given below.

General case:

$$\frac{d\bar{w}}{d\bar{x}} = \bar{\psi} \tag{70a}$$

$$\frac{d\bar{v}}{d\bar{x}} = \bar{\nu} \tag{70b}$$

$$\frac{d\bar{\psi}}{d\bar{x}} = C_{31}\,\bar{M}_x + C_{32}\,\bar{M}_y + C_{33}\,\bar{M}_z + C_{31}\,\bar{T}\,\bar{e}_A \sin\beta\,\bar{\nu}$$

$$- C_{31}\,\bar{T}\,\bar{e}_A \cos\beta\,\bar{\psi} + (C_{32}\cos\beta - C_{33}\sin\beta)\bar{T}\,\bar{e}_A\,\bar{\phi} \tag{70c}$$

$$\frac{d\bar{\nu}}{d\bar{x}} = C_{21}\,\bar{M}_x + C_{22}\,\bar{M}_y + C_{23}\,\bar{M}_z$$

$$+ C_{21}\,\bar{T}\,\bar{e}_A \sin\beta\,\bar{\nu} - C_{21}\,\bar{T}\,\bar{e}_A \cos\beta\,\bar{\psi}$$

$$+ (C_{22}\cos\beta - C_{23}\sin\beta)\,\bar{T}\,\bar{e}_A\,\bar{\phi} \qquad (70d)$$

$$\frac{d\bar{\phi}}{d\bar{x}} = C_{11}\,\bar{M}_x + C_{12}\,\bar{M}_y + C_{13}\,\bar{M}_z$$

$$+ C_{11}\,\bar{T}\,\bar{e}_A \sin\beta\,\bar{\nu} - C_{11}\,\bar{T}\,\bar{e}_A \cos\beta\,\bar{\psi}$$

$$+ (C_{12}\cos\beta - C_{13}\sin\beta)\,\bar{T}\,\bar{e}_A\,\bar{\phi} \qquad (70e)$$

$$\frac{d\bar{M}_x}{d\bar{x}} = [\bar{\Omega}^2\,\frac{m}{m_o}\,\bar{x}\sin\beta(\bar{e}_A - \bar{e}) - \bar{T}\,\bar{e}_A' \sin\beta - \bar{T}\,\bar{e}_A\,\beta'\cos\beta]\bar{\nu}$$

$$+ [\bar{\Omega}^2\,\frac{m}{m_o}\,\bar{x}\cos\beta(\bar{e} - \bar{e}_A) + \bar{T}\,\bar{e}_A' \cos\beta - \bar{T}\,\bar{e}_A\,\beta'\sin\beta]\bar{\psi}$$

$$+ [(\bar{\Omega}^2 + \bar{\omega}^2)\,\frac{m}{m_o}\,\bar{e}\sin\beta]\bar{v} - \bar{\omega}^2\,\frac{m}{m_o}\,\bar{e}\cos\beta\,\bar{w}$$

$$+ [\bar{\Omega}^2\,\frac{m}{m_o}\{(\bar{k}_{m_2}^2 - \bar{k}_{m_1}^2)\cos 2\beta + \bar{e}\,\bar{e}_o\cos\beta\} - \bar{\omega}^2\,\frac{m}{m_o}\,\bar{k}_m^2]\,\bar{\beta}$$

(70f)

$$\frac{d\bar{M}_z}{d\bar{x}} = \bar{T}\,\bar{\nu} - \bar{V}_y - \bar{\Omega}^2\,\frac{m}{m_o}\,\bar{e}\,\bar{x}\sin\beta\,\bar{\phi} \qquad (70g)$$

$$\frac{d\bar{M}_y}{d\bar{x}} = \bar{T}\,\bar{\psi} - \bar{V}_z + \bar{\Omega}^2\,\frac{m}{m_o}\,\bar{e}\,\bar{x}\cos\beta\,\bar{\phi} \qquad (70h)$$

$$\frac{-d\bar{V}_y}{d\bar{x}} = (\bar{\Omega}^2 + \bar{\omega}^2)\,\frac{m}{m_o}\,\bar{v} - (\bar{\Omega}^2 + \bar{\omega}^2)\,\frac{m}{m_o}\,\bar{e}\,\sin\beta\,\bar{\phi} \tag{70i}$$

$$\frac{-d\bar{V}_z}{d\bar{x}} = \bar{\omega}^2\,\frac{m}{m_o}\,\bar{w} + \bar{\omega}^2\,\frac{m}{m_o}\,\bar{e}\,\cos\beta\,\bar{\phi} \tag{70j}$$

where

$$C_{11} = (a_{22}\,a_{33} - a_{23}\,a_{32})/D$$

$$C_{12} = (a_{13}\,a_{32} - a_{12}\,a_{33})/D$$

$$C_{13} = (a_{12}\,a_{23} - a_{13}\,a_{22})/D$$

$$C_{21} = (a_{23}\,a_{31} - a_{21}\,a_{33})/D$$

$$C_{22} = (a_{11}\,a_{33} - a_{13}\,a_{31})/D$$

$$C_{23} = (a_{13}\,a_{21} - a_{11}\,a_{23})/D$$

$$C_{31} = (a_{21}\,a_{32} - a_{22}\,a_{31})/D$$

$$C_{32} = (a_{12}\,a_{31} - a_{11}\,a_{32})/D$$

$$C_{33} = (a_{11}\,a_{22} - a_{12}\,a_{21})/D$$

$$D = \begin{vmatrix} a_{11} & a_{12} & a_{13} \\ a_{21} & a_{22} & a_{23} \\ a_{31} & a_{32} & a_{33} \end{vmatrix}$$

$$a_{11} = \left(\frac{R}{b_o}\right)^2 \frac{GJ}{EI_{10}} + \bar{T}\,\bar{k}_A^2 + \frac{EB_1(\beta')^2}{EI_{10}b_o^2}$$

$$a_{12} = -\frac{E\,B_2\beta'}{EI_{10}b_o}\cos\beta = a_{31}$$

$$a_{13} = -\frac{E\,B_2\beta'}{EI_{10}b_o}\sin\beta = a_{21}$$

$$a_{22} = \left(\frac{EI_2}{EI_{10}} - \frac{EI_1}{EI_{10}}\right) \sin\beta\cos\beta = a_{33}$$

$$a_{23} = \frac{EI_1}{EI_{10}}\cos^2\beta + \frac{EI_2}{EI_{10}}\sin^2\beta$$

$$a_{32} = \frac{EI_1}{EI_{10}}\sin^2\beta + \frac{EI_2}{EI_{10}}\cos^2\beta$$

$$\bar{T} = \frac{TR^2}{EI_{10}} = \bar{\Omega}^2 \int_{\bar{x}}^{1} \frac{m}{m_o}\,\bar{x}\,d\bar{x}$$

Case I:

$$\frac{d\bar{w}}{d\bar{x}} = \bar{\psi} \tag{71a}$$

$$\frac{d\bar{v}}{d\bar{x}} = \bar{\nu} \tag{71b}$$

$$\frac{d\bar{\psi}}{d\bar{x}} = a_3 \, EI_{10} \, \bar{M}_y - a_2 \, EI_{10} \, \bar{M}_z \tag{71c}$$

$$\frac{d\bar{v}}{d\bar{x}} = a_1 \, EI_{10} \, \bar{M}_z - a_2 \, EI_{10} \, \bar{M}_y \tag{71d}$$

$$\frac{d\bar{M}_z}{d\bar{x}} = \bar{T} \, \bar{v} - \bar{V}_y \tag{71e}$$

$$\frac{d\bar{M}_y}{d\bar{x}} = T \, \bar{\psi} - \bar{V}_z \tag{71f}$$

$$\frac{-d\bar{V}_y}{d\bar{x}} = \bar{\Omega}^2 \, \frac{m}{m_o} \, \bar{v} + \bar{\omega}^2 \, \frac{m}{m_o} \, \bar{v} \tag{71g}$$

$$\frac{-d\bar{V}_z}{d\bar{x}} = \bar{\omega}^2 \, \frac{m}{m_o} \, \bar{w} \tag{71h}$$

where

$$a_1 = \frac{C_1}{C_1C_3 - C_2^2} \; ; \quad a_2 = \frac{C_2}{C_1C_3 - C_2^2} \; ; \quad a_3 = \frac{C_3}{C_1C_3 - C_2^2}$$

$$C_1 = EI_1 \cos^2 \beta + EI_2 \sin^2 \beta$$

$$C_2 = (EI_2 - EI_1) \sin \beta \cos \beta$$

$$C_3 = EI_1 \sin^2 \beta + EI_2 \cos^2 \beta$$

$$\bar{T} = \bar{\Omega}^2 \int_{\bar{x}}^{1} \frac{m}{m_o} (\bar{x} + \bar{x}_o) d\bar{x}$$

$$\bar{x}_o = \frac{x_o}{R}$$

x_o = distance from axis of rotation to the root of the elastic beam.

In this particular case the axis of rotation is assumed to be different from the root of the elastic portion of the blade. This particular case may be of more interest in the case of propeller blades.

Case II:

$$\frac{d\bar{w}}{d\bar{x}} = \bar{\psi} \tag{72a}$$

$$\frac{d\bar{\psi}}{d\bar{x}} = \bar{T}\,\frac{EI_{10}}{EI_1}\,\bar{e}_A\,\bar{\phi} + \frac{EI_{10}}{EI_1}\,\bar{M}_y \tag{72b}$$

$$\frac{d\bar{\phi}}{d\bar{x}} = \frac{\bar{M}_x}{\frac{GJ}{EI_{10}}\left(\frac{R}{b_o}\right)^2 + \bar{T}\,\bar{k}_A^2} \tag{72c}$$

$$\frac{d\bar{M}_x}{d\bar{x}} = -\,\bar{\omega}^2\,\frac{m}{m_o}\,\bar{e}\,\bar{w} + \bar{\Omega}^2\,\frac{m}{m_o}\,\bar{e}\,\bar{x}\,\bar{\psi} + \left[\frac{m}{m_o}\,\bar{\Omega}^2(\bar{k}_{m_2}^2 - \bar{k}_{m_1}^2 + \bar{e}\,\bar{e}_o) - \bar{\omega}^2\,\bar{k}_m^2 - \bar{T}^2\,\bar{e}_A^2\,\frac{EI_{10}}{EI_1}\right]\bar{\phi} - \bar{T}\,\bar{e}_A\,\frac{EI_{10}}{EI_1}\,\bar{M}_y \tag{72d}$$

$$\frac{d\bar{M}_y}{d\bar{x}} = \bar{T}\,\bar{\psi} + \bar{\Omega}^2\,\frac{m}{m_o}\,\bar{e}\,\bar{x}\,\bar{\phi} - \bar{V}_z \tag{72e}$$

$$\frac{-d\bar{V}_z}{d\bar{x}} = \bar{\omega}^2 \frac{m}{m_o} \bar{w} + \bar{\omega}^2 \frac{m}{m_o} \bar{e} \bar{\phi} \tag{72f}$$

where

$$\bar{T} = \bar{\Omega}^2 \int_x^1 \frac{m}{m_o} \bar{x} \, d\bar{x}$$

Case III:

$$\frac{d\bar{w}}{d\bar{x}} = \bar{\psi} \tag{73a}$$

$$\frac{d\bar{\psi}}{d\bar{x}} = \frac{EI_{10}}{EI_1} \bar{M}_y \tag{73b}$$

$$\frac{d\bar{M}_y}{d\bar{x}} = \bar{T} \bar{\psi} - \bar{V}_z \tag{73c}$$

$$\frac{-d\bar{V}_z}{d\bar{x}} = \bar{\omega}^2 \frac{m}{m_o} \bar{w} \tag{73d}$$

where $\bar{T} = \bar{\Omega}^2 \int_{\bar{x}}^1 \frac{m}{m_o} \bar{x} \, d\bar{x}$

Case IV:

$$\frac{d\bar{v}}{d\bar{x}} = \bar{\nu} \tag{74a}$$

$$\frac{d\bar{\nu}}{d\bar{x}} = \frac{EI_{20}}{EI_2} \bar{M}_z \tag{74b}$$

$$\frac{d\bar{M}_z}{d\bar{x}} = \bar{T} \bar{\nu} - \bar{V}_y \tag{74c}$$

$$\frac{-d\bar{V}_y}{d\bar{x}} = (\bar{\omega}^2 + \bar{\Omega}^2)\ \frac{m}{m_o}\ \bar{w} \tag{74d}$$

where $\bar{T} = \bar{\Omega}^2 \int_{\bar{x}}^{1} \frac{m}{m_o}\ \bar{x}\ d\bar{x}$

Case V:

$$\frac{d\bar{\phi}}{d\bar{x}} = \frac{\left(\frac{b_o}{R}\right)\bar{M}_x}{\frac{GJ}{GJ_o} + \bar{T}\left(\frac{b_o}{R}\right)^2 \bar{k}_A^2} \tag{75a}$$

$$\frac{d\bar{M}_x}{d\bar{x}} = \bar{\Omega}^2\ \frac{m}{m_o}\left(\frac{b_o}{R}\right)(\bar{k}_{m_2}^2 - \bar{k}_{m_1}^2)\ \bar{\phi}$$

$$- \bar{\omega}^2\ \frac{m}{m_o}\ \bar{k}_m^2 \left(\frac{b_o}{R}\right)\bar{\phi} \tag{75b}$$

where $\bar{T} = \bar{\Omega}^2 \int_{\bar{x}}^{1} \frac{m}{m_o}\ \bar{x}\ d\bar{x}$

Equations (70) to (75) will be used to define the elements of matrix [A] in Equation (36) for evaluation of the transmission matrices of the general case and five subcases considered. The required initial conditions are given by Equation (43). Having determined the transmission matrix, the frequency determinant can then be obtained for any set of boundary conditions. Two sets of boundary conditions are considered, namely, Fixed-Free and Hinge-Free. These

conditions can be described as follows:

$$\begin{aligned} &\text{Fixed} : \bar{w} = \bar{v} = \bar{\psi} = \bar{\nu} = \bar{\phi} = 0 \\ &\text{Hinge} : \bar{w} = \bar{v} = \bar{M}_z = \bar{M}_y = \bar{\phi} = 0 \\ &\text{Free} : \bar{M}_x = \bar{M}_y = \bar{M}_z = \bar{V}_y = \bar{V}_z = 0 \end{aligned} \tag{76}$$

By definition of the transmission matrix

$$\begin{Bmatrix} \bar{w} \\ \bar{v} \\ \bar{\psi} \\ \bar{\nu} \\ \bar{\phi} \\ \bar{M}_x \\ \bar{M}_z \\ \bar{M}_y \\ -\bar{V}_y \\ -V_z \end{Bmatrix}_{\bar{x}=1} = [T_{ij}] \begin{Bmatrix} \bar{w} \\ \bar{v} \\ \bar{\psi} \\ \bar{\nu} \\ \bar{\phi} \\ \bar{M}_x \\ \bar{M}_z \\ \bar{M}_y \\ -V_y \\ -V_z \end{Bmatrix}_{\bar{x}=0} \tag{77}$$

By substituting the fixed boundary conditions into the input state vector ($\bar{x}=0$) and the free boundary conditions into output state vector ($\bar{x}=1$), the following frequency determinant can be obtained for the Fixed-Free system. T_{ij} represents the (i,j) th element of the transmission matrix corresponding to $\bar{x} = 1$.

$$\begin{vmatrix} T_{66} & T_{67} & T_{68} & T_{69} & T_{610} \\ T_{76} & T_{77} & T_{78} & T_{79} & T_{710} \\ T_{86} & T_{87} & T_{88} & T_{89} & T_{810} \\ T_{96} & T_{97} & T_{98} & T_{99} & T_{910} \\ T_{106} & T_{107} & T_{108} & T_{109} & T_{1010} \end{vmatrix} = 0 \qquad (78)$$

Similarly by substituting the Hinge boundary conditions into the input state vector and the free conditions into the output state vector, the following frequency determinant can be obtained for the Hinge-Free system

$$\begin{vmatrix} T_{63} & T_{64} & T_{66} & T_{69} & T_{610} \\ T_{73} & T_{74} & T_{76} & T_{79} & T_{710} \\ T_{83} & T_{84} & T_{86} & T_{89} & T_{810} \\ T_{93} & T_{94} & T_{96} & T_{99} & T_{910} \\ T_{103} & T_{104} & T_{106} & T_{109} & T_{1010} \end{vmatrix} = 0$$

Similarly the corresponding frequency determinants can be obtained for Fixed-Free and Hinge-free systems of the sub-cases as shown below.

Case I:

Fixed-Free

$$\begin{vmatrix} T_{55} & T_{56} & T_{57} & T_{58} \\ T_{65} & T_{66} & T_{67} & T_{68} \\ T_{75} & T_{76} & T_{77} & T_{78} \\ T_{85} & T_{86} & T_{87} & T_{88} \end{vmatrix} = 0$$

Hinge-Free

$$\begin{vmatrix} T_{53} & T_{54} & T_{57} & T_{58} \\ T_{63} & T_{64} & T_{67} & T_{68} \\ T_{73} & T_{74} & T_{77} & T_{78} \\ T_{83} & T_{84} & T_{87} & T_{88} \end{vmatrix} = 0$$

Case II:

Fixed-Free

$$\begin{vmatrix} T_{44} & T_{45} & T_{46} \\ T_{54} & T_{55} & T_{56} \\ T_{64} & T_{65} & T_{66} \end{vmatrix} = 0$$

Hinge-Free

$$\begin{vmatrix} T_{42} & T_{44} & T_{46} \\ T_{52} & T_{54} & T_{56} \\ T_{62} & T_{64} & T_{66} \end{vmatrix} = 0$$

Case III and Case IV:

Fixed-Free

$$\begin{vmatrix} T_{33} & T_{34} \\ T_{43} & T_{44} \end{vmatrix} = 0$$

Hinge-Free

$$\begin{vmatrix} T_{32} & T_{34} \\ T_{42} & T_{44} \end{vmatrix} = 0$$

Case V:

Fixed-Free

$$T_{22} = 0$$

Mode Shapes

Having determined the natural frequencies, the corresponding mode shapes can be obtained in the following fashion.

General case:

$$\begin{Bmatrix} \bar{W} \\ \bar{V} \\ \bar{\psi} \\ \bar{\nu} \\ \bar{\phi} \\ \cdot \\ \cdot \\ \cdot \\ -\bar{V}_z \end{Bmatrix}_{\bar{x}} = [T_{ij}(\bar{x})] \begin{Bmatrix} \bar{W} \\ \bar{V} \\ \bar{\psi} \\ \bar{\nu} \\ \bar{\phi} \\ \cdot \\ \cdot \\ \cdot \\ -\bar{V}_z \end{Bmatrix}_{\bar{x}=0} \tag{79}$$

Fixed-Free.

Substituting fixed boundary conditions into the input state vector and extracting the first, second and fifth rows of Equation (79) while assigning arbitrarily, $\bar{V}_z(0) = 1$, the following matrix equation is obtained.

$$\begin{Bmatrix} \bar{w}(\bar{x}) \\ \bar{v}(\bar{x}) \\ \bar{\phi}(\bar{x}) \end{Bmatrix} = \begin{bmatrix} T_{16}(\bar{x}) & T_{17}(\bar{x}) & T_{18}(\bar{x}) & T_{19}(\bar{x}) \\ T_{26}(\bar{x}) & T_{27}(\bar{x}) & T_{28}(\bar{x}) & T_{29}(\bar{x}) \\ T_{56}(\bar{x}) & T_{57}(\bar{x}) & T_{58}(\bar{x}) & T_{59}(\bar{x}) \end{bmatrix} \begin{Bmatrix} \bar{M}_x(0) \\ \bar{M}_z(0) \\ \bar{M}_y(0) \\ -\bar{V}_y(0) \end{Bmatrix} - \begin{Bmatrix} T_{110}(\bar{x}) \\ T_{210}(\bar{x}) \\ T_{510}(\bar{x}) \end{Bmatrix} \tag{80}$$

Substituting fixed boundary conditions into the input state vector, free boundary conditions into the output state vector, extracting the sixth to ninth rows of Equation (77), and assigning arbitrarily, $\bar{V}_z(0) = 1$, the following matrix equation is obtained

$$\begin{bmatrix} T_{66} & T_{67} & T_{68} & T_{69} \\ T_{76} & T_{77} & T_{78} & T_{79} \\ T_{86} & T_{87} & T_{88} & T_{89} \\ T_{96} & T_{97} & T_{98} & T_{99} \end{bmatrix} \begin{Bmatrix} \bar{M}_x(0) \\ \bar{M}_z(0) \\ \bar{M}_y(0) \\ -\bar{V}_y(0) \end{Bmatrix} = \begin{Bmatrix} T_{610} \\ T_{710} \\ T_{810} \\ T_{910} \end{Bmatrix} \tag{81}$$

Solving Equation (81)

$$\begin{Bmatrix} \bar{M}_x(0) \\ \bar{M}_z(0) \\ \bar{M}_y(0) \\ -\bar{V}_y(0) \end{Bmatrix} = \begin{bmatrix} T_{66} & T_{67} & T_{68} & T_{69} \\ T_{76} & T_{77} & T_{78} & T_{79} \\ T_{86} & T_{87} & T_{88} & T_{89} \\ T_{96} & T_{97} & T_{98} & T_{99} \end{bmatrix}^{-1} \begin{Bmatrix} T_{610} \\ T_{710} \\ T_{810} \\ T_{910} \end{Bmatrix} = \begin{Bmatrix} \alpha_1 \\ \alpha_2 \\ \alpha_3 \\ \alpha_4 \end{Bmatrix} \tag{82}$$

Substituting Equation (82) into Equation (80) it is obvious that

$$\begin{Bmatrix} \bar{w}(\bar{x}) \\ \bar{v}(\bar{x}) \\ \bar{\phi}(\bar{x}) \end{Bmatrix} = \begin{bmatrix} T_{16}(\bar{x}) & T_{17}(\bar{x}) & T_{18}(\bar{x}) & T_{19}(\bar{x}) \\ T_{26}(\bar{x}) & T_{27}(\bar{x}) & T_{28}(\bar{x}) & T_{29}(\bar{x}) \\ T_{56}(\bar{x}) & T_{57}(\bar{x}) & T_{58}(\bar{x}) & T_{59}(\bar{x}) \end{bmatrix} \begin{Bmatrix} \alpha_1 \\ \alpha_2 \\ \alpha_3 \\ \alpha_4 \end{Bmatrix} - \begin{Bmatrix} T_{110}(\bar{x}) \\ T_{210}(\bar{x}) \\ T_{510}(\bar{x}) \end{Bmatrix} \tag{83}$$

The mode shapes can be obtained from Equation (83). If the differential equations of motion given by Equations (59) to (61) are decoupled by virtue of some parameters being zero, then the frequency determinant for the coupled system will turn out to be the product of frequency determinants of the uncoupled system so the eigenvalues can be obtained from the general formulation. But then the coefficient matrix in Equation (81) will be singular and hence can not be inverted. As a result solutions to subcases can not be obtained from the general formulation.

By adopting the above procedure for the mode shapes of the Hinge-Free system, the following equation for these shapes can be obtained.

$$\begin{Bmatrix} \bar{w}(\bar{x}) \\ \bar{v}(\bar{x}) \\ \bar{\phi}(\bar{x}) \end{Bmatrix} = \begin{bmatrix} T_{13}(\bar{x}) & T_{14}(\bar{x}) & T_{16}(\bar{x}) & T_{19}(\bar{x}) \\ T_{23}(\bar{x}) & T_{24}(\bar{x}) & T_{26}(\bar{x}) & T_{29}(\bar{x}) \\ T_{53}(\bar{x}) & T_{54}(\bar{x}) & T_{56}(\bar{x}) & T_{59}(\bar{x}) \end{bmatrix} \begin{Bmatrix} \alpha_1 \\ \alpha_2 \\ \alpha_3 \\ \alpha_4 \end{Bmatrix} - \begin{Bmatrix} T_{110}(\bar{x}) \\ T_{210}(\bar{x}) \\ T_{510}(\bar{x}) \end{Bmatrix} \tag{84}$$

where

$$\begin{Bmatrix} \alpha_1 \\ \alpha_2 \\ \alpha_3 \\ \alpha_4 \end{Bmatrix} = \begin{bmatrix} T_{63} & T_{64} & T_{66} & T_{69} \\ T_{73} & T_{74} & T_{76} & T_{79} \\ T_{83} & T_{84} & T_{86} & T_{89} \\ T_{93} & T_{94} & T_{96} & T_{99} \end{bmatrix}^{-1} \begin{Bmatrix} T_{610} \\ T_{710} \\ T_{810} \\ T_{910} \end{Bmatrix}$$

The mode shapes can be similarly obtained for the subcases and the pertinent equations are given below.

Case I:

Fixed-Free

$$\begin{Bmatrix} \bar{w}(\bar{x}) \\ \bar{v}(\bar{x}) \end{Bmatrix} = \begin{bmatrix} T_{15}(\bar{x}) & T_{16}(\bar{x}) & T_{17}(\bar{x}) \\ T_{25}(\bar{x}) & T_{26}(\bar{x}) & T_{27}(\bar{x}) \end{bmatrix} \begin{Bmatrix} \alpha_1 \\ \alpha_2 \\ \alpha_3 \end{Bmatrix} - \begin{Bmatrix} T_{18}(\bar{x}) \\ T_{28}(\bar{x}) \end{Bmatrix}$$

where

$$\begin{Bmatrix} \alpha_1 \\ \alpha_2 \\ \alpha_3 \end{Bmatrix} = \begin{bmatrix} T_{55} & T_{56} & T_{57} \\ T_{65} & T_{66} & T_{67} \\ T_{75} & T_{76} & T_{77} \end{bmatrix}^{-1} \begin{Bmatrix} T_{58} \\ T_{68} \\ T_{78} \end{Bmatrix}$$

Hinge-Free

$$\begin{Bmatrix} \bar{w}(\bar{x}) \\ \bar{v}(\bar{x}) \end{Bmatrix} = \begin{bmatrix} T_{13}(\bar{x}) & T_{14}(\bar{x}) & T_{17}(\bar{x}) \\ T_{23}(\bar{x}) & T_{24}(\bar{x}) & T_{27}(\bar{x}) \end{bmatrix} \begin{Bmatrix} \alpha_1 \\ \alpha_2 \\ \alpha_3 \end{Bmatrix} - \begin{Bmatrix} T_{18}(\bar{x}) \\ T_{28}(\bar{x}) \end{Bmatrix}$$

where

$$\begin{Bmatrix} \alpha_1 \\ \alpha_2 \\ \alpha_3 \end{Bmatrix} = \begin{bmatrix} T_{53} & T_{54} & T_{57} \\ T_{63} & T_{64} & T_{67} \\ T_{73} & T_{74} & T_{77} \end{bmatrix}^{-1} \begin{Bmatrix} T_{58} \\ T_{68} \\ T_{78} \end{Bmatrix}$$

Case II:

Fixed-Free

$$\begin{Bmatrix} \bar{w}(\bar{x}) \\ \bar{\phi}(\bar{x}) \end{Bmatrix} = \begin{bmatrix} T_{14}(\bar{x}) & T_{15}(\bar{x}) \\ T_{34}(\bar{x}) & T_{35}(\bar{x}) \end{bmatrix} \begin{Bmatrix} \alpha_1 \\ \alpha_2 \end{Bmatrix} - \begin{Bmatrix} T_{16}(\bar{x}) \\ T_{36}(\bar{x}) \end{Bmatrix}$$

where

$$\begin{Bmatrix} \alpha_1 \\ \alpha_2 \end{Bmatrix} = \begin{bmatrix} T_{44} & T_{45} \\ T_{54} & T_{55} \end{bmatrix}^{-1} \begin{Bmatrix} T_{46} \\ T_{56} \end{Bmatrix}$$

Hinge-Free

$$\begin{Bmatrix} \bar{w}(\bar{x}) \\ \bar{\phi}(\bar{x}) \end{Bmatrix} = \begin{bmatrix} T_{12}(\bar{x}) & T_{14}(\bar{x}) \\ T_{32}(\bar{x}) & T_{34}(\bar{x}) \end{bmatrix} \begin{Bmatrix} \alpha_1 \\ \alpha_2 \end{Bmatrix} - \begin{Bmatrix} T_{16}(\bar{x}) \\ T_{36}(\bar{x}) \end{Bmatrix}$$

where

$$\begin{Bmatrix} \alpha_1 \\ \alpha_2 \end{Bmatrix} = \begin{bmatrix} T_{42} & T_{44} \\ T_{52} & T_{54} \end{bmatrix}^{-1} \begin{Bmatrix} T_{46} \\ T_{56} \end{Bmatrix}$$

Case III:

Fixed-Free

$$\bar{w}(x) = \frac{T_{34}}{T_{33}} T_{13}(\bar{x}) - T_{14}(\bar{x})$$

Hinge-Free

$$\bar{w}(\bar{x}) = \frac{T_{34}}{T_{32}} T_{12}(\bar{x}) - T_{14}(\bar{x})$$

Case IV:

Fixed-Free

$$\bar{v}(\bar{x}) = \frac{T_{34}}{T_{33}} T_{13}(\bar{x}) - T_{14}(\bar{x})$$

Hinge-Free

$$\bar{v}(\bar{x}) = \frac{T_{34}}{T_{32}} T_{12}(\bar{x}) - T_{14}(\bar{x})$$

Case V:

Fixed-Free

$$\bar{\phi}(\bar{x}) = T_{12}(\bar{x})$$

CHAPTER IV

DYNAMIC CHARACTERISTICS OF ROTOR BLADES: INTEGRATING AND DIFFERENTIATING MATRIX METHOD

In this chapter the application of integrating and differentiating matrices to obtain the dynamic characteristics of fixed-free rotor blades for (1) flapwise bending and (2) coupled flapwise bending and torsion is discussed. Some aspects of this method are indicated together with the method of solution.

Basic Equations

Integrating and differentiating matrices are used to obtain the dynamic characteristics of non-uniform, rotating rotor blades for

1) Flapwise bending only

2) Coupled flapwise bending and torsion.

The differential equations of motion for the above two cases are given by Equations (65) to (67). These equations are given below with $k_A = e_A = e_o = 0$

1. Flapwise bending

$$(EIw'')'' - (Tw')' - \omega^2 m w = 0 \tag{85a}$$

$$T' + \Omega^2 m x = 0 \tag{85b}$$

2. Coupled flapwise bending and torsion

$$-(GJ\phi')' + \Omega^2 m x e w' + \Omega^2 m(k_{m_2}^2 - k_{m_1}^2)\phi$$

$$-\omega^2(m e w + m k_m^2 \phi) = 0 \qquad (86)$$

$$(EIw")" - (Tw')' - (\Omega^2 m x e\phi)' - \omega^2(m w + m e \phi) = 0 \qquad (87)$$

$$T' + \Omega^2 m x = 0 \qquad (88)$$

The integration and differentiation matrices are given in Appendix A and are denoted by [I] and [D] respectively. The differential equations of motion are integrated with the use of integrating and differentiating matrices to obtain an eigenvalue problem the solution of which defines the natural frequencies and associated modal vectors.

Formulation of the Eigenvalue Problem

Flapwise Bending

Equation (85) is expressed in matrix notation as

$$([EI_1]\{w"\})" - ([T]\{w'\})' - \omega^2[m]\{w\} = \{0\} \qquad (89)$$

where the elements of the diagonal matrices are merely the coefficients appearing in the differential equations at equal intervals along the rotor. The integrating matrix developed corresponds precisely to these intervals. Integration of Equation (89) is performed by premultiplying the equation by the integrating matrix [I] giving

$$([EI_1]\{w''\})' - [T]\{w'\} - \omega^2[I][m]\{w\} + \{k_1\} = \{0\} \quad (90)$$

Now consider the following relation.

$$(TW)' = Tw' + T'w \quad (91)$$

Substituting Equation (88) into (91) yields

$$(Tw)' = Tw' - \Omega^2 m x w \quad (92)$$

In matrix notation, Equation (92) after rearrangement becomes

$$[T]\{w'\} = ([T]\{w\})' + \Omega^2[m][x]\{w\} \quad (93)$$

Substituting this equation into Equation (90) and integrating once yields

$$[EI_1]\{w''\} - [T]\{w\} - \Omega^2[I][m][x]\{w\} - \omega^2[I]^2[m]\{w\} + [I]\{k_1\} + \{k_2\} = \{0\} \quad (94)$$

Premultiplying Equation (94) by $[EI]^{-1}$ and integrating once gives

$$\begin{aligned}\{w'\} &- [I][EI_1]^{-1}[T]\{w\} \\ &-\Omega^2[I][EI_1]^{-1}[I][m][x]\{w\} \\ &-\omega^2[I][EI_1]^{-1}[I]^2[m]\{w\} \\ &+ [I][EI_1]^{-1}[I]\{k_1\} + [I][EI_1]^{-1}\{k_2\} \\ &+ \{k_3\} = \{0\}\end{aligned} \quad (95)$$

Integrating Equation (95) once again yields

$$\{w\} - [I]^2 \lfloor EI_1 \rfloor^{-1} \lfloor T \rfloor \{w\}$$

$$- \Omega^2 [I]^2 \lfloor EI_1 \rfloor^{-1} [I] \lfloor m \rfloor \lfloor x \rfloor \{w\}$$

$$- \omega^2 [I]^2 \lfloor EI_1 \rfloor^{-1} [I]^2 \lfloor m \rfloor \{w\} + [I]^2 \lfloor EI_1 \rfloor^{-1} [I] \{k_1\}$$

$$+ [I]^2 \lfloor EI_1 \rfloor^{-1} \{k_2\} + [I] \{k_3\} + \{k_4\} = \{0\} \qquad (96)$$

$\{k_1\}$, $\{k_2\}$, $\{k_3\}$ and $\{k_4\}$ are constant-of-integration matrices wherein each column contains identical elements, which are evaluated by using the boundary conditions of the problem. These constants are evaluated from the following fixed-free boundary conditions.

$$w_o = 0 \qquad (97)$$

$$w_o' = 0 \qquad (98)$$

$$(EI_1 w'')_n = 0 \qquad (99)$$

$$(EI_1 w'')_n' = 0 \qquad (100)$$

$$T_n = 0 \qquad (101)$$

where n is the last station of the interval.

The matrices $[D_o]$ and $[D_n]$, which are used in evaluating the constants of integration matrices are defined as

$$[D_o] = \begin{bmatrix} 1 & 0 & 0 & \dots & 0 & 0 & 0 \\ 1 & 0 & 0 & \dots & 0 & 0 & 0 \\ \vdots & & & & & & \\ 1 & 0 & 0 & \dots & 0 & 0 & 0 \end{bmatrix}$$

$$[D_n] = \begin{bmatrix} 0 & 0 & 0 & \dots & 0 & 0 & 1 \\ 0 & 0 & 0 & \dots & 0 & 0 & 1 \\ \vdots & & & & & & \\ 0 & 0 & 0 & \dots & 0 & 0 & 1 \end{bmatrix}$$

The constant of integration $\{k_1\}$ is evaluated by premultiplying Equation (90) by $[D_n]$ and applying the boundary conditions given by Equations (100) and (101). Since $[D_n]\{k_1\} = \{k_1\}$ premultiplication leads to

$$\{k_1\} = \omega^2 [D_n][I][m]\{w\} \tag{101a}$$

Premultiplying Equation (94) by $[D_n]$ and applying the boundary conditions given by Equations (99) and (101) and substituting for $\{k_1\}$ yields

$$\begin{aligned} \{k_2\} = {} & \Omega^2 [D_n][I][m][x]\{w\} \\ & + \omega^2 [D_n][I]^2[m]\{w\} \\ & - \omega^2 [D_n][I][D_n][I][m]\{w\} \end{aligned} \tag{102}$$

Premultiplying Equations (95) and (96) by $[D_o]$ and applying the boundary conditions given by Equations (97) and (98) yields

$$\{k_3\} = \{k_4\} = \{0\} \tag{103}$$

Since $[D_o][I]$ and $[D_o][I]^2$ are null matrices.
Expressing Equation (88) in matrix notation gives

$$\{T\} + \Omega^2 \lfloor m \rfloor \lfloor x \rfloor \{1\} + \{k_5\} = \{0\} \tag{104}$$

premultiplying this equation by $[D_n]$ and applying the condition given by Equation (101)

$$\{k_5\} = -\Omega^2 [D_n][I] \lfloor m \rfloor \lfloor x \rfloor \{1\} \tag{105}$$

substituting this equation into Equation (105) and rearranging yields

$$\{T\} = \Omega^2 [F] \lfloor m \rfloor \lfloor x \rfloor \{1\} \tag{106}$$

where $[F] = ([D_n] - \lfloor 1 \rfloor)[I]$

let $$\lfloor T \rfloor = \Omega^2 [\ P\ ] \tag{107}$$

where $\lfloor P \rfloor = \text{diag}[F] \lfloor m \rfloor \lfloor x \rfloor \{1\}$

substituting Equations (101a), (102), (103) and (107) into Equation (96) gives

$$\left[\lfloor 1 \rfloor + \Omega^2 [I]^2 \lfloor EI_1 \rfloor^{-1} \left[-\lfloor P \rfloor + [F] \lfloor m \rfloor \lfloor x \rfloor \right] \right.$$

$$\left. - \omega^2 [I]^2 \lfloor EI_1 \rfloor^{-1} [F]^2 \lfloor m \rfloor \right] \{w\} = \{0\} \qquad (108)$$

Rearrangement of this equation gives

$$[G]\{w\} = \lambda [H]\{w\} \qquad (109)$$

where $\lambda = \frac{1}{\omega^2}$

$$[G] = [I]^2 \lfloor EI_1 \rfloor^{-1} [F]^2 \lfloor m \rfloor$$

$$[H] = \lfloor 1 \rfloor + \Omega^2 [I]^2 \lfloor EI_1 \rfloor^{-1} \left[-\lfloor P \rfloor + [F] \lfloor m \rfloor \lfloor x \rfloor \right]$$

Premultiplying Equation (109) by $[H]^{-1}$ yields

$$[H]^{-1}[G]\{w\} = \lambda \{w\} \qquad (110)$$

Equation (110) is the eigenvalue problem resulting from integration of the differential equation, (89), using the integrating matrix. Solutions of the eigenvalue problem describe the natural frequencies and the associated modal vectors.

Coupled Flapwise Bending and Torsion

Equations (86) to (88) can be expressed in matrix notation as

$$(\lceil EI_1 \rfloor\{w''\})'' - (\lceil T \rfloor\{w'\})' - \Omega^2(\lceil me \rfloor\lceil x \rfloor\{\phi\})' - \omega^2\lceil m \rfloor\{w\} - \omega^2\lceil me \rfloor\{\phi\} = \{0\} \quad (111)$$

$$-([\ GJ\ ]\{\phi'\})' + \Omega^2\lceil me \rfloor\lceil x \rfloor[D]\{w\} + \Omega^2\lceil m(k_{m_2}^2 - k_{m_1}^2) \rfloor\{\phi\} - \omega^2\lceil me \rfloor\{w\} - \omega^2\lceil m\ k_m^2 \rfloor\{\phi\} = \{0\} \quad (112)$$

$$\{T\} + \Omega^2\lceil m \rfloor\lceil x \rfloor\{1\} = \{0\} \quad (113)$$

The matrix [D] in Equation (112) represents the differentiating matrix described in Appendix A. It can be observed that the introduction of the differentiating matrix is not necessary in the case of flapwise bending problem. But it is required in the case of coupled flapwise bending and torsion problem. This is because of the term Ω^2 m x e w' present in the differential equation of motion. Presence of such terms needs the introduction of the differentiating matrix. The boundary conditions for the fixed-free system are

$$
\left.
\begin{aligned}
& w_o = 0 \\
& w_o' = 0 \\
& \phi_o = 0 \\
& (EI_1 w'')_n = 0 \\
& \{(EI_1 w'')' - Tw' - \Omega^2 \, m \, x \, e\phi\}_n = 0 \\
& (GJ\phi')_n = 0 \\
& T_n = 0
\end{aligned}
\right\} \qquad (114)
$$

Integrating Equations (111) to (113) using the integrating matrix and evaluating the constants of integration by applying the boundary conditions given by Equation (114) by adopting a similar procedure used in the case of flapwise bending, the following equations are obtained.

$$
\begin{aligned}
& \{w\} + \Omega^2 [I]^2 \lfloor EI_1 \rfloor^{-1} [F] \lfloor m \rfloor \lfloor x \rfloor \{w\} \\
& + \Omega^2 [I]^2 \lfloor EI_1 \rfloor^{-1} [F] \lfloor me \rfloor \lfloor x \rfloor \{\phi\} \\
& - \Omega^2 [I]^2 \lfloor EI_1 \rfloor^{-1} \lfloor P \rfloor \{w\} \\
& - \omega^2 [I]^2 \lfloor EI_1 \rfloor^{-1} [F]^2 \lfloor m \rfloor \{w\} \\
& - \omega^2 [I]^2 \lfloor EI_1 \rfloor [F]^2 \lfloor me \rfloor \{\phi\} = \{0\}
\end{aligned} \qquad (115)
$$

$$\{\phi\} + \Omega^2[I]\lceil GJ \rfloor^{-1}[F]\lceil me \rfloor\lceil x \rfloor[D]\{w\}$$

$$+ \Omega^2[I]\lceil GJ \rfloor^{-1}[F]\lceil m(k_{m_2}^2 - k_{m_1}^2) \rfloor\{\phi\}$$

$$- \omega^2[I]\lceil GJ \rfloor^{-1}[F]\lceil me \rfloor\{w\}$$

$$- \omega^2[I]\lceil GJ \rfloor^{-1}[F]\lceil m\, k_m^2 \rfloor\{\phi\} = \{0\} \qquad (116)$$

where

$$[F] = ([D_n] - \lceil 1 \rfloor)[I]$$

$$\lceil P \rfloor = \text{diag}[F\{\lceil m \rfloor\lceil x \rfloor\{1\}$$

Equations (115) and (116) can be rearranged as

$$\omega^2[A_1]\{w\} + \omega^2[A_2]\{\phi\} = [B_1]\{w\} + [B_2]\{\phi\} \qquad (117)$$

$$\omega^2[A_3]\{w\} + \omega^2[A_4]\{\phi\} = [B_3]\{w\} + [B_4]\{\phi\} \qquad (118)$$

where

$$[A_1] = [I]^2\lceil EI_1 \rfloor^{-1}[F]^2\lceil m \rfloor$$

$$[A_2] = [I]^2\lceil EI_1 \rfloor^{-1}[F]^2\ \lceil me \rfloor$$

$$[A_3] = [I]\lceil GJ \rfloor^{-1}[F]\lceil me \rfloor$$

$$[A_4] = [I]\lceil GJ \rfloor^{-1}[F]\lceil m\, k_m^2 \rfloor$$

$$[B_1] = \left[\lceil 1 \rfloor + \Omega^2[I]^2\lceil EI_1 \rfloor^{-1}([F]\lceil m \rfloor\lceil x \rfloor - \lceil P \rfloor)\right]$$

$$[B_2] = \Omega^2 [I]^2 \left\lfloor EI_1 \right\rfloor^{-1} [F] \left\lfloor me \right\rfloor \left\lfloor x \right\rfloor$$

$$[B_3] = \Omega^2 [I] \left\lfloor GJ \right\rfloor^{-1} [F] \left\lfloor me \right\rfloor \left\lfloor x \right\rfloor [D]$$

$$[B_4] = \left\lfloor 1 \right\rfloor + \Omega^2 [I] \left\lfloor GJ \right\rfloor^{-1} [F] \left\lfloor m(k_{m_2}^2 - k_{m_1}^2) \right\rfloor$$

Equations (117) and (118) can be combined into a single matrix equation as shown below

$$\omega^2 \begin{bmatrix} [A_1] & [A_2] \\ \hline [A_3] & [A_4] \end{bmatrix} \begin{Bmatrix} \{w\} \\ \hline \{\phi\} \end{Bmatrix} =$$

$$\begin{bmatrix} [B_1] & [B_2] \\ \hline [B_3] & [B_4] \end{bmatrix} \begin{Bmatrix} \{w\} \\ \hline \{\phi\} \end{Bmatrix}$$

or

$$\omega^2 [G]\{\alpha\} = [H]\{\alpha\} \tag{119}$$

where $$\{\alpha\} = \begin{Bmatrix} \{w\} \\ \hline \{\phi\} \end{Bmatrix}$$

Equation (119) can be written in a standard form of the eigenvalue problem by dividing by ω^2 and premultiplying by $[H]^{-1}$ which gives

$$[H]^{-1}[G]\{\alpha\} = \lambda\{\alpha\} \tag{120}$$

where $\lambda = \frac{1}{\omega^2}$

Equation (120) is the eigenvalue problem obtained by application of the integrating and differentiating matrix approach for coupled flapwise bending and torsion. The solution of the eigenvalue problem describes the natural frequencies and the associated natural mode shapes.

Discussion of the Method

An examination of the product matrix $[H]^{-1}[G]$ shows that it is "simply degenerate" (rank of the matrix is one less than the order of the matrix) in the case of flapwise bending and "multiply degenerate" of order two in the case of coupled flapwise bending and torsion. This degeneracy leads to zero eigenvalues (λ=0), only one in the case of flapwise bending and once repeated zero eigenvalues in the case of coupled flapwise bending and torsion. These vanishing eigenvalues correspond to infinite natural frequencies and hence have no physical significance. The zero eigenvalues are due to the fact that the integrating matrix contains all zeros as its first row. This kind of situation may appear in other instances of structural dynamic problems, viz., when a flexibility type of formulation is used for lumped parameter and semidefinite systems. Furthermore it

can be observed that neither [G] nor [H] is a symmetric matrix. The eigenvalue problem resulting from this method is not a self-adjoint eigenvalue problem. Consequently, the modal vectors defined by the eigenvalue problem are not orthogonal in the normal sense. A lumped parameter approximation, Rayleigh-Ritz procedure or Galerkin's approach for the solution of originally continuous systems also yields an eigenvalue problem of the same form. In those cases the [G] and [H] matrices are symmetric. By virtue of symmetry of [G] and [H], the modal vectors in these cases (Rayleigh-Ritz, Galerkin's methods etc.) are orthogonal i.e., orthogonal with respect to [G] and [H] matrices as weighting matrices. So the integrating and differentiating matrix method does not yield a self-adjoint eigenvalue problem even though the original continuous system constitutes a self-adjoint eigenvalue problem. This sort of thing is not uncommon in structural dynamics; for example the collocation technique yields a similar nonself-adjoint eigenvalue problem.

The present method breaks down when applied to a system containing rigid-body degrees of freedom. To illustrate this problem, the method is applied to a uniform continuous non-rotating beam for flapwise bending with Hinge-Free boundary conditions.

The equation of motion for simple harmonic free vibration with frequency, ω, is given by

$$w'''' - \lambda w = 0 \tag{121}$$

where $\lambda = \frac{m\omega^2}{EI}$

Successive integration of Equation (121) with the help of integrating matrices, yields the following equations

$$\{w'''\} - \lambda[I]\{w\} + \{k_1\} = \{0\} \tag{122}$$

$$\{w''\} - \lambda[I]^2\{w\} + [I]\{k_1\} + \{k_2\} = \{0\} \tag{123}$$

$$\{w'\} - \lambda[I]^3\{w\} + [I]^2\{k_1\} + [I]\{k_2\} + \{k_3\} = \{0\} \tag{124}$$

$$\{w\} - \lambda[I]^4\{w\} + [I]^3\{k_1\} + [I]^2\{k_2\} + [I]\{k_3\} + \{k_4\} = \{0\} \tag{125}$$

Boundary conditions of the problem are

$$w_o = 0 \tag{126}$$

$$w''_o = 0 \tag{127}$$

$$w''_n = 0 \tag{128}$$

$$w'''_n = 0 \tag{129}$$

Premultiplying Equation (125) by $[D_o]$ and applying the boundary condition of Equation (126) yields

$$\{k_4\} = \{0\} \tag{130}$$

similarly by premultiplying Equation (123) by $[D_o]$ and using the boundary of condition of Equation (127) gives

$$\{k_2\} = \{0\} \tag{131}$$

Premultiplying Equation (122) by $[D_n]$ and using the boundary condition of Equation (129) leads to

$$\{k_1\} = \lambda[D_n][I]\{w\} \tag{132}$$

Now by premultiplying Equation (123) by $[D_n]$ and applying the boundary condition of Equation (128) gives

$$\{k_2\} = \lambda[D_n][I]^2\{w\} - [D_n][I]\{k_1\}$$

or

$$\{k_2\} = \lambda([D_n][I]^2 - [D_n][I][D_n][I])\{w\} \tag{133}$$

The constants of integration $\{k_1\}$ and $\{k_4\}$ are determined uniquely, $\{k_3\}$ is left undetermined, and $\{k_2\}$ has non-unique values given by Equations (131) and (133). So the method breaks down when the system has a rigid-body degree of freedom. Other boundary conditions, for example, fixed-fixed and simply supported-simply supported cases, do not pose any problem even though a slight variation in the method of evaluating the constants of integration is required. The reason for the failure of the integrating matrix method for semi-definite systems is that this approach is leading to a flexibility type of formulation (in the sense

that the eigenvalue $\lambda = 1/\omega^2$) and such a formulation can not exist for a semi-definite system. One can always convert a differential equation into an integral equation and rigid-body modes can be swept out from the integral equation formulation. The integrating matrix can then be used to solve the integral equation, but the simplicity of this approach is lost since the integral equation requires the determination of the flexibility influence function.

Method of Solution

Since the modal vectors of the eigenvalue problem given by Equation (120) or (110) are not orthogonal, the sweeping and iteration method leads to convergence problems from the second mode onwards. Even though the original continuous system has orthogonality properties for its eigenfunctions, they can not be used to solve Equations (120) or (110), since any approximate formulation must be self contained. In such cases the biorthogonality relationships can be used. Use of the biorthogonality relationships involves the solution of two eigenvalue problems, namely, the original eigenvalue problem and the adjoint eigenvalue problem. However this approach has a restriction that the eigenvalues must be sufficiently far apart for satisfactory convergence. If more than one eigenvalue is required it is preferable to use methods like the LR or QR-transformations

[17]. The LR-transformation is the most significant advance which has been made in connection with the solution of the eigenvalue problem. The QR-transformation further eliminates the difficulties associated with the LR-transformation, since the [G] and [H] matrices are non-symmetric the possibility of complex eigenvalues exists and as such the complex QR-transformation is preferable to use for the solution of the eigenvalue problem.

CHAPTER V

RESULTS AND DISCUSSION OF RESULTS

The object of this study is to develop a comprehensive method and computer program to obtain the dynamic characteristics of twisted, non-uniform rotating blades for coupled flapwise bending, chordwise bending and torsion with five of its subcases. The transmission matrix approach is used to satisfy this objective. The integrating and differentiating matrix technique is used to obtain the dynamic characteristics of rotating blades for 1) coupled flapwise bending and torsion and 2) flapwise bending. Numerical results are compared with available experimental and analytical results. The results obtained by the transmission matrix approach and the integrating and differentiating matrix method are also compared.

Results

Pure Torsion

Natural frequencies and mode shapes were computed using the transmission matrix for a uniform blade with fixed-free end conditions and the results were compared with the exact solutions. The natural frequencies of non-rotating and rotating blades are presented in Table 1 and the modal deflections are given in Table 2.

Table 1. Comparison of Natural Frequencies, Pure Torsion, Fixed-Free

R = 40.0 in, m = 0.0015 slugs/inch, GJ = 9000 Lb-in^2

$k^2_{m_1}$ = 0.18 in^2, $k^2_{m_2}$ = 0.55 in^2

Mode No.	Frequencies Rad/Sec Transmission Matrix	Frequencies Rad/Sec Exact [18]	Percentage	Frequencies Rad/Sec Transmission Matrix
	Ω=0.0 Rad/Sec	Ω=0.0 Rad/Sec	Error	Ω=60.0 Rad/Sec
1	389.9999	390.0001	+0.000051	392.3325
2	1169.9993	1170.0003	0.000086	1170.7806
3	1949.9986	1950.0004	0.000092	1950.4782
4	2730.0530	2730.0006	-0.00192	2730.3872
5	3510.1826	3510.0008	-0.00518	3510.4425

Table 2. Comparison of Mode Shapes, Pure Torsion, Fixed-Free

Station $\bar{x}$	I Mode, Ω=0.0 Rad/Sec		II Mode, Ω=0.0 Rad/Sec	
	TM	Exact [18]	TM	Exact [18]
0.0	0.0000	0.0000	0.0000	0.0000
0.1	0.1564	0.1564	-0.4540	-0.4540
0.2	0.3090	0.3090	-0.8090	-0.8090
0.3	0.4540	0.4540	-0.9877	-0.9877
0.4	0.5878	0.5878	-0.9511	-0.9511
0.5	0.7071	0.7071	-0.7071	-0.7071
0.6	0.8090	0.8090	-0.3090	-0.3090
0.7	0.8910	0.8910	0.1564	0.1564
0.8	0.9511	0.9511	0.5878	0.5878
0.9	0.9877	0.9877	0.8910	0.8910
1.0	1.0000	1.0000	1.0000	1.0000

Station $\bar{x}$	III Mode, Ω=0.0 Rad/Sec		IV Mode, Ω=0.0 Rad/Sec		V Mode, Ω=0.0 Rad/Sec	
	TM	Exact [18]	TM	Exact [18]	TM	Exact [18]
0.0	0.0000	0.0000	0.0000	0.0000	0.0000	0.0000
0.1	0.7071	0.7071	-0.8910	-0.8910	0.9878	0.9877
0.2	1.0000	1.0000	-0.8090	-0.8090	0.3091	0.3090
0.3	0.7071	0.7071	0.1564	0.1564	-0.8911	-0.8910
0.4	0.0000	0.0000	0.9511	0.9511	-0.5878	-0.5878
0.5	-0.7071	-0.7071	0.7071	0.7071	0.7072	0.7071
0.6	-1.0000	-1.0000	-0.3090	-0.3090	0.8091	0.8090
0.7	-0.7071	-0.7071	-0.9877	-0.9877	-0.4540	-0.4540
0.8	0.0000	0.0000	-0.5878	-0.5878	-0.9511	-0.9511
0.9	0.7071	0.7071	0.4540	0.4540	0.1564	0.1564
1.0	1.0000	1.0000	1.0000	1.0000	1.0000	1.0000

Flapwise Bending

Natural frequencies and mode shapes were computed for rotating and nonrotating uniform blades with fixed-free end conditions using the 1) transmission matrix and 2) integrating matrix methods. The solutions obtained are presented in Tables 3 to 5. The results obtained for both uniform and nonuniform Hinge-Free systems are given in Tables 6 to 8 and are compared with available solutions. The following nonuniform data pertains to the results shown in Tables 7 and 8

$$EI_1(\bar{x}) = 2.5 \times 10^7 \ \text{Lb-in}^2, \quad 0 \leq \bar{x} \leq 0.2$$

$$EI_1(\bar{x}) = (4.332005 - 15.366799\ \bar{x} + 26.696032\ \bar{x}^2 - 15.153439\ \bar{x}^3) \times 10^7 \ \text{Lb-in}^2, \quad 0.2 < \bar{x} \leq 1.0$$

$$m(\bar{x}) = (0.397549 + 93.7898\ \bar{x} - 462.665\ \bar{x}^2) \ \text{Lb/in} \qquad 0 \leq \bar{x} \leq 0.2$$

$$m(\bar{x}) = (1.101767 - 0.512333\ \bar{x}) \ \text{Lb/in} \quad 0.2 < \bar{x} \leq 1.0$$

$R = 432$ inches

$\Omega = 20$ rad/sec

Table 3. Comparison of Natural Frequencies, Flapwise Bending, Fixed-Free

$R = 40.0$ in, $m = 0.0015$ slugs/inch, $EI_1 = 25{,}000$ Lb-in^2

$\Omega = 0.0$ Rad/Sec

Mode No.	Frequencies Rad/Sec: Integrating Matrix Method 5 Stations	Integrating Matrix Method 6 Stations	Integrating Matrix Method 10 Stations	Integrating Matrix Method 11 Stations
1	31.0743	31.0768	31.0775	31.0775
2	190.3132	193.4180	194.7359	194.7489
3	586.6048	539.9401	544.5727	544.9658
4	2882.5440	1448.2540	1067.4440	1067.5010
5		8692.1060	1819.5690	1787.9350

Mode No.	Frequencies Rad/Sec: IM 15 Stations	IM 16 Stations	IM 20 Stations	IM 21 Stations
1	31.0775	31.0775	31.0775	31.0775
2	194.7586	194.7589	194.7592	194.7592
3	545.3089	545.3207	545.3326	545.3332
4	1068.5480	1068.6090	1068.6600	1068.6590
5	1768.0040	1767.5330	1766.8860	1766.8270

Mode No.	Frequencies Rad/Sec: IM 25 Stations	IM 26 Stations	IM 30 Stations	TM	Exact [18]
1	31.0775	31.0775	31.0775	31.0765	31.0740
2	194.7593	194.7592	194.7592	194.7574	194.7517
3	545.3322	545.3320	545.3321	545.3349	545.3652
4	1068.6470	1068.6430	1068.6380	1068.6839	1068.7213
5	1766.6590	1766.6330	1766.5800	1766.6662	1766.4833

Table 4. Comparison of Mode Shapes, Flapwise Bending, Fixed-Free

Stations $\frac{x}{R}$	I Mode			II Mode		
	IM 6 Stations	IM 11 Stations	TM	IM 6 Stations	IM 11 Stations	TM
0.0	0.0000	0.0000	0.0000	0.0000	0.0000	0.0000
0.1		0.0168	0.0168		-0.0927	-0.0926
0.2	0.0639	0.0639	0.0639	-0.3081	-0.3013	-0.3011
0.3		0.1365	0.1365		-0.5264	-0.5261
0.4	0.2299	0.2299	0.2299	-0.6864	-0.6838	-0.6835
0.5		0.3395	0.3395		-0.7139	-0.7137
0.6	0.4611	0.4611	0.4611	-0.5891	-0.5897	-0.5895
0.7		0.5909	0.5909		-0.3172	-0.3171
0.8	0.7255	0.7255	0.7255	0.0644	0.0700	0.0700
0.9		0.8624	0.8624		0.5237	0.5237
1.0	1.0000	1.0000	1.0000	1.0000	1.0000	1.0000

Stations $\frac{x}{R}$	III Mode			IV Mode		
	IM 6 Stations	IM 11 Stations	TM	IM 6 Stations	IM 11 Stations	TM
0.0	0.0000	0.0000	0.0000	0.0000	0.0000	0.0000
0.1		0.2323	0.2281		-0.4254	-0.3849
0.2	0.6165	0.6115	0.6045	-0.4684	-0.7942	-0.7536
0.3		0.7622	0.7563		-0.4429	-0.4338
0.4	0.4638	0.5287	0.5259	0.1396	0.3289	0.3155
0.5		0.0196	0.0197		0.7188	0.7069
0.6	-0.3915	-0.4749	-0.4738	0.1730	0.3312	0.3264
0.7		-0.6584	-0.6574		-0.3900	-0.3973
0.8	-0.3815	-0.3960	-0.3949	-0.3548	-0.6362	-0.6428
0.9		0.2259	0.2285		-0.0681	-0.0508
1.0	1.0000	1.0000	1.0000	1.0000	1.0000	1.0000

Table 4 (Continued)

Stations $\frac{x}{R}$	V Mode			
	IM	IM	IM	TM
	6 Stations	11 Stations	26 Stations	
0.00	0.0000	0.0000	0.0000	0.0000
0.04			0.1306	0.1305
0.08			0.4032	0.4031
0.10		0.6911	-	0.5403
0.12			0.6538	0.6540
0.16			0.7597	0.7603
0.20	0.2324	0.7262	0.6625	0.6633
0.24			0.3782	0.3789
0.28			-0.0129	-0.0127
0.30		-0.2630	-	-0.2124
0.32			-0.3936	-0.3941
0.36			-0.6481	-0.6494
0.40	-0.2637	-0.7311	-0.6988	-0.7004
0.44			-0.5308	-0.5322
0.48			-0.1969	-0.1975
0.50		0.0019	-	0.0008
0.52			0.1987	0.1992
0.56			0.5328	0.5345
0.60	0.1911	0.6835	0.7017	0.7041
0.64			0.6533	0.6557
0.68			0.4036	0.4052
0.70		0.2392	-	0.2270
0.72			0.0320	0.0319
0.76			-0.3434	-0.3452
0.80	-0.2639	-0.5305	-0.6010	-0.6040
0.84			-0.6524	-0.6555
0.88			-0.4675	-0.4695
0.90		-0.3171	-	-0.2961
0.92			-0.0786	-0.0813
0.96			0.4380	0.4343
1.00	1.0000	1.0000	1.0000	1.0000

Table 5. Comparison of Natural Frequencies, Flapwise Bending, Fixed-Free

R = 40.0 in, m = 0.0015 slugs/inch, EI_1 = 25,000 Lb-in^2, Ω = 60.0 Rad/Sec

Mode No.	Frequencies, Rad/Sec					
	IM 5 Stations	IM 6 Stations	IM 10 Stations	IM 11 Stations	IM 15 Stations	IM 16 Stations
1	71.6291	71.5952	71.5862	71.5859	71.5854	71.5854
2	242.3845	246.2130	247.4413	247.4583	247.4751	247.4760
3	632.9143	592.5546	600.1895	600.6313	601.0585	601.0778
4	2943.3516	1496.6176	1125.5619	1125.9220	1127.3040	1127.3970
5		8759.7170	1877.9530	1847.3020	1828.4330	1828.0500

Mode No.	Frequencies, Rad/Sec					
	IM 20 Stations	IM 21 Stations	IM 25 Stations	IM 26 Stations	IM 30 Stations	TM
1	71.5853	71.5853	71.5853	71.5853	71.5853	71.5844
2	247.4774	247.4775	247.4777	247.4778	247.4778	247.4762
3	601.1032	601.1050	601.1080	601.1084	601.1091	601.1136
4	1127.5080	1127.5120	1127.5170	1127.5170	1127.5150	1127.5787
5	1827.5580	1827.5070	1827.3940	1827.3770	1827.3310	1825.9995

Table 6. Comparison of Natural Frequencies, Flapwise Bending, Hinge-Free

R = 40.0 in, m = 0.0015 slugs/inch, EI_1 = 25,000 Lb-in^2

Mode No.	Frequencies, Rad/Sec			
	TM Ω=0.0 Rad/Sec	Exact [18] Ω=0.0 Rad/Sec	TM Ω=139.7542 Rad/Sec	Reference 19 Ω=139.7542 Rad/Sec
1	0.0000	0.0000	139.7542	139.7542
2	136.2758	136.3066	374.1612	374.5134
3	441.6321	441.6833	729.9141	726.1212
4	921.4557	921.4282	1239.9997	
5	1575.7496	1575.6967	1904.9995	

Table 7. Comparison of Natural Frequencies, Flapwise Bending, Hinge-Free

Mode No.	Frequencies, Rad/Sec		
	TM	Reference 20	Exact [19]
1	19.9978	-	20.0000
2	44.1942	44.1873	
3	67.0057	67.0052	
4	98.0901	98.1565	
5	139.5464	139.6660	

Table 8. Comparison of Mode Shapes, Flapwise Bending, Hinge-Free

$\bar{x}$	II Mode		III Mode	
	TM	Ref. 4	TM	Ref. 4
0.0	0.0000	0.0000	0.0000	0.0000
0.1	-0.2096	-0.2097	0.2774	0.2769
0.2	-0.3463	-0.3466	0.3175	0.3173
0.3	-0.4119	-0.4121	0.1681	0.1676
0.4	-0.4194	-0.4194	-0.0621	-0.0628
0.5	-0.3629	-0.3627	-0.2994	-0.3001
0.6	-0.2348	-0.2346	-0.4608	-0.4612
0.7	-0.0301	-0.0297	-0.4569	-0.4569
0.8	0.2525	0.2529	-0.2110	-0.2106
0.9	0.6050	0.6053	0.3034	0.3039
1.0	1.0000	1.0000	1.0000	1.0000

$\bar{x}$	IV Mode		V Mode	
	TM	Ref. 4	TM	Ref. 4
0.0	0.0000	0.0000	0.0000	0.0000
0.1	-0.2136	-0.2134	0.1914	0.1920
0.2	-0.0643	-0.0645	-0.1614	-0.1614
0.3	0.2575	0.2576	-0.4834	-0.4835
0.4	0.4621	0.4625	-0.2994	-0.2989
0.5	0.3824	0.3825	0.2530	0.2538
0.6	0.0207	0.0204	0.5417	0.5416
0.7	-0.4061	-0.4066	0.1398	0.1387
0.8	-0.5264	-0.5264	-0.5024	-0.5028
0.9	-0.0265	-0.0260	-0.3144	-0.3134
1.0	1.0000	1.0000	1.0000	1.0000

Chordwise Bending

With equal stiffness properties in flapwise and chordwise directions, the natural frequencies and mode shapes will be identical for nonrotating systems. But when $\Omega > 0$, the natural frequencies and mode shapes will be different in both the directions. This is evident from the differential equations of motion given by Equations (67) and (68). To find the effect of rotation of the blade on chordwise bending frequencies, numerical results were computed using the transmission matrix and are given in Table 9. To find the relative effect of rotation between chordwise bending frequencies and flapwise bending frequencies, comparisons are made between the results for a system with identical stiffness distribution in both the directions.

Coupled Flapwise Bending and Torsion

Natural frequencies and mode shapes were computed for rotating and non-rotating blades with fixed-free end conditions using the (1) transmission matrix and 2) integrating and differentiating matrix methods. The solutions obtained are presented in Tables 10 to 12, 14 and 15. The results obtained by both the methods were compared. Natural frequencies for a hinge-hinge system were computed and are compared with the exact solutions in Table 13.

Table 9. Comparison of Natural Frequencies between Chordwise Bending and Flapwise Bending

R = 40.0 in, m = 0.0015 slugs/inch, EI_1 = 25,000 Lb-in^2, EI_2 = 25,000 Lb-in^2

Mode No.	Frequencies, Rad/Sec					
	Fixed-Free			Hinge-Free		
	Chordwise Bending		Flapwise Bending	Chordwise Bending		Flapwise Bending
	Ω = 0.0 Rad/Sec	Ω = 60.0 Rad/Sec	Ω = 60.0 Rad/Sec	Ω = 0.0 Rad/Sec	Ω = 60.0 Rad/Sec	Ω = 60.0 Rad/Sec
1	31.0765	39.0438	71.5844	0.0000	0.0000	60.0000
2	194.7574	240.0939	247.4762	136.2758	194.4000	203.4485
3	545.3349	598.1087	601.1136	441.6321	505.3673	508.9165
4	1068.6839	1125.9372	1127.5787	921.4557	987.1619	989.0524
5	1766.6662	1823.9995	1825.9995	1575.7496	1642.4996	1644.1996

Table 10. Comparison of Natural Frequencies, Coupled Flapwise Bending and Torsion, Fixed-Free

$R = 40.0$ in, $b_o = 2.0$ in, $EI_1 = 25{,}000$ Lb-in^2, $GJ = 9{,}000$ Lb-in^2, $e = 0.4$ in, $k^2_{m_1} = 0.18$ in^2, $k^2_{m_2} = 0.71$ in^2, $k^2_A = e_A = e_o = \Omega = 0$

Mode No.	Frequencies, Rad/Sec					
	IM 5	IM 6	IM 10	IM 11	IM 15	TM
1	31.0541	31.0566	31.0573	31.0573	31.0573	31.0566
2	189.3711	192.4270	193.7237	193.7364	193.7460	193.7456
3	390.8059	390.8278	390.8773	390.8782	390.8789	390.8779
4	578.9344	534.2687	538.8281	539.2106	539.5430	539.5630
5	1168.2270	1171.4130	1042.8690	1042.9530	1043.9400	1041.7426

Table 11. Comparison of Mode Shapes, Coupled Flapwise Bending and Torsion, Fixed-Free

	I Mode			
	IM, 11		TM	
$\bar{x}$	w	ϕ	w	ϕ
0.0	0.0000	0.0000	0.0000	0.0000
0.1	0.0168	0.0040	0.0168	0.0007
0.2	0.0639	0.0081	0.0639	0.0014
0.3	0.1365	0.0121	0.1365	0.0020
0.4	0.2299	0.0159	0.2299	0.0026
0.5	0.3395	0.0195	0.3395	0.0032
0.6	0.4611	0.0227	0.4611	0.0038
0.7	0.5909	0.0255	0.5909	0.0042
0.8	0.7255	0.0276	0.7255	0.0046
0.9	0.8624	0.0290	0.8624	0.0048
1.0	1.0000	0.0295	1.0000	0.0049

	II Mode			
	IM, 11		TM	
$\bar{x}$	w	ϕ	w	ϕ
0.0	0.0000	0.0000	0.0000	0.0000
0.1	-0.0909	-0.1034	-0.0908	-0.0172
0.2	-0.2952	-0.2020	-0.2950	-0.0337
0.3	-0.5152	-0.2872	-0.5149	-0.0479
0.4	-0.6681	-0.3499	-0.6678	-0.0583
0.5	-0.6956	-0.3838	-0.6953	-0.0639
0.6	-0.5712	-0.3874	-0.5710	-0.0646
0.7	-0.3010	-0.3658	-0.3009	-0.0610
0.8	0.0817	-0.3299	0.0817	-0.0550
0.9	0.5297	-0.2950	0.5298	-0.0491
1.0	1.0000	-0.2791	1.0000	-0.0465

Table 11 (Continued)

	III Mode			
	IM, 11		TM	
$\bar{x}$	w	ϕ	w	ϕ
0.0	0.0000	0.0000	0.0000	0.0000
0.1	-0.0015	0.1569	-0.0091	0.1569
0.2	-0.0060	0.3093	-0.0361	0.3093
0.3	-0.0129	0.4534	-0.0772	0.4534
0.4	-0.0207	0.5860	-0.1242	0.5860
0.5	-0.0277	0.7042	-0.1664	0.7042
0.6	-0.0324	0.8057	-0.1946	0.8057
0.7	-0.0340	0.8881	-0.2041	0.8881
0.8	-0.0327	0.9493	-0.1962	0.9493
0.9	-0.0296	0.9871	-0.1772	0.9871
1.0	-0.0257	1.0000	-0.1541	1.0000

	IV Mode			
	IM, 11		TM	
$\bar{x}$	w	ϕ	w	ϕ
0.0	0.0000	0.0000	0.0000	0.0000
0.1	0.2239	0.2815	0.2199	0.0464
0.2	0.5890	0.4727	0.5825	0.0783
0.3	0.7340	0.4606	0.7285	0.0766
0.4	0.5101	0.2059	0.5075	0.0347
0.5	0.0231	-0.2101	0.0230	-0.0342
0.6	-0.4476	-0.6208	-0.4468	-0.1024
0.7	-0.6172	-0.8654	-0.6167	-0.1430
0.8	-0.3572	-0.8819	-0.3566	-0.1455
0.9	0.2484	-0.7474	0.2506	-0.1229
1.0	1.0000	-0.6496	1.0000	-0.1068

Table 12. Comparison of Natural Frequencies, Coupled Flapwise Bending and Torsion, Fixed-Free

$R = 40.0$ in, $b_o = 2.0$ in, $EI_1 = 25{,}000$ Lb-in^2, $GJ = 9{,}000$ Lb-in^2, $e = 0.4$ in, $k^2_{m_1} = 0.18$ in^2, $k^2_{m_2} = 0.71$ in^2, $k^2_A = e_A = e_o = 0$, $\Omega = 60$ Rad/Sec

Mode No.	Frequencies, Rad/Sec					
	IM, 5	IM, 6	IM, 10	IM, 11	IM, 15	TM
1	71.6286	71.5947	71.5857	71.5853	71.5849	71.5842
2	238.5975	242.2124	243.3731	243.3891	243.4048	243.4068
3	396.1727	396.3372	396.4195	396.4211	396.4231	396.4220
4	621.7557	583.8138	591.3070	591.7329	592.1436	592.1875
5	1173.3870	1176.9320	1095.6540	1095.9590	1097.2320	-

Table 13. Comparison of Natural Frequencies, Coupled Flapwise Bending and Torsion, Hinge-Hinge

$R = 40.0$ in, $b_o = 2.0$ in,

$m = 0.0015$ slugs/inch, $e = 0.4$ in,

$GJ = 9{,}000$ Lb-in^2, $EI_1 = 25{,}000$ Lb-in^2

$k^2_{m_1} = 0.18$ in^2, $k^2_{m_2} = 0.71$ in^2 $\Omega = 0.0$

Mode No.	Frequencies, Rad/Sec	
	TM	Exact [21]
1	87.1144	87.1149
2	346.9486	346.9476
3	774.7238	774.4656
4	778.4611	781.0821

Table 14. The Effect of 'e' on Natural Frequencies, Coupled Flapwise Bending and Torsion, Fixed-Free

The data is same as given in Table 13.

Transmission Matrix Approach

Mode No.	Frequencies, Rad/Sec					
	Torsion e = 0	Bending e = 0	e = 0.1	e = 0.2	e = 0.3	3 = 0.4
1		31.0765	31.0753	31.0715	31.0653	31.0566
2		194.7574	194.6918	194.4948	194.1762	193.7456
3	353.2085		355.2697	361.6643	373.0741	390.8779
4		545.3349	544.9474	543.7975	541.9663	539.5630
5		1068.6839	1060.8828	1054.4512	-	1041.7426

Integrating and differentiating matrix method

Mode No.	Frequencies, Rad/Sec					
	e = 0.0		e = 0.1	e = 0.2	e = 0.3	3 = 0.4
	Bending	Torsion				
1	31.0775		31.0762	31.0724	31.0661	31.0573
2	194.7489		194.6824	194.4858	194.1660	193.7364
3		353.2084	355.2713	361.6660	373.0742	390.8782
4	544.9659		544.5774	543.4351	541.6052	539.2106
5	1067.5010		1062.2640	1059.2590	1052.2550	1042.9530

The following data pertain to Table 15.

Data: $R = 40.0$ inches, $m = 0.0015(2-\bar{x})$ slugs/inch,

$GJ = 9{,}000(2-\bar{x})$ Lb-in^2, $EI_1 = 25{,}000(2-\bar{x})$ Lb-in^2,

$e = 0.4(2-\bar{x})$ inches, $k^2_{m_1} = 0.18(2-\bar{x})$ in^2, $k^2_{m_2} = 0.71(2-\bar{x})$ in^2,

$k^2_A = 0$, $e_A = 0$, $e_o = 0$, $b_o = 2.0$ inches

Table 15. Comparison of Natural Frequencies, Coupled Flapwise Bending and Torsion, Fixed-Free

Mode No.	Frequencies, Rad/Sec, $\Omega = 0.0$ Rad/Sec			
	1M, 5	IM, 10	IM, 15	TM
1	38.1066	38.0963	38.0963	38.0954
2	198.4039	204.6921	204.7077	204.7063
3	405.1039	406.0001	406.0171	406.0164
4	565.4224	542.4926	543.1884	543.2036
5	1065.4790	995.7279	998.1369	994.4802

Mode No.	Frequencies, Rad/Sec, $\Omega = 60.0$ Rad/Sec			
	IM, 5	IM, 10	IM, 15	TM
1	75.6448	75.5338	75.5324	75.5317
2	237.7916	243.8943	243.9037	243.9027
3	413.7955	415.1411	415.1513	415.1523
4	594.0282	580.8276	581.5386	581.5135
5	1075.1110	1025.7030	1028.0330	1030.5374

Coupled Flapwise Bending and Chordwise Bending

The numerical results for coupled flapwise bending and chordwise bending were computed using the transmission matrix for a system with the following data

$$\left.\begin{aligned} &R = 40.0 \text{ inches} \\ &x_o = 0.0 \\ &\beta = 45° \\ &m = 0.0015 \text{ slugs/inch} \\ &EI_1 = 25{,}000 \text{ Lb-in}^2 \\ &EI_2 = 75{,}000 \text{ Lb-in}^2 \\ &\Omega = 0.0 \end{aligned}\right\} \qquad (134)$$

The natural frequencies and associated mode shapes are presented in Tables 16 and 17. These results were compared with the exact solutions. The exact solution for the above system can be obtained as follows. Substituting the data given by Equations (134) into the differential equations of motion given by Equations (63) and (64) yields the following relations

$$50{,}000\, w'''' + 25{,}000\, v'''' - 0.0015\omega^2 w = 0 \qquad (135a)$$

$$25{,}000\, w'''' + 50{,}000\, v'''' - 0.0015\omega^2 v = 0 \qquad (135b)$$

Adding the above equations and subtracting the one equation from the another yields

$$75{,}000\ (w'''' + v'''') - 0.0015\ \omega^2 (w + v) = 0 \qquad (136a)$$

$$25{,}000\ (w'''' - v'''') - 0.0015\ \omega^2 (w - v) = 0 \qquad (136b)$$

Making use of the coordinate transformation

$$r = w + v \qquad (137a)$$

$$s = w - v \qquad (137b)$$

Equations (136) become

$$75{,}000\ r'''' - 0.0015\ \omega^2\ r = 0 \qquad (138a)$$

$$25{,}000\ s'''' - 0.0015\ \omega^2\ s = 0 \qquad (138b)$$

Solving for w and v in terms of r and s

$$w = \tfrac{1}{2}(r + s) \quad ; \quad v = \tfrac{1}{2}(r - s)$$

Equations (138) are decoupled set of equations and they are similar to equation of motion governing simple harmonic transverse vibration of a beam with uniform properties. The exact solutions to Equation (138) viz., eigenvalues and eigenfunctions can be obtained. Equations (138) and (135) are equivalent and hence the exact solutions to the system described by Equations (135) are known. The solution to Equation (138a) of the form

$$\omega = \bar{\omega}, \quad r = \bar{r} \quad \text{and} \quad \bar{s} = 0.$$

The solution $\bar{s} = 0$ follows from the fact that Equation (138a) is an uncoupled equation in r, and $\bar{\omega}$ is not an eigenvalue of the uncoupled Equation (138b) in s. Since $\bar{\omega}$ is not an eigenvalue of Equation (138b) the only solution for this equation corresponding to $\omega = \bar{\omega}$ is $s = 0$. Further from Equation (137b) it follows that

$$w = v \tag{139}$$

so the eigenvalues $\omega = \bar{\omega}$ are eigenvalues of the system described by Equations (135) and the corresponding eigenfunctions must be such that they satisfy the relation given by Equation (139).

Again the solution to Equation (138b) is of the form

$$\omega = \bar{\bar{\omega}} \quad , \quad s = \bar{\bar{s}} \quad \text{and} \quad r = 0$$

The relation $r = 0$ can be obtained by following a reasoning similar to that used for the solution of Equation (138a). Further $r = 0$ implies from Equation (137a)

$$w = -v \tag{140}$$

so the eigenvalues $\omega = \bar{\bar{\omega}}$ are eigenvalues of the system described by Equations (135) and the corresponding eigenfunctions must be such that they satisfy the relation given by Equation (140).

When the boundary conditions for the coupled flapwise bending and chordwise bending problem are Hinge-Free, two rigid body modes are possible. If the rotational velocity ($\Omega = 0$) is zero, then $\omega = 0$ is a once repeated eigenvalue and the associated linearly independent modal functions are given by the following equations.

$$\left.\begin{aligned} w(x) &= C_1 x \\ v(x) &= 0 \end{aligned}\right\} \tag{141}$$

and

$$\left.\begin{aligned} w(x) &= 0 \\ v(x) &= C_2 x \end{aligned}\right\} \tag{142}$$

where C_1 and C_2 are arbitrary constants.

If the rotational velocity has a non-zero value ($\Omega \neq 0$) then $\omega = 0$ and $\omega = \Omega$ are both eigenvalues of the system and the associated modal functions are given by the following relations.

Eigenvalue	Modal functions	
$\omega = 0$	$w(x) = 0$, $v(x) = C_3 x$	(143)
$\omega = \Omega$	$w(x) = C_4 x$, $v(x) = 0$	(144)

where C_3 and C_4 are arbitrary constants.

The eigenvalues corresponding to rigid body modes can be obtained and are included in Table 16.

Table 16. Comparison of Natural Frequencies, Coupled Flapwise Bending and Chordwise Bending

Mode No.	Frequencies, Rad/Sec					
	Fixed-Free			Hinge-Free		
	$\Omega = 0$ TM	$\Omega = 0$ Exact	Ω =60.0 Rad/Sec TM	$\Omega = 0$ TM	$\Omega = 0$ Exact	Ω=60 Rad/Sec TM
1	31.0775	31.0740	47.6325	0.0000	0.0000	0.0000
2	53.8277	53.8218	79.9485	0.0000	0.0000	60.0000
3	194.7594	194.7517	243.7269	136.2790	136.3036	198.7602
4	337.3333	337.3198	367.9180	236.0422	236.0899	277.4052
5	545.3369	545.3652	599.6112	441.6340	441.6833	507.1379
6	944.5513	944.6002	977.0149	764.9326	765.0179	804.7467
7				921.4544	921.4282	

Table 17. Mode Shapes, Coupled Flapwise Bending and Chordwise Bending, Fixed-Free

$\bar{x}$	I Mode		II Mode	
	w	v	w	v
0.0	0.0000	0.0000	0.0000	0.0000
0.1	-0.0168	0.0168	0.0168	0.0168
0.2	-0.0639	0.0639	0.0639	0.0639
0.3	-0.1365	0.1365	0.1365	0.1365
0.4	-0.2299	0.2299	0.2699	0.2699
0.5	-0.3395	0.3395	0.3395	0.3395
0.6	-0.4611	0.4611	0.4611	0.4611
0.7	-0.5909	0.5909	0.5909	0.5909
0.8	-0.7255	0.7255	0.7255	0.7255
0.9	-0.8624	0.8624	0.8624	0.8624
1.0	-1.0000	1.0000	1.0000	1.0000

$\bar{x}$	III Mode		IV Mode	
	w	v	w	v
0.0	0.0000	0.0000	0.0000	0.0000
0.1	0.0926	-0.0926	-0.0926	-0.0926
0.2	0.3011	-0.3011	-0.3011	-0.3011
0.3	0.5261	-0.5261	-0.5261	-0.5261
0.4	0.6835	-0.6835	-0.6835	-0.6835
0.5	0.7137	-0.7137	-0.7137	-0.7137
0.6	0.5895	-0.5895	-0.5895	-0.5895
0.7	0.3171	-0.3171	-0.3171	-0.3171
0.8	-0.0700	0.0700	0.0700	0.0700
0.9	-0.5238	0.5238	0.5238	0.5238
1.0	-1.0000	1.0000	1.0000	1.0000

The natural frequencies were computed using the transmission matrix for the system with the following non-uniform properties. The results are presented in Table 18 and are compared with the experimental and analytical results of Reference 9.

Data: x_o = 6.0 inches

R = 18.0 inches

x inches	m Lb-Sec^2/in^2	EI_1 Lb-in^2	EI_2 Lb-in^2	β deg
0.0	1.026×10^{-3}	0.200×10^6	63×10^6	30.5
2.0	0.696	0.110	49	25.2
4.0	0.660	0.083	46	20.0
6.0	0.608	0.058	44	14.8
8.0	0.564	0.042	43	9.6
10.0	0.535	0.031	43	4.7
12.0	0.520	0.027	44	0
14.0	0.506	0.026	47	-4.2
16.0	0.498	0.025	51	-7.6
18.0	0.498	0.024	56	-10.0

Table 18. Comparison of Natural Frequencies, Coupled Flapwise Bending and Chordwise Bending, Fixed-Free

Mode No.	Ω RPM	ω, Hz		
		TM	Expt [9]	IM [9]
1	1567	40.9617	40.08	40.77
2		109.2179	-	-
3		279.7851	-	-
1	1589	41.3525	-	-
2		109.7746	107.53	109.05
3		280.4674	-	-
1	2609	60.0708	58.73	59.85
2		139.5231	-	-
3		309.4012	-	-
1	2614	60.1640	-	-
2		139.6827	137.02	139.03
3		319.6220	-	-
1	3583	78.3389	76.52	78.08

Coupled Flapwise Bending, Chordwise Bending and Torsion

The natural frequencies and mode shapes for coupled flapwise bending, chordwise bending and torsion were computed using the transmission matrix for a system with the following properties.

$$
\left.
\begin{aligned}
&R = 40.0 \text{ in} \\
&\beta = 45^\circ \\
&EI_1 = 25{,}000 \text{ Lb-in}^2 \\
&EI_2 = 75{,}000 \text{ Lb-in}^2 \\
&GJ = 9{,}000 \text{ Lb-in}^2 \\
&m = 0.0015 \text{ slugs/inch} \\
&k_{m_1}^2 = 1.0 \text{ in}^2 \\
&k_{m_2}^2 = 1.0 \text{ in}^2 \\
&e = \sqrt{2} \text{ in} \\
&b_o = 2.0 \text{ in} \\
&B_1 = B_2 = e_A = e_o = k_A = \Omega = 0
\end{aligned}
\right\} \qquad (145)
$$

The natural frequencies and the associated mode shapes are presented in Tables 19 and 20. These results were compared with the exact solutions and the solutions obtained by an equivalent coupled flapwise bending and torsion problem. The exact solutions and the equivalent coupled flapwise bending and torsion problem can be obtained as follows.

Substitute the data given by Equations (145) into the governing equations of motion given by Equations (59), (60) and (61). This yields the following equations.

$$-9000\ \phi'' - 0.003\ \omega^2\phi + 0.0015\ \omega^2(v - w) = 0 \qquad (146a)$$

$$50{,}000\ w'''' + 25{,}000\ v'''' - 0.0015\ \omega^2(w + \phi) = 0 \qquad (146b)$$

$$25{,}000\ w'''' + 50{,}000\ v'''' - 0.0015\ \omega^2(v - \phi) = 0 \qquad (146c)$$

Adding Equations (146b) and (146c) yields

$$75{,}000\ (w'''' + v'''') - 0.0015\ \omega^2(w + v) = 0 \qquad (147a)$$

Subtracting Equation (146c) from Equation (146b) yields

$$25{,}000(w'''' - v'''') - 0.0015\ \omega^2(w - v) - 0.003\ \omega^2\phi = 0 \qquad (147b)$$

Making use of the co-ordinate transformation given by Equations (137), Equations (146) become

$$9000\ \phi'' + 0.003\ \omega^2\phi + 0.0015\ \omega^2 s = 0 \qquad (148a)$$

$$25{,}000\ s'''' - 0.0015\ \omega^2 s - 0.003\ \omega^2\phi = 0 \qquad (148b)$$

$$75{,}000\ r'''' - 0.0015\ \omega^2 r = 0 \qquad (148c)$$

Equation (148c) is a decoupled equation and is similar to equation of motion governing simple harmonic transverse vibration of a beam with uniform properties. The exact solution to Equation (148c) viz., eigenvalues and eigenfunctions can be obtained. The solution to this equation is

of the form

$$\omega = \bar{\omega} \ , \ r = \bar{r} \ , \ \phi = 0 \text{ and } \bar{s} = 0$$

The solution $\bar{s} = 0$, and $\phi = 0$ follows from the fact that Equation (148c) is an uncoupled equation in r, and $\bar{\omega}$ is not an eigenvalue of the coupled Equations (148a) and (148b). The relation s = 0 implies from Equation (137b)

$$v = w \tag{149}$$

so the eigenvalues $\omega = \bar{\omega}$ are eigenvalues of the system described by Equations (146) and the corresponding eigenfunctions must be such that they satisfy the relation given by Equation (149).

Equations (148a) and (148b) can be written as

$$4{,}500 \ \phi'' + 0.0015 \ \omega^2 \ (\frac{s}{2} + \phi) = 0 \tag{150a}$$

$$25{,}000 \ \frac{s''''}{2} - 0.0015 \ \omega^2 \ (\frac{s}{2} + \phi) = 0 \tag{150b}$$

The solution to Equations (150) is of the form

$$\omega = \bar{\bar{\omega}} \ , \ s = \bar{\bar{s}}, \ \phi = \bar{\bar{\phi}} \text{ and } r = 0$$

The relation r = 0 implies from Equations (137)

$$v = -w \tag{151a}$$

$$s/2 = w \tag{151b}$$

Substituting Equation (151b) into Equations (150) gives

$$4{,}500\ \phi'' + 0.0015\ \omega^2(\phi + w) = 0 \tag{152a}$$

$$25{,}000\ w'''' - 0.0015\ \omega^2(\phi + w) = 0 \tag{152b}$$

The above system of Equations are equivalent to a coupled flapwise bending and torsion problem with the following data

$$\left.\begin{aligned} &R = 40.0 \text{ in} \\ &EI_1 = 25{,}000 \text{ Lb-in}^2 \\ &GJ = 4{,}500 \text{ Lb-in}^2 \\ &m = 0.0015 \text{ slugs/in} \\ &k_{m_1}^2 = 0.5 \text{ in}^2 \\ &k_{m_2}^2 = 0.5 \text{ in}^2 \\ &e = 1.0 \text{ in} \\ &k_A = \Omega = 0 \end{aligned}\right\} \tag{153}$$

If w and ϕ represent the mode shapes of coupled flapwise bending and torsion for the equivalent system then the original system mode shapes must be such that v = -w. The system given by Equations (146) and the system described by Equations (148c) and (152) are equivalent. Hence the solutions to Equations (148c) and (152) form a complete set of solutions to original system described by Equations (146).

The orthogonality relation for coupled flapwise bending, chordwise bending and torsion is derived in Appendix B and is given by the following equations.

$$\int_o^R m[k_m^2 \phi_r\phi_s + w_r w_s + v_r v_s - e \sin\beta(\phi_r v_s + \phi_s v_r) + e \cos\beta(\phi_r w_s + \phi_s w_r)]\, dx = 0, \quad r \neq s \tag{154}$$

$$\int_o^R m[k_m^2 \phi_r^2 + w_r^2 + v_r^2 - 2e \sin\beta\phi_r v_r + 2e \cos\beta\phi_r w_r]dx = M_r$$

orthogonality was checked between the natural modes presented in Table 20. For verification of orthogonality between the natural modes, deflections at 50 equally spaced stations were used. The numerical values of M_{r_s} (r,s = 1,5) are given in Table 21. The effect of Ω and e on the natural frequencies was studied and the results are presented in Tables 22 and 23. The data of the system considered is given below.

R = 40.0 in

b_o = 2.0 in

β = 45°

EI_1 = 25,000 Lb-in^2

EI_2 = 75,000 Lb-in^2

GJ = 9,000 Lb-in^2

m = 0.0015 slugs/in

$k_{m_1}^2$ = 0.18 in^2

Table 19. Comparison of Natural Frequencies, Coupled Flapwise Bending, Chordwise Bending and Torsion, Fixed-Free

Mode No.	Frequencies, Rad/Sec			Nature of Mode Shapes
	TM	Exact	Equivalent System	
1	30.8295		30.8274	v = -w
2	53.8277	53.8218		v=w, ϕ=0
3	184.6175		184.6150	v = -w
4	337.3333	337.3198		v=w, ϕ=0
5	484.3373		484.3266	v = -w

Table 20. Mode Shapes, Coupled Flapwise Bending, Chordwise Bending and Torsion, Fixed-Free

	I Mode			II Mode		
$\bar{x}$	w	v	ϕ	w	v	ϕ
0.0	0.0000	0.0000	0.0000	0.0000	0.0000	0.0000
0.1	-0.0168	0.0168	-0.0034	0.0168	0.0168	0.0000
0.2	-0.0639	0.0639	-0.0067	0.0639	0.0639	0.0000
0.3	-0.1366	0.1366	-0.0100	0.1365	0.1365	0.0000
0.4	-0.2300	0.2300	-0.0132	0.2299	0.2299	0.0000
0.5	-0.3396	0.3396	-0.0162	0.3395	0.3395	0.0000
0.6	-0.4612	0.4612	-0.0188	0.4611	0.4611	0.0000
0.7	-0.5910	0.5910	-0.0211	0.5909	0.5909	0.0000
0.8	-0.7255	0.7255	-0.0229	0.7255	0.7255	0.0000
0.9	-0.8624	0.8624	-0.0240	0.8624	0.8624	0.0000
1.0	-1.0000	1.0000	-0.0244	1.0000	1.0000	0.0000

	III Mode			IV Mode		
$\bar{x}$	w	v	ϕ	w	v	ϕ
0.0	0.0000	0.0000	0.0000	0.0000	0.0000	0.0000
0.1	0.0783	-0.0783	0.0639	-0.0926	-0.0926	0.0000
0.2	0.2526	-0.2526	0.1242	-0.3011	-0.3011	0.0000
0.3	0.4366	-0.4366	0.1750	-0.5261	-0.5261	0.0000
0.4	0.5581	-0.5581	0.2101	-0.6835	-0.6835	0.0000
0.5	0.5670	-0.5670	0.2253	-0.7137	-0.7137	0.0000
0.6	0.4414	-0.4414	0.2204	-0.5895	-0.5895	0.0000
0.7	0.1878	-0.1878	0.1991	-0.3171	-0.3171	0.0000
0.8	-0.1640	0.1640	0.1694	0.0700	0.0700	0.0000
0.9	-0.5724	0.5724	0.1422	0.5238	0.5238	0.0000
1.0	-1.0000	1.0000	0.1322	1.0000	1.0000	0.0000

Table 21. Orthogonality of Natural Modes, Coupled Flapwise Bending, Chordwise Bending and Torsion, Fixed-Free

s \ r	1	2	3	4	5
1	0.5164	0.3848×10^{-5}	-0.2203×10^{-6}	-0.8462×10^{-6}	-0.1685×10^{-5}
2	0.3848×10^{-5}	0.5000	-0.2042×10^{-7}	0.5465×10^{-6}	0.2602×10^{-5}
3	-0.2165×10^{-6}	-0.2047×10^{-7}	0.4604	-0.1158×10^{-5}	-0.1414×10^{-5}
4	-0.8462×10^{-6}	0.5465×10^{-6}	-0.1158×10^{-5}	0.5000	0.3304×10^{-5}
5	-0.1679×10^{-5}	0.2602×10^{-5}	-0.1414×10^{-5}	0.3305×10^{-5}	0.8111

$$k_{m_2}^2 = 0.71 \text{ in}^2$$

$$e_A = k_A^2 = e_o = 0$$

The effect of collective pitch on the natural frequencies and mode shapes was studied for the blade with the following data and the results are tabulated in Tables 24 to 26.

Data:

x	m	EI_1	EI_2	GJ
in	slugs/in	Lb-in^2	Lb-in^2	Lb-in^2
0.0	1.2312×10^{-2}	0.200×10^6	63×10^6	0.9×10^4
2.0	0.8352	0.110	49	0.9
4.0	0.7920	0.083	46	0.9
6.0	0.7296	0.058	44	0.9
8.0	0.6768	0.042	43	0.9
10.0	0.6420	0.031	43	0.9
12.0	0.6240	0.027	44	0.9
14.0	0.6072	0.026	47	0.9
16.0	0.5976	0.025	51	0.9
18.0	0.5976	0.024	56	0.9

x	e	k_{m_1}	k_{m_2}	β
in	in			deg
0.0	0.4	0.18	0.71	30.5
2.0	0.4	0.18	0.71	25.2
4.0	0.4	0.18	0.18	20.0
6.0	0.4	0.18	0.71	14.8
8.0	0.4	0.18	0.71	9.6
10.0	0.4	0.18	0.71	4.7
12.0	0.4	0.18	0.71	0
14.0	0.4	0.18	0.18	-4.2
16.0	0.4	0.18	0.71	-7.6
18.0	0.4	0.18	0.71	-10.0

Table 22. The Effect of Rotational Velocity on Natural Frequencies, Coupled Flapwise Bending, Chordwise Bending and Torsion, Fixed-Free

Mode No.	Frequencies, Rad/Sec; e = 0.4 in						Nature of Mode Shape
	Ω=0.0 Rad/Sec	Ω=30.0 Rad/Sec	Ω=60.0 Rad/Sec	Ω=90.0 Rad/Sec	Ω=130.0 Rad/Sec	Ω=150.0 Rad/Sec	
1	31.0584	41.3281	52.6219	59.5278	65.7668	71.8132	Flapwise Bending
2	53.8190	58.1973	76.7514	103.8823	132.8339	162.3355	Chordwise Bending
3	193.7445	207.1084	241.4782	284.3316	319.8837	336.3856	Flapwise Bending
4	337.3339	344.8945	366.6794	399.9802	425.0262	467.7667	Chordwise Bending
5	390.8759	391.7929	395.0279	403.8684	444.0840	494.8650	Torsion

Table 23. The Effect of 'e' on Natural Frequencies, Coupled Flapwise Bending, Chordwise Bending and Torsion, Fixed-Free

Mode No.	Frequencies, Rad/Sec, $\Omega = 0$						Nature of Mode Shape
	e = 0 in	e = 0.2 in	e = 0.4 in	e = 0.6 in	e = 0.8 in	e = 1.0 in	
1	31.0775	31.0738	31.0584	31.0329	30.9974	30.9537	Flapwise Bending
2	53.8277	53.8191	53.8190	53.8190	53.8190	53.8190	Chordwise Bending
3	194.7594	194.4935	193.7445	192.6047	191.1869	189.5765	Flapwise Bending
4	337.3333	337.3389	337.3339	337.3319	337.3306	337.3298	Chordwise Bending
5	353.2085	361.6539	390.8759	458.4458	-	-	Torsion

Table 24. The Effect of Collective Pitch on Natural Frequencies, Non-rotating Blade, Coupled Flapwise Bending, Chordwise Bending and Torsion, Fixed-Free

Mode No.	Frequencies, Rad/Sec, $\Omega = 0$		
	Collective Pitch = 0 deg	Collective Pitch = 15 deg	Collective Pitch = 30 deg
1	21.8304	21.8303	21.8303
2	70.7422	70.7422	70.7422
3	86.3694	86.3693	86.3692
4	198.3834	198.3834	198.3834

Table 25. The Effect of Collective Pitch on Natural Frequencies, Rotating Blade, Coupled Flapwise Bending, Chordwise Bending and Torsion, Fixed-Free

Mode No.	Frequencies, Rad/Sec, Ω = 160.0 Rad/Sec					
	CP = 0°	CP=15°	CP=20°	CP=30°	CP=45°	CP=60°
1	35.5875	33.6161	32.7959	31.0337	28.4729	26.6919
2	70.2060	69.8182	69.5587	68.8853	67.6428	66.4174
3	102.1790	102.1691	102.1354	102.0272	101.7879	101.5204
4	198.9166	198.7310	198.6310	198.3917	197.9886	197.6305

Mode No.	Frequencies, Rad/Sec, Ω = 160.0 Rad/Sec				
	CP=75°	CP=-15°	CP=-30°	CP=-45°	CP=-60°
1	26.3260	36.5254	36.2417	34.7930	32.4767
2	65.5464	69.9535	69.1237	67.9246	66.6672
3	101.3034	102.0620	101.8591	101.6091	101.3825
4	197.4128	198.8993	198.6835	198.3264	197.9230

Table 26. The Effect of Collective Pitch on Mode Shapes, Coupled Flapwise Bending, Chordwise Bending and Torsion, Fixed-Free

	I Mode w, Ω = 160.0 Rad/Sec					
$\bar{x}$	β = 0°	β = 15°	β = 30°	β = 45°	β = 60°	β = 75°
0.0	0.0000	0.0000	0.0000	0.0000	0.0000	0.0000
0.1	0.0107	0.0103	-0.0082	-0.0036	-0.0002	0.0026
0.2	0.0462	0.0450	-0.0365	-0.0170	-0.0024	0.0096
0.3	0.1069	0.1050	-0.0865	-0.0420	-0.0087	0.0194
0.4	0.1917	0.1893	-0.1582	-0.0797	-0.0206	0.0297
0.5	0.2980	0.2957	-0.2502	-0.1301	-0.0393	0.0387
0.6	0.4223	0.4204	-0.3594	-0.1920	-0.0650	0.0452
0.7	0.5595	0.5581	-0.4811	-0.2625	-0.0966	0.0489
0.8	0.7039	0.7030	-0.6099	-0.3384	-0.1321	0.0502
0.9	0.8516	0.8511	-0.7418	-0.4116	-0.1694	0.0502
1.0	1.0000	1.0000	-0.8744	-0.4953	-0.2073	0.0498

	I Mode v, Ω = 160.0 Rad/Sec					
$\bar{x}$	β = 0°	β = 15°	β = 30°	β = 45°	β = 60°	β = 75°
0.0	0.0000	0.0000	0.0000	0.0000	0.0000	0.0000
0.1	-0.0059	-0.0099	0.0136	0.0126	0.0115	0.0104
0.2	-0.0237	-0.0408	0.0567	0.0530	0.0491	0.0450
0.3	-0.0513	-0.0902	0.1267	0.1197	0.1122	0.1044
0.4	-0.0860	-0.1545	0.2196	0.2098	0.1991	0.1876
0.5	-0.1252	-0.2300	0.3307	0.3193	0.3066	0.2928
0.6	-0.1667	-0.3130	0.4550	0.4426	0.4308	0.4167
0.7	-0.2090	-0.4003	0.5874	0.5778	0.5667	0.5543
0.8	-0.2511	-0.4895	0.7239	0.7170	0.7091	0.7001
0.9	-0.2930	-0.5792	0.8618	0.8583	0.8542	0.8496
1.0	-0.3348	-0.6691	1.0000	1.0000	1.0000	1.0000

Table 26 (Continued)

	I Mode ϕ, Ω = 160.0 Rad/Sec					
$\bar{x}$	β = 0°	β = 15°	β = 30°	β = 45°	β = 60°	β = 75°
0.0	0.0000	0.0000	0.0000	0.0000	0.0000	0.0000
0.1	0.0039	0.0037	-0.0039	-0.0038	-0.0043	-0.0053
0.2	0.0078	0.0073	-0.0078	-0.0075	-0.0086	-0.0106
0.3	0.0116	0.0108	-0.0116	-0.0112	-0.0129	-0.0159
0.4	0.0153	0.0143	-0.0152	-0.0148	-0.0170	-0.0211
0.5	0.0188	0.0176	-0.0187	-0.0182	-0.0210	-0.0260
0.6	0.0222	0.0207	-0.0220	-0.0213	-0.0247	-0.0306
0.7	0.0252	0.0234	-0.0249	-0.0242	-0.0280	-0.0347
0.8	0.0278	0.0257	-0.0273	-0.0265	-0.0308	-0.0382
0.9	0.0296	0.0274	-0.0290	-0.0282	-0.0327	-0.0407
1.0	0.0302	0.0280	-0.0297	-0.0288	-0.0334	-0.0416

	II Mode ϕ, Ω = 160.0 Rad/Sec					
$\bar{x}$	β = 0°	β = 15°	β = 30°	β = 45°	β = 60°	β = 75°
0.0	0.0000	0.0000	0.0000	0.0000	0.0000	0.0000
0.1	0.1675	0.1685	0.1690	0.1691	0.1687	0.1678
0.2	0.3287	0.3304	0.3315	0.3316	0.3309	0.3294
0.3	0.4826	0.4849	0.4865	0.4869	0.4861	0.4842
0.4	0.6213	0.6239	0.6258	0.6265	0.6257	0.6238
0.5	0.7391	0.7416	0.7435	0.7442	0.7436	0.7418
0.6	0.8335	0.8356	0.8371	0.8377	0.8372	0.8357
0.7	0.9023	0.9037	0.9046	0.9048	0.9043	0.9032
0.8	0.9526	0.9534	0.9538	0.9538	0.9534	0.9526
0.9	0.9880	0.9882	0.9884	0.9884	0.9882	0.9880
1.0	1.0000	1.0000	1.0000	1.0000	1.0000	1.0000

Table 26 (Continued)

$\bar{x}$	II Mode w, Ω = 160.0 Rad/Sec					
	β = 0°	β = 15°	β = 30°	β = 45°	β = 60°	β = 75°
0.0	0.0000	0.0000	0.0000	0.0000	0.0000	0.0000
0.1	0.0013	0.0011	0.0009	0.0005	0.0000	-0.0004
0.2	0.0041	0.0038	0.0029	0.0017	0.0002	-0.0011
0.3	0.0055	0.0052	0.0041	0.0023	0.0001	-0.0018
0.4	0.0008	0.0011	0.0008	-0.0003	-0.0015	-0.0024
0.5	-0.0160	-0.0141	-0.0121	-0.0100	-0.0073	-0.0038
0.6	-0.0516	-0.0473	-0.0406	-0.0318	-0.0208	-0.0080
0.7	-0.1105	-0.1030	-0.0893	-0.0698	-0.0454	-0.0173
0.8	-0.1925	-0.1814	-0.1586	-0.1250	-0.0823	-0.0332
0.9	-0.2929	-0.2780	-0.2447	-0.1944	-0.1298	-0.0554
1.0	-0.4035	-0.3848	-0.3405	-0.2721	-0.1838	-0.0816

$\bar{x}$	II Mode v, Ω = 160.0 Rad/Sec					
	β = 0°	β = 15°	β = 30°	β = 45°	β = 60°	β = 75°
0.0	0.0000	0.0000	0.0000	0.0000	0.0000	0.0000
0.1	-0.0007	-0.0011	-0.0014	-0.0016	-0.0017	-0.0015
0.2	-0.0021	-0.0035	-0.0046	-0.0054	-0.0055	-0.0051
0.3	-0.0031	-0.0050	-0.0068	-0.0079	-0.0080	-0.0072
0.4	-0.0023	-0.0033	-0.0044	-0.0048	-0.0042	-0.0028
0.5	+0.0009	0.0039	0.0065	0.0090	0.0117	0.0141
0.6	0.0063	0.0183	0.0290	0.0382	0.0456	0.0505
0.7	0.0129	0.0400	0.0646	0.0854	0.1011	0.1104
0.8	0.0190	0.0672	0.1114	0.1489	0.1769	0.1930
0.9	0.0236	0.0977	0.1662	0.2246	0.2681	0.2933
1.0	0.0269	0.1296	0.2251	0.3066	0.3677	0.4033

Table 26 (Continued)

	III Mode w, Ω = 160.0 Rad/Sec					
$\bar{x}$	β = 0°	β = 15°	β = 30°	β = 45°	β = 60°	β = 75°
0.0	0.0000	0.0000	0.0000	0.0000	0.0000	0.0000
0.1	-0.0404	-0.0298	-0.0207	-0.0115	-0.0006	-0.0141
0.2	-0.1570	-0.1171	-0.0828	-0.0480	-0.0068	-0.0491
0.3	-0.3168	-0.2377	-0.1697	-0.1009	-0.0194	-0.0919
0.4	-0.4686	-0.3514	-0.2510	-0.1494	-0.0289	-0.1362
0.5	-0.5493	-0.4061	-0.2839	-0.1604	-0.0137	-0.1873
0.6	-0.4971	-0.3486	-0.2224	-0.0951	0.0562	-0.2622
0.7	-0.2806	-0.1501	-0.0394	0.0719	0.2044	-0.3809
0.8	+0.0789	0.1735	0.2535	0.3338	0.4294	-0.5492
0.9	0.5251	0.5739	0.6151	0.6565	0.7057	-0.7540
1.0	1.0000	1.0000	1.0000	1.0000	1.0000	-0.9723

	III Mode v					
$\bar{x}$	β = 0°	β = 15°	β = 30°	β = 45°	β = 60°	β = 75°
0.0	0.0000	0.0000	0.0000	0.0000	0.0000	0.0000
0.1	0.0226	0.0291	0.0349	0.0408	0.0478	-0.0556
0.2	0.0831	0.1088	0.1319	0.1557	0.1836	-0.2153
0.3	0.1616	0.2142	0.2615	0.3106	0.3682	-0.4339
0.4	0.2392	0.3168	0.3868	0.4598	0.5458	-0.6442
0.5	0.3035	0.3912	0.4707	0.5543	0.6534	-0.7662
0.6	0.3521	0.4209	0.4842	0.5521	0.6337	-0.7240
0.7	0.3930	0.4056	0.4197	0.4381	0.4623	-0.4816
0.8	0.4367	0.3594	0.2946	0.2329	0.1638	-0.0673
0.9	0.4873	0.2990	0.1368	-0.0242	-0.2091	0.4496
1.0	0.5415	0.2351	-0.0308	-0.2974	-0.6060	1.0000

Table 26 (Continued)

	III Mode ϕ, Ω = 160.0 Rad/Sec					
$\bar{x}$	β = 0°	β = 15°	β = 30°	β = 45°	β = 60°	β = 75°
0.0	0.0000	0.0000	0.0000	0.0000	0.0000	0.0000
0.1	0.0200	0.0190	0.0191	0.0201	0.0222	-0.0255
0.2	0.0423	+0.0400	0.0402	0.0423	0.0468	-0.0540
0.3	0.0752	0.0707	0.0708	0.0746	0.0828	-0.0962
0.4	0.1263	0.1178	0.1175	0.1238	0.1381	-0.1617
0.5	0.2003	0.1854	0.1843	0.1943	0.2176	-0.2566
0.6	0.2970	0.2735	0.2710	0.2858	0.3211	-0.3808
0.7	0.4076	0.3738	0.3696	0.3898	0.4390	-0.5225
0.8	0.5229	0.4782	0.4722	0.4982	0.5621	-0.6710
0.9	0.6217	0.5676	0.5602	0.5913	0.6682	-0.7991
1.0	0.6622	0.6042	0.5961	0.6293	0.7115	-0.8516

Discussion of Results

It can be observed from the comparisons made in the previous tables that the transmission matrix approach yields extremely accurate results for natural frequencies and associated modal functions for coupled flapwise bending, chordwise bending and torsion and five of its subcases. Furthermore it can be observed from Table 21 that the transmission approach gives good orthogonality of natural modes defined by the differential equations of motion. In Tables 1 and 2 natural frequencies obtained by the transmission matrix approach for a pure torsion problem were given. These solutions were compared with the exact solutions and it can be observed from these comparisons that the transmission matrix gives almost exact solutions in the case of pure torsion.

In Tables 3 to 5 comparisons were made between the results obtained by the transmission matrix approach and the integrating matrix method for flapwise bending problem with fixed-free end conditions. It can be observed from Table 3 that the first four natural frequencies obtained by the integrating matrix method with 15 stations are very accurate and are identical up to 4 significant digits with the exact solutions and the solutions obtained by the transmission matrix approach. The fifth natural frequency agrees up to four significant digits with the exact and transmission matrix solution, when 20 stations are used in the integrating

matrix method of solution. As is expected it can be observed from Table 3 that the accuracy improves with increasing the number of stations. Results for a rotating blade are presented in Table 5 and are quite similar to the non-rotating case.

Natural mode deflections obtained by both the transmission and integrating matrices are presented in Table 4. It can be observed from this table that the integrating matrix using six stations gives very accurate mode deflections for the first two natural modes, eleven stations gives moderately accurate solutions for third and fourth modes. For higher modes more stations are required; for example, for the fifth mode, twenty six stations give very accurate solutions.

The Fortran program written for the integrating matrix method of solution for the flapwise bending problem with fixed-free end conditions requires a memory of 31,071 words decimal. The Fortran program written for transmission matrix approach for flapwise bending problem which can take care of both fixed-free and hinge-free boundary conditions requires a memory of only 11,531 words decimal. So the transmission matrix approach requires appreciably less memory than the integrating matrix method for numerical computation on a digital computer.

On the UNIVAC 1108 computer, the time for actual solution of 5 natural frequencies and the associated natural

modes shapes for both methods are given below [for results shown in Tables 3 and 4]

IM 6 Stations	IM 11 Stations	IM 26 Stations	TM
380 MLSEC	656 MLSEC	4,356 MLSEC	29,857 MLSEC

It can be observed from Tables 3 and 4 that the integrating matrix solution with 26 stations and the transmission matrix approach give almost identical accuracy. So the integrating matrix method is much faster than the transmission matrix method for computation on a digital computer.

Because of the method of solution (QR-transformation) for the eigenvalue problem yielded by the integrating matrix method, all the eigenvalues of the problem were obtained simultaneously even though only a few of them are normally required. The eigenvectors can be obtained corresponding to any individual eigenvalue separately. In the transmission matrix approach only the required number of eigenvalues need be computed. The number of ordinates available for any natural mode computed by the transmission matrix approach is determined by the number of steps used in integrating the differential equations governing the elements of the transmission matrix. The numerical integration scheme used normally determines the step size of the integration (In the present case 50 steps are used), where as in the integration matrix method the number of ordinates available is equal to

number of stations used. In the case of the flapwise bending problem the order of the eigenvalue problem is equal to the number of stations.

The natural frequencies for the flapwise bending problem with hinge-free end conditions computed by the transmission matrix approach are shown in Table 6. The first five natural frequencies of the non-rotating blade were compared with the exact frequencies and all of them agree up to the first three significant digits. Rotating system frequencies were compared with the solutions obtained by Galerkin's method. As mentioned in Chapter IV, the integrating matrix method can not be applied to hinge-free systems since the method fails when the system has rigid body degrees of freedom. In Tables 7 and 8 the natural frequencies and the associated natural mode shapes for non-uniform rotating blade as computed by the transmission matrix for flapwise bending are given. These results were compared with the results obtained by the finite difference technique in Reference 20. In this case also the agreement is quite good.

In Table 9 the natural frequencies for chordwise bending are given for non-rotating and rotating blades. They are compared with the flapwise bending frequencies of a rotating blade. It can be observed from this table for a hinge-free system that $\omega = 0$ corresponds to a rigid body mode for chordwise bending and $\omega = \Omega$ corresponds to a rigid body

mode for flapwise bending. Furthermore it can be observed that the effect of centrifugal force is more predominant on flapwise bending frequencies than on the chordwise bending frequencies. For higher modes it can be observed that this difference in the effect of centrifugal force is less predominant.

Natural frequencies for a uniform blade with hinge-hinge boundary conditions were computed using the transmission matrix for coupled flapwise bending and torsion. The results are presented in Table 13 and are compared with the exact solutions. It can be observed from this table that the first three natural frequencies agree up to three significant digits and the percentage error of the fourth frequency is 0.335.

In Tables 10 to 12 and 15 comparisons are made between the results obtained by the transmission matrix approach and the integrating and differentiating matrix method for flapwise bending and torsion. It can be observed from Tables 10, 12 and 15 that the integrating and differentiating matrix method with 10 stations gives accurate results and are in good agreement with the results obtained by the transmission matrix. Further it can be observed from these tables that the accuracy of the frequencies increases with the increasing number of stations and approach the solutions obtained by the transmission matrix method. In Table

11 comparisons are made between the mode shapes obtained by both the methods. The first two natural modes presented in Table 11 are predominantly flapwise bending modes, and it can be observed from this table that flapwise bending deflections given by both methods are in good agreement. However the torsional deflections obtained by the two methods differ significantly. The third natural mode is predominantly a torsional mode and torsional deflections are in good agreement but the flapwise deflections differ significantly. For predominant bending, the integrating matrix method gives higher values for ϕ, and for predominant torsion the integrating matrix method gives smaller values for w. The integrating method gives a non-self adjoint eigenvalue problem and as such the eigenvectors need not be orthogonal. The transmission matrix method gives natural modes which are orthogonal. Furthermore it is a straight forward matter to obtain the natural modes ofter obtaining the natural frequencies using the transmission matrix approach. So the integrating matrix method gives an accurate predominant deflection mode but not the nonsignificant deflection. In the case of uncoupled problems, for example, flapwise bending, as mentioned earlier the integrating matrix method does give accurate mode shapes. The difference in the application of the integrating matrix method to flapwise bending problem and the coupled flapwise bending and torsion is that in the case of the latter problem the differentiating

matrix needs to be introduced. However, for non-rotating blade the differentiating matrix is eliminated. Since the results presented in Table 11 correspond to non-rotating blade the discrepancies in nonsignificant deflection are not due to use of the differentiating matrix. Further investigations are necessary to pindown why these discrepancies are coming using the integrating matrix method.

The Fortran program written for the integrating matrix method of solution for coupled flapwise bending and torsion with fixed-free end conditions requires a memory of 33,179 words decimal. The Fortran program written for the transmission matrix approach for the coupled flapwise bending and torsion problem which can take care of both fixed-free and hinge-free boundary conditions requires a memory of 14,860 words decimal. On the UNIVAC 1108 computer, time for actual solution of 5 natural frequencies and the associated modes shapes for both methods are given below.

IM 6 Stations	IM 11 Stations	TM
696 MLSEC	2,484 MLSEC	25,630 MLSEC

So as in the case of the flapwise bending problem, the integrating matrix method is in this case faster than the transmission matrix approach for computation on a digital computer but requires more memory than the transmission matrix approach.

All other remarks made in connection with the flapwise bending problem comparing the two methods are also applicable here, except in this case the order of the eigenvalue problem is twice the number of stations used. Some times the comparison between the time required for actual computation for both the methods is misleading since in the case of the transmission matrix approach the time of computation is mainly dependent on the interval of frequency scanning. For example, by doubling the interval of frequency scanning the time of actual computation can be cut down by half. If any two frequencies are close smaller interval for frequency scanning is required. But this scanning procedure guarantees the detection of all frequencies provided that they are separated at least by the interval of frequency scanning used.

By varying the 'e' the natural frequencies were computed and are given in Table 14. From this table it can be observed that the effect of 'e' is not significant on the natural frequencies associated with predominantly flapwise bending. The effect is significant on the natural frequencies associated with predominantly torsional modes. Further it is observed that the effect is insignificant on mode shapes whether they are predominantly torsion or bending.

In Tables 16 and 17 the natural frequencies and mode shapes as computed by the transmission matrix approach for coupled chordwise bending and flapwise bending are presented.

The results corresponding to a non-rotating blade were compared with the exact solutions and the agreement can be observed to be good. The exact solutions were obtained and the corresponding mode shapes are such that they satisfy either v = w or v = -w. The first and third natural frequencies shown in Table 16 correspond to the case v = -w and the second and fourth natural frequencies correspond to the case v = w. It can be observed from Table 17 that this is precisely the situation. Natural frequencies for a non-uniform rotating propeller blade were computed using the transmission matrix. These results were compared with experimental and analytical solutions of Reference 9. It can be observed from this table that the experimental and analytical solutions agree very well with the transmission matrix solutions.

Using the transmission matrix approach, natural frequencies and mode shapes were computed for coupled flapwise bending, chordwise bending and torsion. These results are presented in Tables 19 and 20. The natural frequencies are compared with exact solutions and solutions obtained by solving an equivalent coupled flapwise bending and torsion problem. The mode shapes are such that they satisfy either (1) $\phi = 0$, v = w or (2) v = -w. This can be observed in Table 20. This provides an excellent means of checking the efficacy of the transmission matrix approach for the most general case of the rotor blade bending problem. In Table 21

the orthogonality of these natural modes defined by the differential equation of motion is presented.

The effect of 'Ω' and 'e' on the natural frequencies corresponding to coupled flapwise bending, chordwise bending and torsion was studied and the results are presented in Tables 22 and 23 respectively. As expected it was observed that the natural frequencies increase with increasing rotational velocity. This effect was more significant on natural frequencies associated with predominantly flapwise bending or chordwise bending as compared with the frequencies associated with predominantly torsion. The results obtained by varying e are shown in Table 23. The natural frequencies associated with predominantly chordwise bending are almost invariant with e. The effect of e on natural frequencies associated with predominantly flapwise bending is also very little, while its effect on frequencies associated with predominantly torsional is significant.

The effect of collective pitch on coupled flapwise bending, chordwise bending and torsional frequencies and mode shapes was studied and the results are presented in Tables 24 to 26. From Tables 24 to 26 the following observations can be made.

1. The natural frequencies of non-rotating blades do not vary with collective pitch.
2. The natural frequencies decrease with the increase of collective pitch either clockwise or counter clockwise

for rotating blades. This effect is more predominant on natural frequencies associated with predominantly bending as compared to the frequencies associated with predominantly torsion.

3. The effect of collective pitch on bending deflection is significant.

Discussion of Methods

The transmission matrix by definition is independent of the boundary conditions. Having determined the transmission matrix the boundary conditions can be simply imposed on the input and output state vectors which will yield the frequency determinant. So all the problems corresponding to various boundary conditions can be analyzed easily. Rigid body degrees of freedom present no difficulty for this approach. Having determined the natural frequencies, the corresponding natural modes can easily be obtained. For some lower order uniform continuous systems and for lumped elements, transmission matrices can be obtained analytically. If analytical solutions for transmission matrices are not possible, numerical solutions can be obtained. For example, if Rubin's method is used the Runge-kutta procedure can be utilized to solve the differential equations governing the elements of the transmission matrix. One distinguishing advantage of the transmission matrix approach is that together with the mode shapes all other physical quantities

(slopes, moments, shears, etc.) are also known. The number of stations at which these properties are known is dependent only on the step size of the integration. The incremental step size can be selected arbitrarily and then the result compared with that obtained for a smaller increment. In this way an optimal value for step size can be obtained. A much smaller step size will lead to round off and truncation errors.

The computer time required for the determination of natural frequencies and mode shapes using the transmission matrix approach is mainly dependent on the frequency scanning interval. If the rotor blade has close natural frequencies, a relatively short frequency scanning interval is required. Doubling the frequency scanning interval, for example, cuts down the time of actual computation by half. Detection of a repeated root can be facilitated by evaluation of the derivative of the frequency determinant. This derivative can be easily evaluated since the derivatives of the transmission matrices are available and hence the derivative of the frequency determinant is also known.

When natural frequencies are to be calculated repeatedly, as in the case of a flutter analysis, the transmission matrix approach has the following advantage. The frequencies associated with a non-rotating blade can be calculated first, then frequencies at a finite rotational velocity can be obtained as follows. Let ω_{1N}, ω_{2N}, ω_{3N}, ω_{4N},

etc. be the non-rotating natural frequencies and ω_{1R}, ω_{2R}, ω_{3R}, ω_{4R} etc., be the natural frequencies of the rotating system. The frequency scanning can be started for the rotational system from ω_{1N} until the root ω_{1R} is obtained. For the second natural frequency the scanning can be started from the maximum value of ω_{1R} and ω_{2N}. This process can be repeated for all higher frequencies.

Integration of differential equations of motion using integrating and differentiating matrices as operators leads to an eigenvalue problem. Unlike the transmission matrix approach, this procedure has to be repeated for each set of boundary conditions. Further this scheme breaks down when the system contains rigid body degrees of freedom. The integrating matrix method leads to a non-self adjoint eigenvalue problem and hence the eigenvectors need not be orthogonal. Since the formulation leads to a non-selfadjoint eigenvalue problem, the possibility of complex eigenvalues and eigenvectors exists. As a result the preferred method of solution for the eigenvalue problem is the QR-transformation.

For uncoupled problems, the order of the eigenvalue problem is equal to the number of stations. For coupled problems the order of the eigenvalue problem increases two-fold, or three fold depending on the number of coupled differential equations. Repeated eigenvalues and close

eigenvalues do not cause any difficulty or require any special attention if the QR-transformation is used to solve the eigenvalue problem.

CHAPTER VI

CONCLUSIONS AND RECOMMENDATIONS

The transmission matrix approach was used to obtain the dynamic characteristics of rotating blades for combined flapwise bending, chordwise bending and torsion and five of its subcases. Hinge-Free and Fixed-Free end conditions were considered. The integrating matrix method was used to obtain the dynamic characteristics of rotating blades for 1) flapwise bending and 2) coupled flapwise bending and torsion. Comparisons were made between the two methods and with available experimental and analytical results.

Conclusions

1. The transmission matrix approach is an efficient means of calculating the dynamic characteristics of rotating blades to obtain accurate results. Various sets of boundary conditions can be incorporated easily with a single formulation. Rigid body degrees of freedom present no difficulty. Mode shapes obtained by this approach are orthogonal as defined by the differential equations of motion.
2. The integrating matrix method leads to a non-self adjoint eigenvalue problem. Hence the natural modes need not be

orthogonal. In the case of coupled problems, the integrating matrix gives accurate mode shapes for predominant motions while non-significant motions may be inaccurate. This method breaks down when rigid body degrees of freedom are present in the system. The reason is that the integrating matrix formulation leads to a flexibility type of formulation and as such can not exist for a semi-definite system.

3. The transmission matrix approach requires significantly less computer memory than the integrating matrix method.
4. The time of actual computation on a digital computer using the integrating matrix method is very much less than the time required by transmission matrix approach.

Recommendations

1. A complete evaluation of the significance of each of the coupling terms associated with the centrifugal forces should be made using the transmission matrix approach for the coupled flapwise bending, chordwise bending and torsion problem.
2. A much faster integration scheme is required for solving the differential equations governing the elements of the transmission matrix.
3. The integrating matrix method should be extended to solve the rotor bending problem for combined flapwise bending, chordwise bending and torsion.

4. A method of using the integrating matrix method on semi-definite systems is required.
5. An experimental investigation would be useful to verify the analytical results obtained by the transmission and integrating matrix methods.

PART II

THE EFFECT OF PHASE ANGLE ON MULTIBLADED ROTOR FLUTTER

CHAPTER VII

INTRODUCTION

In modern flight vehicle design aeroelastic analyses are quite necessary. In the past, classical flutter of helicopter rotor blades has not been a serious problem because it has been customary to place the blade elastic axis and the center of gravity on or near the 25% chord point. This means that the elastic axis, the axis of aerodynamic centers, and the gravity axis are effectively coincident, thus eliminating coupled bending torsion flutter and also single-degree-of-freedom flutter. Placing the three axes in coincidence involves some penalty in weight and increases structural complexity. To provide improved structural efficiency, consideration is being given to moving the axes apart, similar to fixed wing designs. Once the axes are no longer in approximate coincidence, the blade becomes very susceptible to classical flutter. Therefore for helicopter rotors flutter calculations have to be undertaken. This requires use of an unsteady aerodynamic theory. The blade tip Mach number of some current helicopters approaches unity for certain flight conditions so that compressibility effects are very important.

The state of art in unsteady helicopter aerodynamics has not progressed as rapidly as that for unsteady fixed wing aerodynamics. One of the main difficulties of rotor aerodynamic theory lies in the fact that there is usually more than one blade, and mutual interference of their wakes and bound vorticities can not be ignored. The forward motion adds to the already existing complexity. The first notable contributions to the unsteady aerodynamics of rotary wings were made by Loewy [24], Jones [25], and Timman and Van de Vooren [26]. These investigators in similar but independent studies considered the flow to be incompressible. Jones and Rao [27] incorporated compressibility effects on oscillating rotor blades using a model similar to that proposed by Loewy. Their theory takes into account the presence of more than one blade with the assumption that all the blades of the rotor oscillate with same amplitude and frequency but are not necessarily in phase. Hammond and Pierce [28] independently analyzed a slightly different model of the compressible flow problem.

These unsteady aerodynamic theories are currently employed to predict aeroelastic instabilities of rotor systems. White [23] and Viswanathan [29] analyzed a single bladed rotor system for flutter at low inflow conditions. Low inflow conditions occur at blade pitch angles near zero and is of prime importance in wake excited flutter. Since

nearly all helicopters have at least two blades, previous analyses have been simplified by the introduction of the concept of an equivalent single-bladed rotor wherein all blades are presumed to be oscillating in phase. In the present study the effect on flutter of phase difference between blades of a two-bladed rotor is determined at low inflow conditions. For a multibladed rotor a further complication arises from the elastic and inertial couplings which exist between the blades, through the root and rotor shaft. In order to keep the current formulation simple these couplings have been ignored. To obtain the natural vibration characteristics of the rotor blades a transmission matrix approach developed by Murthy [30] is used. Jones and Rao's unsteady aerodynamic theory is employed to obtain the compressible aerodynamic loading.

CHAPTER VIII

UNSTEADY AERODYNAMICS

The unsteady aerodynamic theory used to obtain the compressible aerodynamic loading on a helicopter rotor is briefly discussed in this chapter. Such loadings are required in flutter analyses. The pertinent equations for the computation of unsteady aerodynamic coefficients when the blade is describing simple harmonic plunging and pitching oscillations (about midchord point) are given. The method of computation is also indicated.

Loewy's Flow Model

Loewy [24] has given a complete discussion of the unsteady flow field associated with a helicopter rotor in the hovering and axial flight modes. The basic flow picture consists of a blade and a wake which has been blown below the rotor disk by the inflow velocity through the disk. The wake forms a helical surface of vorticity which extends to infinity below the rotor. The following assumptions were made in order to arrive at a model which is mathematically tractable.

1. For low inflows, only the vorticity contained in a small double azimuth angle straddling the blade is of real consequence.
2. The chord, the amplitude of oscillation in effective angle of attack, and relative airspeed vary slowly enough with span or in a compensatory way so that what occurs aerodynamically at one blade radius station is essentially duplicated on either side of it.

As a result of the first assumption, the azimuthal angularity of shed vorticity with respect to blade may be ignored, as well as the horizontal distance that a spanwise element of shed vorticity is moved out of the vertical plane of blade section at a fixed radius as a result of azimuthal rotation. The second assumption is tantamount to saying that the flow problem at a given radius is two dimensional. With these assumptions the flow model proposed by Loewy is shown in Figure 3. The flow consists of a reference airfoil section and its immediate trailing wake (both in the same horizontal plane) together with a system of horizontal wake layers lying at regularly spaced intervals below the reference section. These wake layers below the reference airfoil account for the wake which was shed by the other blades in the rotor as well as that shed by the reference blade on previous revolutions. Loewy analyzed this model for incompressible flow using an incompressible vortex solution.

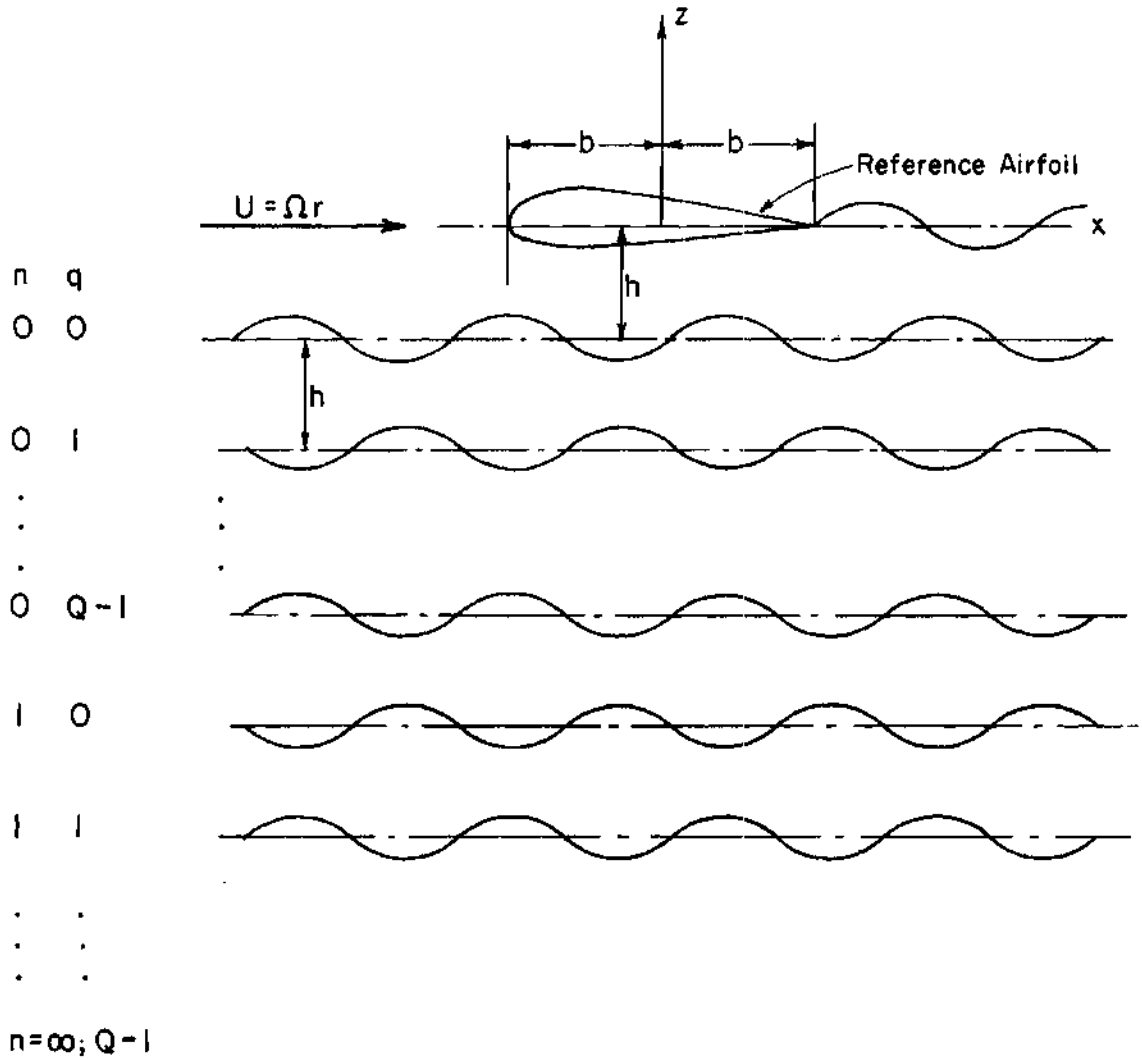

Figure 3. Loewy's Incompressible Flow Model

Compressible Unsteady Aerodynamics

Jones and Rao [27] incorporated compressibility effects using a model similar to that proposed by Loewy. Their analysis of the problem followed a technique developed by Jones [31] for a two-dimensional fixed wing oscillating in subsonic flow. The problem was reduced to one of finding the solution of an integral equation for the velocity potential of the disturbed flow. A doublet distribution function appeared as the unknown in the integral equation. For the solution of the integral equation the doublet distribution was represented by a series of known functions each of which was multiplied by an arbitrary constant. A set of simultaneous linear non-homogeneous equations were derived for the determination of the constants in the series representation of the doublet distribution function. When the doublet distribution function is known the lift distribution is also known and the aerodynamic forces acting on the airfoil can be determined. Following the development of Jones and Rao, the unsteady lift and moment (about the mid-chord) for the airfoil describing simple harmonic plunging and pitching oscillations (about the mid-chord) are given by the following equations.

$$L = \rho_\infty \, b \, U^2 \sum_{n=o} C_n \, R_n \exp(i \, k \, T) \qquad (155)$$

$$M_{c/2} = i\ \rho_\infty\ b^2\ U^2 \sum_{n=o} C_n\ R'_n \exp(i\ k\ T) \qquad (156)$$

where

$$R'_n = \frac{\partial\ R_n(\lambda)}{\partial\ \lambda}$$

$$T = \frac{Ut}{b}$$

$$R_o = 2\ \pi\ \{C(\nu)[J_o(\lambda) - i\ J_1(\lambda)] + \frac{i\ \nu}{2}\ [J_o(\lambda) + J_2(\lambda)]\}$$

$$R_1 = -\pi\left(1 - \frac{\nu}{\pi}\right)\ [J_2(\lambda) + i\ J_1(\lambda)]$$

$$R_n = (-i)^{n+1}\ \ \pi[1 - \frac{\nu}{\lambda}][J_{n+1}(\lambda) + J_{n-1}(\lambda)];\ n \geq 2$$

$$\lambda = \frac{M_\infty^2\ k}{1-M_\infty^2}$$

$$k = \frac{b\ \omega}{U}$$

$$\nu = \frac{k}{1-M_\infty^2}$$

$$C(\nu) = \frac{H_1^{(2)}(\nu)}{H_1^{(2)}(\nu) + i\ H_o^{(2)}(\nu)}$$

J_o , J_1 = Bessel functions

$H_o^{(2)}$, $H_1^{(2)}$ = Hankel functions

The coefficients C_o, C_1 etc., appearing in Equations (155) and (156) are determined from the following simultaneous equations.

$$C_o + \frac{C_1}{2} = \frac{1}{\beta}\left[\alpha^*_{c/2} - k\left(\alpha^*_{c/2} + i\,k\,\frac{w^*_{c/2}}{b}\right)\frac{\partial}{\partial\lambda}\right] J_o(\lambda)$$

$$+ \sum_{n=o} C_n I_{no} - \frac{\pi\, F(Q)}{Q\, D}\, C_o X_o(\nu) J_o(\nu) \qquad (157)$$

$$C_r = \frac{2\, i^r}{\beta}\left[\alpha^*_{c/2} - k\left(\alpha^*_{c/2} + i\,k\,\frac{w^*_{c/2}}{b}\right)\frac{\partial}{\partial\lambda}\right] J_r(\lambda)$$

$$+ \sum_{n=o} C_n I_{nr} - 2\, i^r\, \frac{\pi\, F}{QD}\, C_o X_o(\nu) J_r(\nu),\ r = 1,2,3 \text{ etc.},$$

where

$w^*_{c/2}$ = amplitude of simple harmonic plunging oscillations about midchord, positive down

$\alpha^*_{c/2}$ = amplitude of simple harmonic pitching oscillations about midchord, positive nose up

$\beta^2 = 1 - M_\infty^2$

$$F(Q) = \frac{Q\,k\,h}{b(e^{\gamma}-1)}\left[1 + \sum_{q=1}^{Q-1} \exp i\,\psi_q + \frac{Q-q}{Q}\,\gamma\right]$$

$$\gamma = i\,\frac{2\,\pi\,\omega}{\Omega} + \frac{Q\,k\,h}{b}$$

$$D = \frac{h\,\beta}{b}$$

$$X_o(\nu) = C(\nu)\, J_o(\nu) + i[1 - C(\nu)]\, J_1(\nu)$$

The formulae for the coefficients I_{nr} are given in Reference 31.

Computation of Aerodynamic Coefficients

It is assumed that sufficient accuracy would be given when only four terms are used in the series expression for the doublet distribution function, i.e., all values of C_r for $r > 3$ are assumed to be zero in the system of Equations (157). The four equations that are used in the computation of the aerodynamic coefficients are given below in matrix form.

$$\underset{4x4}{[B]} \quad \underset{4x1}{\begin{Bmatrix} C_o \\ C_1 \\ C_2 \\ C_3 \end{Bmatrix}} = \underset{4x2}{[D]} \underset{2x1}{\begin{Bmatrix} \frac{w^*_{c/2}}{b} \\ \\ \alpha^*_{c/2} \end{Bmatrix}} \tag{158}$$

where

$$B_{11} = I_{00} - A_1 J_o(\nu) - 1 \; ; \; B_{12} = I_{10} - \tfrac{1}{2}$$

$$B_{13} = I_{20} \; ; \; B_{14} = I_{30}$$

$$B_{21} = I_{01} - i\, 2\, A_1 J_1(\nu) \; ; \; B_{22} = I_{11} - 1$$

$$B_{23} = I_{21} \; ; \; B_{24} = I_{31}$$

$$B_{31} = I_{02} + 2\, A_1 J_2(\nu) \; ; \; B_{32} = I_{12}$$

$$B_{33} = I_{22} - 1 \qquad ; \; B_{34} = I_{32}$$

$$B_{41} = I_{03} + i\ 2\ A_1 J_3(\nu) \qquad ; \; B_{42} = I_{13}$$

$$B_{43} = I_{23} \qquad ; \; B_{44} = I_{33} - 1$$

$$D_{11} = -\frac{i\ k^2}{\beta} J_o'(\lambda) \qquad ; \; D_{12} = \frac{1}{\beta}\left[1 - k\ J_o'(\lambda)\right]$$

$$D_{21} = \frac{2\ k^2}{\beta} J_1'(\lambda) \qquad ; \; D_{22} = \frac{2i}{\beta}\left[1 - k\ J_1'(\lambda)\right]$$

$$D_{31} = \frac{i\ 2\ k^2}{\beta} J_2'(\lambda) \qquad ; \; D_{32} = \frac{-2}{\beta}\left[1 - k\ J_2'(\lambda)\right]$$

$$D_{41} = \frac{-2k^2}{\beta} J_3'(\lambda) \qquad ; \; D_{42} = \frac{-2i}{\beta}\left[1 - k\ J_3'(\lambda)\right]$$

$$A_1 = \frac{\pi\ F(Q)}{Q\ D} X_o(\nu)$$

$$I_{00} = i\ \nu\ X_o(\nu)\ J_o(\nu)\ P + \frac{M_\infty^2}{2}\left[1 - C(\nu) + i\ \nu\ G\{C(\nu) + \frac{i\ \nu}{2}\}\right] +$$

$$\frac{M_\infty^4}{32}\left[G\{\frac{3\nu^4}{4} - 2\ i\ \nu^3\ C + 2\ \nu^2(C - 1)\right.$$

$$\left. + 4\ i\ \nu\ C\} + \frac{\nu^4}{16} - \frac{i\ \nu^3\ C}{2} +\right.$$

$$\left.\frac{3\ \nu^2(C - 1)}{2} + 4(1 - C) + 3\ i\ \nu\ C\right]$$

$$I_{01} = -2\,\nu\,X_o(\nu)\,J_1(\nu)\,P + \frac{i\,\nu^3\,M_\infty^2(1-C)}{2}$$

$$- \frac{M_\infty^4}{16}\left[G\{2\,\nu^2\,C + i\,\nu^3(1-C)\} + \frac{i\,\nu^3(1-C)}{2}\right.$$

$$\left. + \frac{3\,C\,\nu^2}{2} + 2\,i\,\nu(C-1)\right]$$

$$I_{02} = -\,2\,i\,\nu\,X_o(\nu)\,J_2(\nu)\,P - \frac{M_\infty^2\,\nu^2}{8}$$

$$\frac{-\,i\,\nu^3\,M_\infty^4\,G}{32}\left(C + \frac{i\nu}{2}\right) +$$

$$\frac{M_\infty^4}{16}\left[\frac{5\,\nu^4}{48} - \frac{3\,i\,\nu^3\,C}{8} + \frac{\nu^2(C-1)}{2}\right]$$

$$I_{03} = 2\,\nu\,X_o(\nu)\,J_3(\nu)\,P - \frac{i\,\nu^3(1-C)M_\infty^4}{192}$$

$$I_{10} = -\frac{\theta^2 G}{8} + \frac{3\theta^4}{256}\left(G + \frac{1}{12}\right)$$

$$I_{11} = \frac{\theta^2}{16} - \frac{\theta^4}{128}\left(G + \frac{5}{12}\right)$$

$$I_{12} = -\frac{\theta^2}{16} + \frac{\theta^4}{128}\left(G + \frac{5}{12}\right)$$

$$I_{13} = -\frac{\theta^2}{48} - \frac{\theta^4}{1024}$$

$$I_{20} = \frac{\theta^2 G}{8} - \frac{\theta^4 G}{96}$$

$$I_{22} = \frac{\theta^2}{12} - \frac{\theta^4}{128}\left(G + \frac{7}{24}\right)$$

$$I_{23} = I_{30} = I_{32} = I_{21} = 0$$

$$I_{31} = \frac{-\theta^2}{16} + \frac{\theta^4}{128}\left(G + \frac{3}{8}\right)$$

$$I_{33} = \frac{\theta^2}{32} + \frac{3\,\theta^4}{2560}$$

$$\theta = M_\infty \nu$$

$$P = \delta + \frac{M_\infty^2}{2}\left(\frac{1}{2} - \ell n \frac{M_\infty}{2}\right) - \frac{M_\infty^4}{8}\left(\ell n \frac{M_\infty}{2} + \frac{1}{4}\right)$$

$$\delta = \ell n \frac{M_\infty}{2} + \sqrt{1 - M^2}\ \ell n \left[\frac{1 + \sqrt{1 - M_\infty^2}}{M_\infty}\right]$$

$$G = \gamma - \frac{1}{2} + \mathrm{Ln}\frac{\theta}{4} + \frac{i\,\pi}{2}$$

γ = Euler's number = 0.57721566

The expressions for lift and moment for

$n = 3$ become

$$\left.\begin{aligned} L &= \rho_\infty\, b\, U^2 [C_o R_o + C_1 R_1 + C_2 R_2 + C_3 R_3] \exp(i\,k\,T) \\ M_{c/2} &= i\,\rho_\infty\, b^2\, U^2 [C_o R_o' + C_1 R_1' + C_2 R_2' + C_3 R_3'] \exp(i\,k\,T) \end{aligned}\right\} (159)$$

Following the notation of Jones and Rao for the non-dimensional aerodynamic coefficients the lift and moment are defined (about midchord point) as shown below

$$\left.\begin{aligned} L &= \pi\ \rho_\infty\ b\ U^2\left[(\ell_w + i\ k\ \ell_{\dot{w}})\frac{w_{c/2}}{b} + (\ell_\alpha + i\ k\ \ell_{\dot{\alpha}})\alpha_{c/2}\right] \\ M_{c/2} &= \pi\ \rho_\infty\ b^2U^2\left[(m_w + i\ m_{\dot{w}})\frac{w_{c/2}}{b} + (m_\alpha + i\ k\ m_{\dot{\alpha}}\ \alpha_{c/2})\right] \end{aligned}\right\} \quad (160)$$

where $w_{c/2}$ = plunging displacement of the midchord point

$\alpha_{c/2}$ = pitching displacement about the midchord point

Assuming simple harmonic plunging and pitching oscillations with frequency, ω, as

$$w_{c/2} = w^*_{c/2}\ \exp(i\ \omega\ t)$$

$$\alpha_{c/2} = \alpha^*_{c/2}\ \exp(i\ \omega\ t)$$

Then,

$$L = L^*\ \exp(i\ \omega\ t)$$

$$M_{c/2} = M^*_{c/2}\ \exp(i\ \omega\ t)$$

and Equations (160) in matrix form become

$$\frac{1}{\pi\rho_\infty bU^2}\underset{2x1}{\begin{Bmatrix} L^* \\ \\ \dfrac{M^*_{c/2}}{b} \end{Bmatrix}} = \underset{2x2}{\begin{bmatrix} (\ell_w + i\ k\ \ell_{\dot{w}}) & (\ell_\alpha + i\ k\ \ell_{\dot{\alpha}}) \\ \\ (m_w + i\ m_{\dot{w}}) & (m_\alpha + i\ k\ m_{\dot{\alpha}}) \end{bmatrix}}\underset{2x1}{\begin{Bmatrix} \dfrac{w^*_{c/2}}{b} \\ \\ \alpha^*_{c/2} \end{Bmatrix}} \quad (161)$$

For simple harmonic plunging and pitching oscillations

Equations (159) become

$$\frac{1}{\pi\rho_\infty b U^2} \begin{Bmatrix} L^* \\ \\ \frac{M^*_{c/2}}{b} \end{Bmatrix} = [R] \begin{Bmatrix} C_o \\ C_1 \\ C_2 \\ C_3 \end{Bmatrix} \tag{162}$$

where

$$[R] = \frac{1}{\pi} \begin{bmatrix} R_o & R_1 & R_2 & R_3 \\ i\,R_o' & i\,R_1' & i\,R_2' & i\,R_3' \end{bmatrix}$$

From Equation (158)

$$\begin{Bmatrix} C_o \\ C_1 \\ C_2 \\ C_3 \end{Bmatrix} = [B]^{-1}[D] \begin{Bmatrix} \frac{w^*_{c/2}}{b} \\ \\ \alpha^*_{c/2} \end{Bmatrix} \tag{163}$$

Substituting Equation (163) into (162)

$$\frac{1}{\pi\rho_\infty b U^2} \begin{Bmatrix} L^* \\ \\ \frac{M^*_{c/2}}{b} \end{Bmatrix} = [R][B]^{-1}[D] \begin{Bmatrix} \frac{w^*_{c/2}}{b} \\ \\ \alpha^*_{c/2} \end{Bmatrix} \tag{164}$$

2x1 2x4 4x2 2x1

4x4

Equating (164) and (161) the following equation for the aerodynamic coefficients can be obtained

$$\begin{bmatrix} (\ell_w + i\,k\,\ell_{\dot{w}}) & (\ell_\alpha + i\,k\,\ell_{\dot{\alpha}}) \\ (m_w + i\,m_{\dot{w}}) & (m_\alpha + i\,k\,m_{\dot{\alpha}}) \end{bmatrix} = [R][B]^{-1}[D] \qquad (165)$$

It is more customary to use the notation of Smilg and Wasserman [32] to define the unsteady aerodynamic coefficients as shown below

$$\left.\begin{aligned} L &= -\pi\,\rho_\infty\,b^3\omega^2\,\left[L_h\,\frac{W_{c/4}}{b} + L_\alpha\,\alpha_{c/4}\right] \\ M_{c/4} &= \pi\,\rho_\infty\,b^4\omega^2\,\left[M_h\,\frac{W_{c/4}}{b} + M_\alpha\,\alpha_{c/4}\right] \end{aligned}\right\} \qquad (166)$$

where

$W_{c/4}$ = plunging deflection of the quarter-chord point

$\alpha_{c/4}$ = pitching deflection about quarterchord point

$M_{c/4}$ = aerodynamic torque about quarterchord axis

From the geometry of Figure (4) the following relations between the quarter chord and midchord references can be obtained

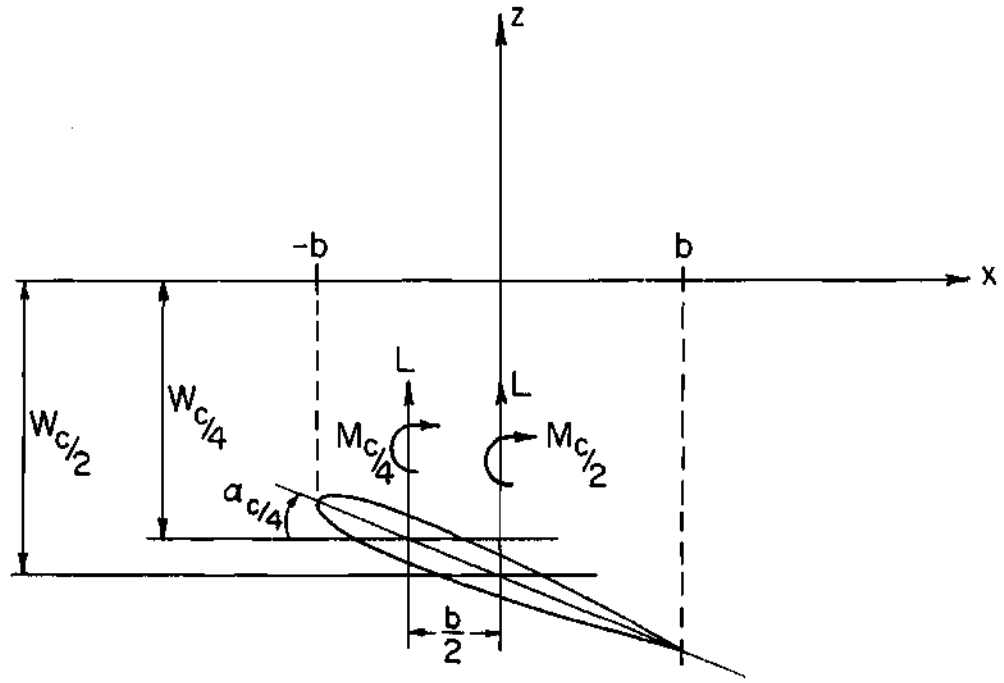

Figure 4. Displacement Relations, Mid-chord to Quarter-chord

$$\left.\begin{aligned} \alpha_{c/4} &= \alpha_{c/2} \\ W_{c/4} &= W_{c/2} - \frac{\alpha_{c/2}\, b}{2} \\ M_{c/2} &= M_{c/4} + \frac{L\, b}{2} \end{aligned}\right\} \qquad (167)$$

Using Equations (166) and (167)

$$L = -\pi\, \rho_\infty\, b^3 \omega^2 \left[L_h \frac{W_{c/2}}{b} + \left(L_\alpha - \frac{L_h}{2} \right) \alpha_{c/2} \right] \qquad (168)$$

$$M_{c/2} = \pi\, \rho_\infty\, b^4 \omega^2 \left[\left(M_h - \frac{L_h}{2} \right) \frac{W_{c/2}}{b} + \left(M_\alpha - \frac{L_\alpha}{2} - \frac{M_h}{2} + \frac{L_h}{4} \right) \alpha_{c/2} \right]$$

comparing Equations (168) and (160) and solving explicitly for L_h, L_α, M_h and M_α the following relations can be obtained

$$\left.\begin{aligned} L_h &= -\frac{1}{k^2} \left[\ell_w + i\, k\, \ell_{\dot{w}} \right] \\ L_\alpha &= -\frac{1}{k^2} \left[\left(\frac{\ell_w}{2} + \ell_\alpha \right) + i\, k \left(\frac{\ell_{\dot{w}}}{2} + \ell_{\dot{\alpha}} \right) \right] \\ M_h &= \frac{1}{k^2} \left[\left(-\frac{\ell_w}{2} + m_w \right) + i\, k \left(-\frac{\ell_{\dot{w}}}{2} + \frac{m_{\dot{w}}}{k} \right) \right] \\ M_\alpha &= \frac{1}{k^2} \left[\left(-\frac{\ell_w}{4} - \frac{\ell_\alpha}{2} + \frac{m_w}{2} + m_\alpha \right) + i\, k \left(-\frac{\ell_{\dot{w}}}{4} - \frac{\ell_{\dot{\alpha}}}{2} + \frac{m_{\dot{w}}}{2k} + m_{\dot{\alpha}} \right) \right] \end{aligned}\right\} \qquad (169)$$

From Equation (165) the non-dimensional unsteady aerocynamic coefficients can be computed numerically when Mach number (M_∞), reduced frequency ($k = \frac{b\omega}{U}$), frequency ratio ($\frac{\omega}{\Omega}$), inflow ratio ($\frac{h}{b}$), number of blades (Q), and the phase differences between oscillations of blades (ψ_q, $q = 1...Q-1$) are specified. Then from Equations (169) L_h, L_α, M_h and M_α can be obtained.

CHAPTER IX

FLUTTER ANALYSIS OF HELICOPTER ROTOR

In this chapter the flutter analysis of helicopter rotor systems is discussed. The case treated here is for a uniform, untwisted rotor blade with flapwise bending and torsional degrees of freedom. The transmission matrix developed in Part I for obtaining the natural vibration characteristics is briefly discussed for fixed-free and hinged-free rotors. The flutter analysis and k-method of solution of the flutter determinant are discussed with the pertinent equations. The numerical procedure suggested by Viswanathan [29] for the k-method is mentioned briefly for completeness.

Vibration Analysis

Equations of Motion

The differential equations of motion for combined flapwise bending and torsion of rotor blades from Reference 16 are given below with $e_A = e_o = 0$

$$- [(GJ + T k_A^2) \Phi']' - \Omega^2 m y e W' +$$

$$\Omega^2 m(k_{m_2}^2 - k_{m_1}^2) \Phi + m k_m^2 \ddot{\Phi} - m e \ddot{W} = M_e \qquad (170)$$

$$- [EI_1 W'']'' + (T W')' - (\Omega^2 m y e \Phi)' + m(-\ddot{W} + e \ddot{\Phi}) = L \tag{171}$$

For simple harmonic free vibration these equations are given by Equations (65) and (66) with $e_A \neq 0$ and $e_o \neq 0$. Note that there is a sign change associated with W, since in this development W is taken as positive down where as in the Reference 16 W is positive up. This sign change is incorporated to be consistent with the development of the unsteady aerodynamics. For simple harmonic free vibration with frequency, ω, Equations (170) and (171) become

$$- [(GJ + T k_A^2) \phi']' - \Omega^2 m y e w' + \Omega^2 m(k_{m_2}^2 - k_{m_1}^2)\phi - \omega^2 m k_m^2 \phi + m e \omega^2 w = 0 \tag{172}$$

$$- [EI_1 w'']'' + (T w')' - (\Omega^2 m y e \phi)' + \omega^2 m(w - e \phi) = 0 \tag{173}$$

These equations are same as Equations (65) and (66) with a sign change associated with w and with $e_A = e_o = 0$ where

$$T = \frac{\Omega^2 m}{2} [R^2 - y^2]$$

Equations (170) and (171) imply that the blade is untwisted and the cross-section has a horizontal plane of symmetry so that the chordwise bending is decoupled.

Natural Vibration Characteristics

The transmission matrix method is used to obtain the natural vibration characteristics of the rotor blades. For completeness the specialized equations for uniform rotor blades for coupled flapwise bending and torsion are given below. The coupled higher order differential Equations (172) and (173) can be reduced to six first-order differential equations and can be arranged into a matrix differential equation of the following form

$$\frac{d}{dy}\{Z\} = [A(y)]\{Z\} \tag{174}$$

where

$$\lfloor Z \rfloor = \lfloor w \ \psi \ \phi \ M_y \ M_x - V_z \rfloor$$

For simplification of the numerical work Equation (174) can be non-dimensionalized by making use of the following non-dimensional relationships

$$\bar{w} = \frac{w}{b} \quad ; \quad \bar{y} = \frac{y}{R}$$

$$\bar{\psi} = \psi \frac{R}{b} \quad ; \quad \bar{\phi} = \phi$$

$$\bar{M}_y = \frac{M_y R^3}{EI_1 b^2} \quad ; \quad \bar{M}_x = \frac{M_x R^2}{b EI_1}$$

$$
[A(y)] = \begin{bmatrix}
0 & -1 & 0 & 0 & 0 & 0 \\
0 & 0 & 0 & 0 & \frac{1}{EI_1} & 0 \\
0 & 0 & 0 & \frac{1}{GJ+T\ k_A^2} & 0 & 0 \\
\omega^2 me & \Omega^2 mye & \Omega^2 m(k_{m_2}^2 - k_{m_1}^2) - \omega^2\ k_m^2 & 0 & 0 & 0 \\
0 & -T & \Omega^2\ m\ y\ e & 0 & 0 & -1 \\
-\omega^2 m & 0 & \omega^2\ m\ e & 0 & 0 & 0
\end{bmatrix}
$$

$$\bar{V}_z = \frac{V_z R^3}{EI_1 b}$$

Then Equation (174) becomes

$$\frac{d}{d\bar{y}} \{\bar{Z}\} = [\bar{A}(\bar{y})] \{\bar{Z}\} \tag{175}$$

where

$$\lfloor \bar{Z} \rfloor = \lfloor \bar{w} \ \bar{\psi} \ \bar{\phi} \ \bar{M}_y \ \bar{M}_x \ -\bar{V}_z \rfloor$$

$$\gamma(\bar{y}) = \frac{b^2}{R^2} \frac{1}{\frac{GJ}{EI_1} + \frac{\bar{\Omega}^2}{2R^2}(1 - \bar{y}^2)}$$

$$\bar{\Omega}^2 = \frac{\Omega^2 m R^4}{EI_1}$$

$$\bar{\omega}^2 = \frac{\omega^2 m R^4}{EI_1}$$

$$\bar{e} = \frac{e}{b}$$

$$\bar{k}_{m_1}^2 = \frac{k_{m_1}}{b^2}$$

$$\bar{k}_{m_2}^2 = \frac{k_{m_2}^2}{b^2}$$

$$\bar{k}_m^2 = \frac{k_m^2}{b^2}$$

$$[\bar{A}(\bar{y})] = \begin{bmatrix} 0 & -1 & 0 & 0 & 0 & 0 \\ 0 & 0 & 0 & 0 & 1 & 0 \\ 0 & 0 & 0 & \gamma(\bar{y}) & 0 & 0 \\ \bar{\omega}^2\,\bar{e} & \bar{\Omega}^2\,\bar{y}\,\bar{e} & \bar{\Omega}^2(\bar{k}_{m_2}^2 - \bar{k}_{m_1}^2) - \bar{\omega}^2\,\bar{k}_m^2 & 0 & 0 & 0 \\ 0 & -\frac{\bar{\Omega}^2}{2}(1-\bar{y}^2) & \bar{\Omega}^2\,\bar{y}\,\bar{e} & 0 & 0 & -1 \\ -\bar{\omega}^2 & 0 & \bar{\omega}^2\,\bar{e} & 0 & 0 & 0 \end{bmatrix}$$

As mentioned earlier the transmission matrix satisfies the following matrix differential equation

$$\frac{d}{d\bar{y}} [T(\bar{y})] = [A(y)][T(y) \tag{176}$$

with initial conditions

$$[T(0)] = [\ 1\ ]$$

By definition of the transmission matrix it follows that

$$\begin{Bmatrix} \bar{w}\ (1) \\ \bar{\psi}\ (1) \\ \bar{M}_y(1) \\ M_x(1) \\ -\bar{V}_z(1) \end{Bmatrix} = [T(\bar{y})]_{\bar{y}=1} \begin{Bmatrix} \bar{w}\ (0) \\ \bar{\psi}\ (0) \\ \bar{M}_y(0) \\ \bar{M}_x(0) \\ -\bar{V}_z(0) \end{Bmatrix} \tag{177}$$

The boundary conditions for the problem at hand are as given below

Tip : $\bar{M}_y(1) = \bar{M}_x(1) = \bar{V}_z(1) = 0$

Hinged Root: $\bar{M}_x(0) = \bar{\phi}(0) = \bar{w}(0) = 0$

Fixed Root : $\bar{w}(0) = \bar{\psi}(0) = \bar{\phi}(0) = 0$

By substituting the appropriate boundary conditions into the input and output state vectors, the following frequency determinants can be obtained

Hinged-Free Rotor

$$\begin{vmatrix} T_{42}(1) & T_{44}(1) & T_{46}(1) \\ T_{52}(1) & T_{54}(1) & T_{56}(1) \\ T_{62}(1) & T_{64}(1) & T_{66}(1) \end{vmatrix} = 0 \qquad (178)$$

Fixed-Free Rotor

$$\begin{vmatrix} T_{44}(1) & T_{45}(1) & T_{46}(1) \\ T_{54}(1) & T_{55}(1) & \bar{T}_{56}(1) \\ T_{64}(1) & T_{65}(1) & T_{66}(1) \end{vmatrix} = 0 \qquad (179)$$

These frequency determinants are functions of frequency, ω, and the roots can be obtained numerically using the frequency scanning technique. The elements of the frequency determinant can be obtained by solving Equation (174). After obtaining the natural frequencies the mode shapes can subsequently be obtained by the following expressions

Hinged-Free Rotor:

$$\left.\begin{aligned} \bar{w}(\bar{y}) &= T_{12}(\bar{y})\alpha_1 + T_{14}(\bar{y})\beta_1 - T_{16}(\bar{y}) \\ \bar{\phi}(\bar{y}) &= T_{32}(\bar{y})\alpha_1 + T_{34}(\bar{y})\beta_1 - T_{36}(\bar{y}) \end{aligned}\right\} \qquad (180)$$

where

$$\alpha_1 = \frac{T_{46}(1)\ T_{54}(1) - T_{44}(1)\ T_{56}(1)}{T_{42}(1)\ T_{54}(1) - T_{44}(1)\ T_{52}(1)}$$

$$\beta_1 = \frac{T_{42}(1)\ T_{56}(1) - T_{46}(1)\ T_{52}(1)}{T_{42}(1)\ T_{54}(1) - T_{44}(1)\ T_{52}(1)}$$

Fixed-Free Rotor:

$$\left.\begin{aligned} \bar{w}(\bar{y}) &= T_{14}(\bar{y})\alpha_2 + T_{15}(\bar{y})\beta_2 - T_{16}(\bar{y}) \\ \bar{\phi}(\bar{y}) &= T_{34}(\bar{y})\alpha_2 + T_{35}(\bar{y})\beta_2 - T_{36}(\bar{y}) \end{aligned}\right\} \qquad (181)$$

where

$$\alpha_2 = \frac{T_{46}(1)\ T_{55}(1) - T_{45}(1)\ T_{56}(1)}{T_{44}(1)\ T_{55}(1) - T_{45}(1)\ T_{54}(1)}$$

$$\beta_2 = \frac{T_{44}(1)\ T_{56}(1) - T_{46}(1)\ T_{54}(1)}{T_{44}(1)\ T_{54}(1) - T_{45}(1)\ T_{55}(1)}$$

Orthogonality and Generalized Equations of Motion

The r-th mode shape $\phi_r(y)$ and $w_r(y)$ and s-th mode shape $\phi_s(y)$ and $w_s(y)$ are orthogonal in the following fashion when they correspond to distinct natural frequencies $\omega_r \neq \omega_s$ as given by Equation (B-20) with a sign change for w.

$$\int_o^R m \{w_r w_s + k_m^2 \phi_r \phi_s - e(w_r \phi_s + w_s \phi_r)\} dy = 0$$

A solution of the following form can be sought for the differential equations (170) and (171),

$$\left.\begin{aligned} \Phi(y,t) &= \sum_{r=1}^{\infty} \phi_r(y)\ \xi_r(t) \\ W(y,t) &= \sum_{r=1}^{\infty} w_r(y)\ \xi_r(t) \end{aligned}\right\} \qquad (182)$$

Then an infinite set of uncoupled ordinary differential equations similar to the single-degree-of-freedom system are obtained in terms of $\xi_r(t)$ as shown below

$$M_r \ddot{\xi}_r(t) + \omega_r^2 M_r \xi_r(t) = \Xi_r(t),\ r = 1,2,3,... \qquad (183)$$

where M_r and $\Xi_r(t)$ denote the generalized mass and generalized force respectively associated with the generalized coordinate $\xi_r(t)$. They are defined by the following equations.

$$M_r = \int_o^R m \{w_r^2 + k_m^2 \phi_r^2 - 2e\ w_r\ \phi_r\}\ dy$$

$$\Xi_r(t) = -\int_o^R L(y,t) w_r(y) dy + \int_o^R M_e(y,t) \phi_r(y) dy$$

The generalized mass and the generalized force can be expressed in terms of non-dimensional mode shapes as

$$M_r = \int_o^1 m\, b^2 R\, \{\bar{w}_r^2 + \bar{k}_m^2\ \ \bar{\phi}_r^2 - 2\ \bar{e}\ \bar{\phi}_r \bar{w}_r\}\ d\bar{y} \tag{184}$$

$$\Xi_r(t) = \int_o^1 \{-bR\ L(\bar{y},t)\bar{w}_r(\bar{y}) + R\ M_e(\bar{y},t)\bar{\phi}_r(\bar{y})\} d\bar{y} \tag{185}$$

Flutter Determinant

Introducing structural damping into the generalized equations of motion (183) to account for the structural damping yields

$$M_r\ \ddot{\xi}_r(t) + (1 + i\ g_r)\omega_r^2\ M_r\ \xi_r(t) = \Xi_r(t), \tag{186}$$

$$r = 1,2,3...$$

where g_r is the structural damping constant of r-th mode. Equations (186) are used in the flutter analysis. It is practical to take only a finite number, N, of these equations. Consequently Equations (182) become

$$\left.\begin{aligned} \Phi(y,t) &= \sum_{r=1}^{N} \phi_r(y)\ \xi_r(t) \\ W(y,t) &= \sum_{r=1}^{N} w_r(y)\ \xi_r(t) \end{aligned}\right\} \tag{187}$$

The flutter speed and frequency are defined, respectively, as the lowest airspeed and the corresponding circular frequency at which a given structure flying at given atmospheric density and temperature will exhibit sustained simple harmonic oscillations. Flight at flutter speed represents a borderline condition or neutral stability boundary, because all small motions must be stable at speeds below flutter speed, where as divergent oscillations can ordinarily occur in a range of speeds above flutter speed. To establish a flutter boundary simple harmonic motion with frequency, ω, is considered as

$$\left.\begin{aligned} \Phi(y,t) &= \phi(y)\ \exp(i\omega t) \\ W(y,t) &= w(y)\ \exp(i\omega t) \\ \xi_r(t) &= \xi_r^*\ \exp(i\omega t) \end{aligned}\right\} \tag{188a}$$

then

$$\left.\begin{aligned} L(y,t) &= L^*(y)\ \exp(i\omega t) \\ M_e(y,t) &= M_e^*(y)\ \exp(i\omega t) \\ \Xi_r(t) &= \Xi_r^*\ \exp(i\omega t) \end{aligned}\right\} \tag{188b}$$

Substituting Equations (188) into (186), (185) and (187) and cancelling the exponential time dependency

$$-\omega^2 M_r \xi_r^* + (1 + i\, g_r)\omega_r^2 M_r \xi_r^* = \Xi_r^*,\ r = 1,2,3\ldots N \tag{189}$$

$$\Xi_r^* = -bR \int_o^1 L^*(\bar{y})\bar{w}_r(\bar{y})d\bar{y} + R \int_o^1 M_e^*(\bar{y})\bar{\phi}_r(\bar{y})d\bar{y} \tag{190}$$

$$\left.\begin{aligned} \bar{\phi}(\bar{y}) &= \sum_{s=1}^{N} \bar{\phi}_s(\bar{y})\xi_s^* \\ \bar{w}(\bar{y}) &= \sum_{s=1}^{N} \bar{w}_s(\bar{y})\xi_s^* \end{aligned}\right\} \tag{191}$$

Following the notation of Smilg and Wasserman [32] the amplitudes of aerodynamic lift and moment are defined as

$$\left.\begin{aligned} L^* &= -\pi \rho_\infty b^3\omega^2 [L_{he} \bar{w} + \bar{L}_{\alpha e} \bar{\phi}] \\ M_e^* &= \pi \rho_\infty b^4\omega^2 [M_{he} \bar{w} + M_{\alpha e} \bar{\phi}] \end{aligned}\right\} \tag{192}$$

L_{he}, $L_{\alpha e}$, M_{he} and $M_{\alpha e}$ are aerodynamic coefficients referenced to the elastic axis and are to be computed from the unsteady aerodynamic theory discussed earlier.

Substituting Equations (191) and (192) into the generalized aerodynamic force expression given by Equation (190).

$$\Xi_r^* = \pi \rho_\infty b^4\omega^2 R \sum_{s=1}^{N} a_{rs} \xi_r^* \tag{193}$$

where

$$a_{rs} = \int_0^1 \{L_{he}\, \bar{w}_r(\bar{y})\bar{w}_s(\bar{y}) + L_{\alpha e}\bar{w}_r(\bar{y})\bar{\phi}_s(\bar{y})$$

$$+ M_{he}\, \bar{\phi}_r(\bar{y})\bar{w}_s(\bar{y}) + M_{\alpha e}\, \bar{\phi}_r(\bar{y})\bar{\phi}_s(\bar{y})\}d\bar{y} \qquad (194)$$

Substituting Equation (193) into (189)

$$\left[-1 + (1 + i\, g_r)\left(\frac{\omega_r}{\omega}\right)^2\right] \bar{M}_r\, \xi_r^* = \sum_{s=1}^{N} a_{rs}\, \xi_r^* \qquad (195)$$

where $\bar{M}_r = \dfrac{M_r}{\pi\, \rho_\infty\, b^4\, R}$

Equation (195) can be written for all r modes in matrix form as

$$\left[\left[-1 + (1 + i\, g_r)\left(\frac{\omega_r}{\omega}\right)^2\right]\bar{M}_r\right] \{\xi^*\} = [A]\{\xi^*\} \qquad (196)$$

Equation (196) is a matrix equation representing a system of linear algebraic homogeneous equations and hence leads to an eigenvalue problem. When the determinant of the coefficient matrix vanishes a non-trivial solution exists for $\{\xi^*\}$. The speed and frequency for which the characteristic determinant vanishes corresponds to states that system can sustain simple harmonic oscillations. The lowest air speed is the flutter speed. The method of solution of characteristic determinant is indicated in the next section.

Method of Solution

The method used to solve the flutter determinant is often called k-method. It requires the introduction of an artificial damping coefficient, g, i.e., $(1 + i\, g_r)$ in Equation (196) is replaced by $(1 + i\, g_r + i\, g)$. Then $(1 + i\, g_r + i\, g)$ can be approximated by the product $(1 + i\, g_r)(1 + i\, g)$ where the error introduced by the approximation vanishes at $g = 0$. This was suggested by Desmairais and Bennett [33]. The introduction of g in the flutter equations provides the subcritical flutter characteristics of the system. The value of g computed by treating it as a dependent variable is the critical value, that is, the structural damping coefficient (in one of the degrees of freedom) required for oscillations of the system to occur at constant amplitude. The magnitude of the critical value of the structural damping coefficient g at a given airspeed indicates whether or not flutter can be expected to occur at that speed. Further it indicates the rapidity with which the flutter oscillations will built up at a given air speed. In addition, the slope of the damping curve when plotted against airspeed, is an indication of the dangers involved in approaching the flutter speed. So the introduction of the structural damping coefficient g provides additional information about subcritical flutter characteristics eventhough the flutter speed can be obtained without it. With the introduction of g Equation (196) can be written as

$$\left[\left[\frac{1}{\bar{M}_r \omega_r^2 (1 + i g_r)} \right] ([A] + [\bar{M}_r]) - \lambda [1] \right] \{\xi^*\} = \{0\} \tag{197}$$

where

$$\lambda = (1 + i g) \left(\frac{1}{\omega}\right)^2$$

If the rotor speed Ω is specified, then the vibration analysis can be performed using the transmission matrix method. The natural frequencies and mode shapes are known, and hence the generalized masses can be calculated. Specifying the modal dependent structural damping constants and the density of the fluid medium only the aerodynamic matrix, [A], will need to be computed in the eigenvalue problem of Equation (197).

Aerodynamic Matrix Computation

The generalized aerodynamic forces (elements of aerodynamic matrix) represent the forces associated with dynamic variations of plunging and pitching motions from the steady state values. The helicopter would probably be flying at some positive angle of attack. There might also be contributions to lift and moment due to camber of the airfoil. For flutter prediction the equilibrated system of steady-state forces and moments are subtracted leaving only time dependent portions. Hence the pitching displacement

due to steady-state angle of attack is not taken into account while calculating the generalized aerodynamic forces. The computation of the elements of the aerodynamic matrix requires a knowledge of the natural vibration characteristics and the unsteady aerodynamic coefficients referenced to the elastic axis at various spanwise locations. The method for obtaining the natural vibration characteristics is already indicated. But the unsteady aerodynamic theory discussed earlier gives the aerodynamic coefficients about the quarter-chord coefficients and the elastic axis coefficients as follows.

Consider an airfoil which is plunging and pitching as shown in Figure 5. Let the distance of the elastic axis from the midchord point be equal to 'ab'. From the geometry of Figure 5 the displacements can be related as follows.

$$\begin{aligned} \alpha_e &= \alpha_{c/4} \\ W_e &= W_{c/4} + (a + \tfrac{1}{2})b\ \alpha_{c/4} \\ M_e &= M_{c/4} + L(a + \tfrac{1}{2})b \end{aligned} \tag{198}$$

Following the notation of Smilg and Wasserman [32], define the lift and moment in terms of aerodynamic coefficients as shown below.

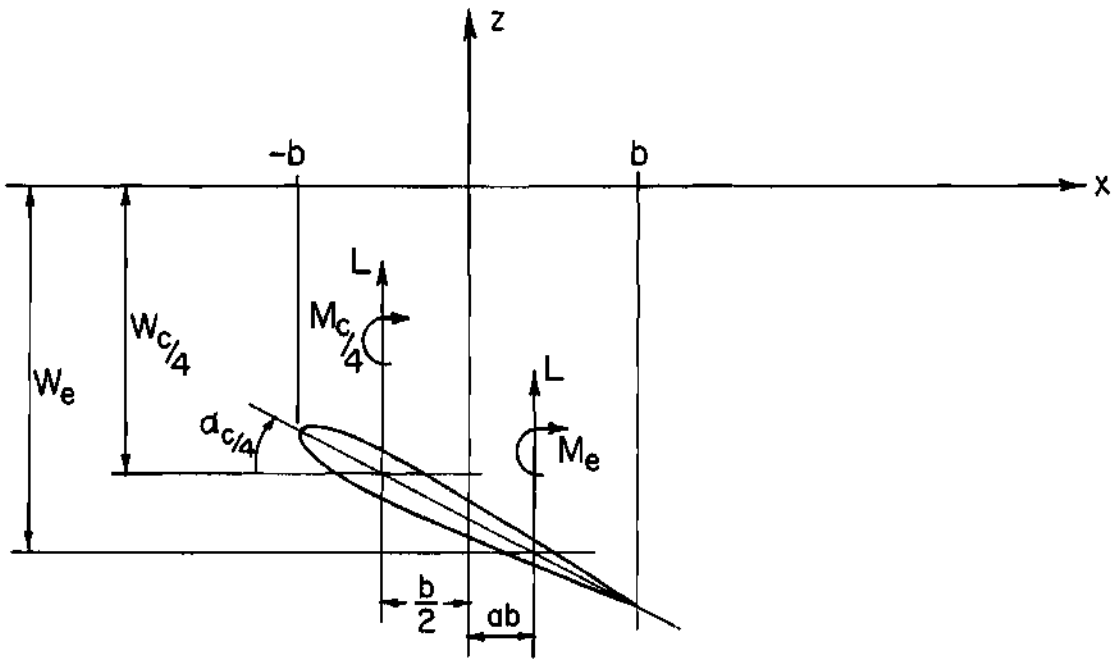

Figure 5. Displacement Relations, Quarter-chord to Elastic Axis

$$L = -\pi \rho_\infty b^3 \omega^2 \left[L_{he} \frac{W_e}{b} + L_{\alpha e} \alpha_e\right]$$

$$M_e = \pi \rho_\infty b^4 \omega^2 \left[M_{he} \frac{W_e}{b} + M_{\alpha e} \alpha_e\right] \tag{199}$$

Using Equations (166), (198) and (199) the following relations can be obtained

$$\begin{aligned} L_{he} &= L_h \\ L_{\alpha e} &= L_\alpha - L_h\left(\tfrac{1}{2} + a\right) \\ M_{he} &= M_h - L_h\left(\tfrac{1}{2} + a\right) \\ M_{\alpha e} &= M_\alpha - \left(L_\alpha + M_h\right)\left(\tfrac{1}{2} + a\right) + L_h\left(\tfrac{1}{2} + a\right)^2 \end{aligned} \tag{200}$$

As already mentioned to compute the aerodynamic coefficients L_h, L_α, M_h and M_α at any spanwise location it is required to know the following

1. number of blades
2. phase differences between oscillations of blades
3. Mach number
4. inflow ratio
5. frequency ratio
6. reduced frequency

Rotor speed, number of blades and phase differences are specified in the problem. Mach number can be calculated (at a given spanwise location, r) since the rotor speed is known. The inflow ratio at a given spanwise location can be

calculated from combined axial momentum and blade element theory. The corresponding equation is given below [23].

$$\bar{h} = \frac{2}{Qb} R \left[\sqrt{\left(\frac{V}{2} + \frac{\bar{a}\,\sigma}{16} \cos\alpha\right)^2 + \frac{\bar{a}\,\sigma\, v}{8R} \sin\alpha} - \left(\frac{V}{2} + \frac{\bar{a}\,\sigma}{16} \cos\alpha\right) \right] \tag{201}$$

where

$\bar{h} = h/b$

α = angle of attack

v = vertical velocity of rotor hub

$\sigma = \frac{2\,b\,Q}{\pi\,R}$

$\bar{a}$ = lift - curve slope $\approx \frac{5.75}{\sqrt{1 - M_\infty^2}}$

If a frequency ratio is chosen then reduced frequency can be calculated for a given spanwise location. So in essence for a given rotor speed, frequency ratio and phase angle the aerodynamic matrix can be computed by specifying the pertinent aerodynamic and structural data of the system.

Numerical Procedure

The following numerical procedure is suggested by Viswanathan [29] for obtaining the flutter speed of a single bladed rotor with appropriate modifications for a multi-bladed rotor.

1. A trial rotor speed Ω_1 is chosen
2. Phase angles ψ_q (q = 1,2...Q-1) are specified (in the case of a two bladed rotor only ψ_1 need be specified)
3. A suitable set of frequency ratios m_1, $m_2 \ldots m_\ell$ are chosen. Corresponding to each frequency ratio the following is done.

Let the frequency ratio be m_j $(1 \leq j \leq \ell)$. As mentioned previously, corresponding to rotor speed Ω_1, frequency ratio m_j, and phase angles ψ_q (q = 1,2...Q-1) the elements of the complex matrix, Equation (197), of the eigenvalue problem can be computed. Complex eigenvalues of the problem can then be computed. Let $\lambda_1^{(j)}$, $\lambda_2^{(j)}, \ldots \lambda_N^{(j)}$ represent these eigenvalues. For the solution of the eigenvalue problem the Francis QR-Transformation [10] or Desmarais and Bennett's procedure [33] can be used. The repeated use of either the QR-Transformation or Desmarais and Bennett's procedure does not make much difference in computer time. The primary advantage in Desmarais and Bennett's procedure is to maintain the continuity of the eigenvalues when going from one frequency ratio to another. For each complex eigenvalue, $\lambda_i^{(j)}$, $1 \leq i \leq N$, ω and g are obtained from the

$$\lambda_i^{(j)} = \left(1 + i\, g_i^{(j)}\right)\left(\frac{1}{\omega_i^{(j)}}\right)^2 \qquad (202)$$

The coefficient i represents $\sqrt{-1}$. The corresponding value for rotor speed can be calculated as

$$\Omega_i^{(j)} = \frac{\omega_i^{(j)}}{m_j} \tag{203}$$

It is required to order the eigenvalues, $\lambda_i^{(j)}$, i = 1,N, on the basis of damped natural frequency $\omega_i^{(j)}$ or $g_i^{(j)}$ or both. The $g_i^{(j)}$ corresponds to damping required in the i-th aeroelastic mode for the j-th frequency ratio.

Having obtained all the dampings for all the aeroelastic modes and frequency ratios, the frequency ratio vs damping plots can be made. Frequency ratio vs damping plots are preferable rather than velocity vs damping ratio plots since damping is a single valued function of the frequency ratio. From these plots the rotor speeds corresponding to g = 0 in all the aeroelastic modes are obtained. Interpolation can be used for this purpose. The lowest value among these rotor speeds is picked. If this lowest value is same as the rotor speed originally specified, then that value is the flutter speed. Four or five iterations are normally required. Each iteration starts with a new rotor speed which can be guessed from the results of the previous iterations. The flutter speed obtained corresponds to the phase angle specified.

CHAPTER X

DISCUSSION OF RESULTS

The object of this study is to determine the effect of phase difference of oscillation for a two bladed rotor on the flutter speed. In this chapter the aerodynamic coefficients computed by the unsteady aerodynamic theory are presented for typical parameters, to show the significance of phase angle. The results of flutter analyses for a sample two bladed rotor are also presented as a function of phase angle.

Aerodynamic Coefficients

The numerical values of aerodynamic coefficients for a two bladed rotor given in Reference 27 were found to be in error. Hence aerodynamic coefficients for typical values of reduced frequency, frequency ratio and inflow ratio have been recomputed and are given in Table 1 for $M_\infty = 0.5$ and various phase angles. For the case considered Real (M_h) and Imag (M_α) do vary greatly. Other aerodynamic coefficients also show considerable variation with phase angle. So before going to the flutter analysis of a two bladed rotor, a conclusion can be drawn that the phase angle could be an important factor for flutter. The aerodynamic coefficients

given in Table 27 correspond to a preselected reference blade. It is interesting to note that they are not symmetric about the phase angle π. This implies that the aerodynamic loads on the reference blade are different when the other blade is leading or lagging the reference blade by the same amount.

Aerodynamic coefficients for typical values of reduced frequency and inflow ratio are given in Table 28 for a two bladed rotor at $M_\infty = 0.5$, $\psi_1 = \frac{3\pi}{2}$. It can be observed from the values of the aerodynamic coefficients that they vary rapidly with the frequency ratio and as such the generalized aerodynamic forces will also vary rapidly with frequency ratio. So the procedure that is usually followed in fixed-wing flutter analyses, viz. computing a very few generalized forces corresponding to preselected reduced frequencies and using a high quality interpolation procedure for obtaining the generalized forces for intermediate values of reduced frequencies, can not be used in the case of a multibladed rotor flutter problem. Finally the aerodynamic coefficients which show significant variation with phase angle are plotted in Figures 6 and 7.

Critical Flutter Speed

A two bladed rotor with uniform properties for coupled bending and torsion degrees of freedom was considered to find the effect of phase angle on flutter speed.

Table 27. Aerodynamic coefficients

$Q = 2$; $M_\infty = 0.5$; $k = 0.1$; $\bar{h} = 0.25$; frequency ratio = 0.75

Phase angle	$R[L_h]$	$I[L_h]$	$R[\alpha_\alpha]$	$I[\alpha_\alpha]$	$R[M_h]$	$I[M_h]$	$R[M_\alpha]$	$I[M_\alpha]$
0	-4.5211	-26.0225	-265.509	19.2804	0.7634	-0.0918	-0.3494	-13.5081
$\pi/16$	-3.5902	-23.4805	-239.141	12.5009	0.7463	-0.0796	-0.2448	-13.3244
$\pi/8$	-3.2908	-21.2936	-216.957	11.6872	0.7305	-0.0729	-0.1935	-13.1598
$3\pi/16$	-3.3653	-19.4607	-198.689	14.2622	0.7166	-0.0697	-0.1756	-13.0177
$\pi/4$	-3.6577	-17.9311	-183.673	18.7148	0.7046	-0.0688	-0.1784	-12.8961
$5\pi/16$	-4.0775	-16.6470	-171.241	24.1969	0.6941	-0.0693	-0.1941	-12.7918
$3\pi/8$	-4.5733	-15.5579	-160.836	30.2461	0.6849	-0.0708	-0.2182	-12.7015
$7\pi/16$	-5.1170	-14.6230	-152.023	36.6199	0.6768	-0.0730	-0.2480	-12.6224
$\pi/2$	-5.6937	-13.8108	-144.471	43.2021	0.6695	-0.0757	-0.2820	-12.5524
$9\pi/16$	-6.2969	-13.0973	-137.932	49.9506	0.6630	-0.0787	-0.3192	-12.4897
$5\pi/8$	-6.9251	-12.4642	-132.223	56.8692	0.6569	-0.0821	-0.3594	-12.4328
$11\pi/16$	-7.5804	-11.8981	-127.212	63.9919	0.6514	-0.0859	-0.4026	-12.3808
$3\pi/4$	-8.2675	-11.3894	-122.807	71.3753	0.6461	-0.0900	-0.4489	-12.3327
$13\pi/16$	-8.9933	-10.9318	-118.952	79.0958	0.6412	-0.0945	-0.4989	-12.2881
$7\pi/18$	-9.7672	-10.5222	-115.625	87.2496	0.6366	-0.0995	-0.5532	-12.2465
$15\pi/16$	-10.6010	-10.1609	-112.841	95.9546	0.6322	-0.1050	-0.6128	-12.2079
π	-11.5095	-9.8524	-110.661	105.3542	0.6280	-0.1112	-0.6788	-12.1724
$17\pi/16$	-12.5111	-9.6070	-109.204	115.6218	0.6241	-0.1182	-0.7527	-12.1406
$9\pi/8$	-13.6280	-9.4427	-108.675	126.9637	0.6206	-0.1262	-0.8366	-12.1135
$19\pi/16$	-14.8873	-9.3903	-109.407	139.6183	0.6177	-0.1355	-0.9330	-12.0932
$10\pi/8$	-16.3192	-9.4995	-111.930	153.8391	0.6156	-0.1465	-1.0447	-12.0831
$21\pi/16$	-17.9533	-9.8511	-117.079	169.8410	0.6149	-0.1595	-1.1751	-12.0891
$11\pi/8$	-19.8053	-10.5735	-126.157	187.6546	0.6165	-0.1748	-1.3270	-12.1208

Table 27 (Continued)

Phase angle	$R[L_h]$	$I[L_h]$	$R[\alpha_\alpha]$	$I[\alpha_\alpha]$	$R[M_h]$	$I[M_h]$	$R[M_\alpha]$	$I[M_\alpha]$
23π/16	-21.8448	-11.8647	-141.113	206.7757	0.6220	-0.1927	-1.5008	-12.1939
3π/2	-23.9203	-14.0037	-164.591	225.4115	0.6338	-0.2126	-1.6883	-12.3319
25π/16	-25.6229	-17.2963	-199.240	239.1651	0.6550	-0.2321	-1.8619	-12.5635
13π/8	-26.1434	-21.8201	-245.032	239.8592	0.6879	-0.2452	-1.9605	-12.9052
27π/16	-24.4514	-26.8996	-294.176	217.8575	0.7294	-0.2429	-1.8957	-13.3183
7π/4	-20.2331	-30.8858	-329.858	171.6647	0.7679	-0.2194	-1.6223	-13.6798
29π/16	-14.7446	-32.2927	-338.461	115.3345	0.7896	-0.1811	-1.2178	-13.8590
15π/8	-9.8472	-31.1979	-322.617	67.4160	0.7914	-0.1422	-0.8264	-13.8380
31π/16	-6.4657	-28.7647	-294.892	36.0045	0.7800	-0.1119	-0.5346	-13.6947
2π	-4.5211	-26.0225	-265.509	19.2804	0.7634	-0.0918	-0.3494	-13.5081

Table 28. Aerodynamic Coefficients

$Q = 2$; $M_\infty = 0.5$; $k = 0.1$; $\bar{h} = 0.25$; Phase Angle = $3\pi/2$

Frequency Ratio	$R[L_h]$	$I[L_h]$	$R[L_\alpha]$	$I[L_\alpha]$	$R[M_h]$	$I[M_h]$	$R[M_\alpha]$	$I[M_\alpha]$
0	0.831	-0.797	-7.7238	-9.1065	0.5853	-0.0003	0.3887	-11.634
0.125	41.990	7.326	114.64	-412.90	0.6083	0.3247	3.6637	-11.540
0.250	4.426	-66.526	-662.32	-110.72	1.0855	-0.1073	-0.1839	-16.746
0.375	-16.179	-42.016	-437.20	119.99	0.8595	-0.2117	-1.4539	-14.589
0.500	-20.079	-31.392	-334.78	169.62	0.7720	-0.2193	-1.6170	-13.721
0.625	-22.636	-23.584	-259.19	203.00	0.7083	-0.2225	-1.7131	-13.086
0.750	-23.920	-14.004	-164.59	225.41	0.6338	-0.2126	-1.6883	-12.332
0.875	-17.572	-1.2715	-30.838	174.59	0.5514	-0.1391	-1.0349	-11.433
1.000	-0.6725	-0.9070	-10.236	5.8302	0.5830	-0.0117	0.2715	-11.623

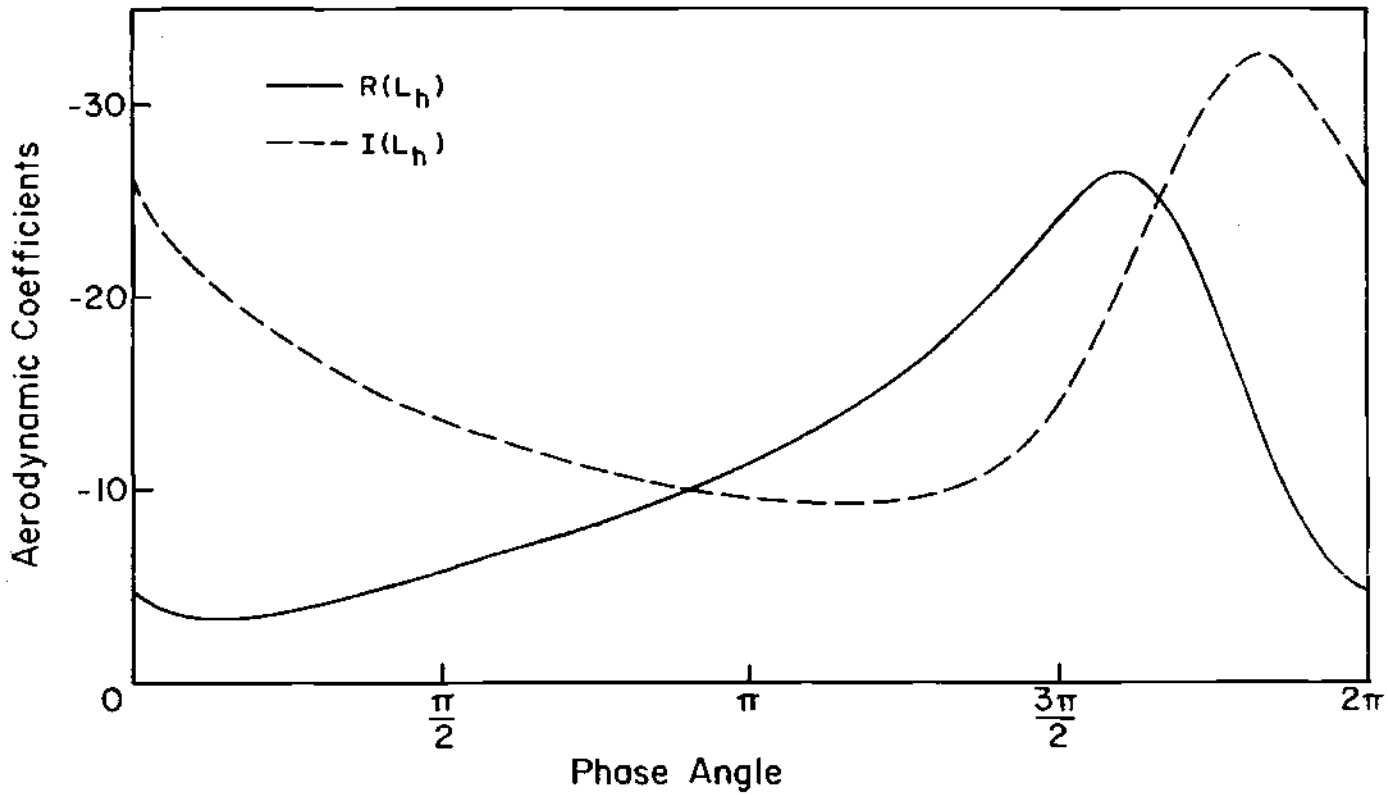

Figure 6. Variation in L_h with Phase Angle

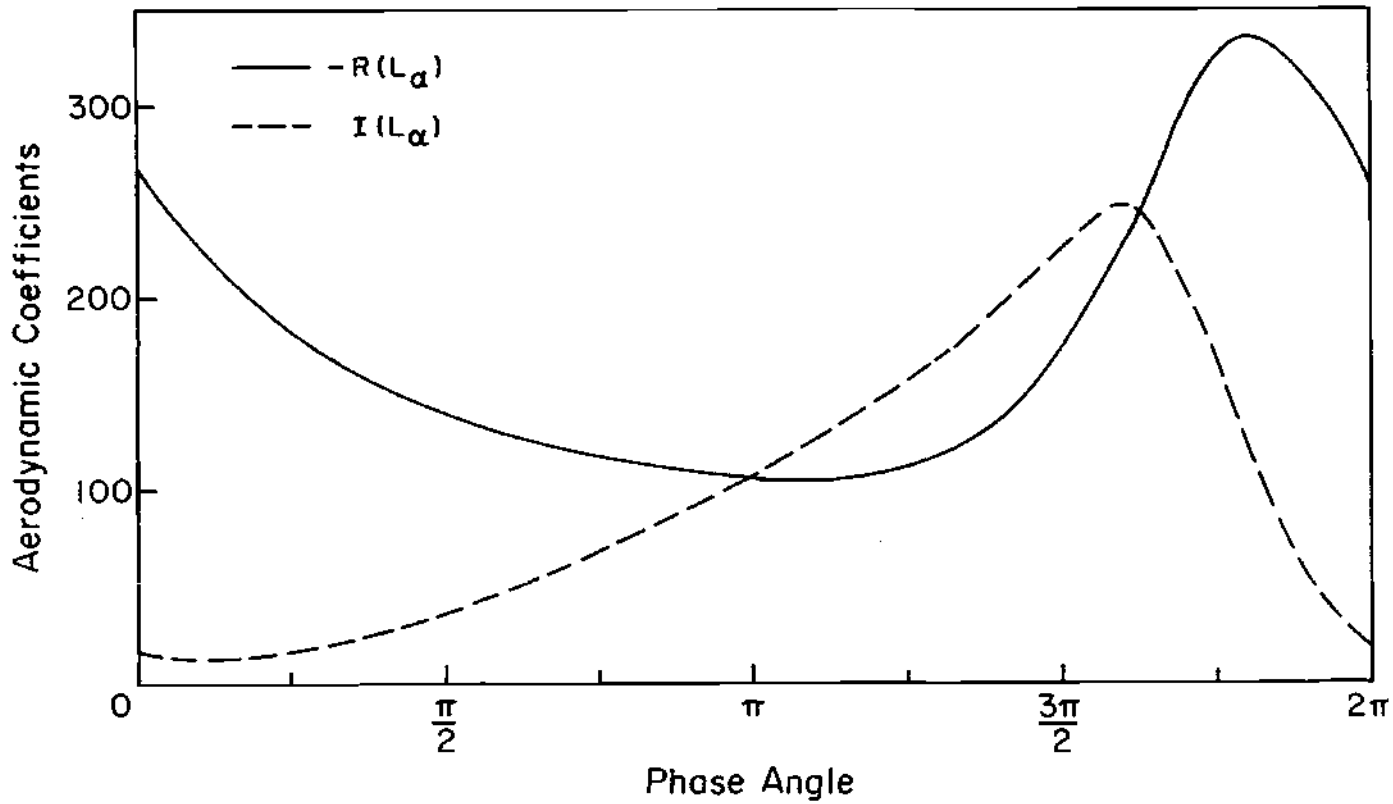

Figure 7. Variation of L_α with Phase Angle

The transmission matrix method was used to obtain the natural vibration characteristics, and Jones and Rao's unsteady aerodynamic theory was used to compute the generalized aerodynamic forces. The k-method as described previously was used to solve the flutter determinant. The flutter speeds for various phase angles (between $0-2\pi$) were computed and the results are presented in Table 29. The flutter speeds are plotted against phase angle in Figure 8. The properties of the two bladed rotor considered are given below.

1. Radius of the rotor = 46.0 inches
2. Semi-chord = 2.0 inches
3. Distance between mass and elastic axis = -0.45 inches
4. Mass per unit span of the blade = 0.00135 slugs/inch
5. Bending stiffness = 26000 $lbf\text{-}in^2$
6. Torsional stiffness = 10000 $lbf\text{-}in^2$
7. Mass radius of gyration squared about an axis normal to major axis at the elastic axis = 0.952576 in^2
8. Polar radius of gyration squared of cross-sectional area effective in carrying tensile stresses, about elastic axis = 0.898704 in^2

9. Mass radius of gyration squared about major axis = 0.01 in^2
10. Density of the fluid far from the rotor = 0.002378 $slugs/ft^3$
11. Speed of sound far from the rotor = 1117 ft/sec
12. Angle of attack of the blade at the root = 4.0 degrees
13. Distance of the elastic axis behind mid chord = -0.92 inches
14. Number of modes used in the flutter analysis = 3
15. Root boundary condition = Hinge
16. Structural damping in all three modes = 0.0

It can be observed from Table 29 that the phase angle $\frac{3\pi}{2}$ corresponds to the lowest flutter speed viz., 67.4942 rad/sec and is the critical flutter speed for the two bladed rotor at hand. The flutter speed corresponding to zero phase angle viz., 79.6322 rad/sec can be obtained from the formulation of a single bladed rotor by using the equivalent single bladed rotor concept. This flutter speed corresponding to equivalent single bladed rotor is 18% higher than the critical flutter speed. Hence the results from the zero phase angle case are unconservative. All helicopters are at least two bladed and it is absolutely

Table 29. Flutter Speeds

Serial Number	Phase Angle Radians	Flutter Speed Rad/Sec
1.	0	79.6322
2.	$\pi/8$	83.5011
3.	$\pi/4$	87.4255
4.	$\pi/3$	84.7550
5.	$5\pi/12$	82.3671
6.	$\pi/2$	80.5264
7.	$5\pi/8$	78.7646
8.	$3\pi/4$	78.8973
9.	$5\pi/6$	80.4528
10.	$11\pi/12$	83.4781
11.	π	88.1924
12.	$51\pi/48$	81.1229
13.	$9\pi/8$	77.0778
14.	$5\pi/4$	71.7921
15.	$11\pi/8$	68.7799
16.	$3\pi/2$	67.4942
17.	$13\pi/8$	67.7465
18.	$7\pi/4$	70.4756
19.	$15\pi/8$	77.0188
20.	2π	79.6322

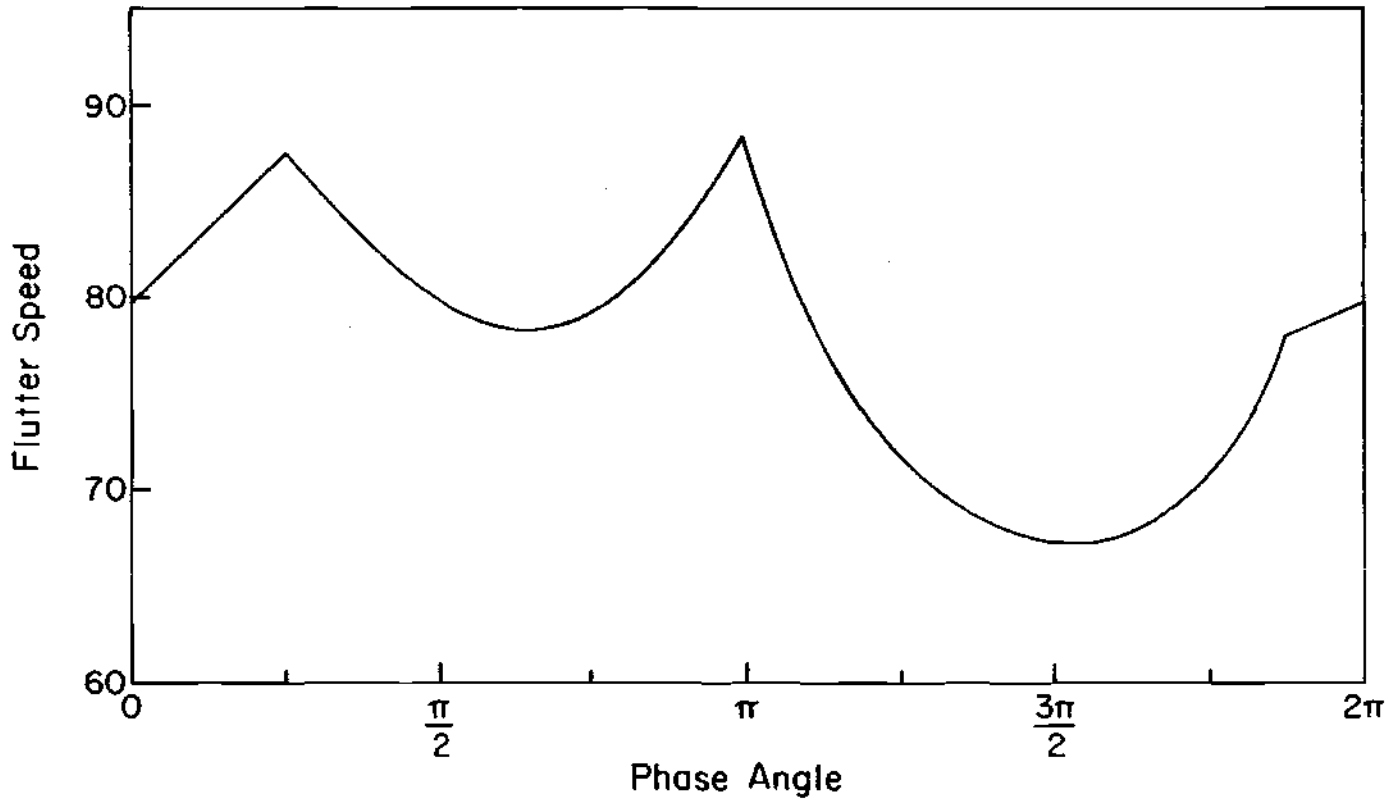

Figure 8. Variation of Flutter Speed with Phase Angle

necessary that flutter speed be calculated sweeping the phase angle between 0 to 2π radians. The highest flutter speed 88.1924 rad/sec corresponds to phase angle π and this value is 30.7% higher than the critical flutter speed. Hence the phase angle has a predominant effect on the flutter speed and thus is an important factor for critical flutter speed of a multibladed rotor.

In general the component of aerodynamic force (or generalized aerodynamic force) which is 90° out of phase with the displacement is directly responsible for any possible flutter. The aerodynamic forces depend on various parameters like dynamic pressure of the flow, rotor geometry, the mode of motion (deflection surface), inflow ratio, frequency ratio and reduced frequency of oscillation etc. It is through these dependences, the inertial and elastic characteristics of the structure exercise their influence. Because of this large number of dependences for flutter, one can not conclude which value of the phase angle leads to critical flutter speed of a two bladed rotor. Hence shape of the curve shown in Figure 8 may vary from one rotor system to another.

The first three normal modes were used in the flutter analysis. The first one is a pure flapping mode, the second is predominantly bending, and the third is predominantly a torsional mode. For all phase angles for which flutter speeds were computed, it was observed that the flutter mode

was the second aeroelastic mode. A similar type of flutter phenomena was observed in all the cases (bending-torsion flutter). So in this case the effect of phase angle on flutter is not due to the occurrence of different kinds of flutter phenomena but due to its effect on the generalized aerodynamic forces through the unsteady aerodynamic coefficients.

When the damping function for any aeroelastic mode has close roots (i.e., when damping vanishes in any aeroelastic mode for nearly equal values of frequency ratio) there exists the possibility of missing that root when the frequency-ratio scanning technique is used. When the roots that are close happen to be the lowest, then there exists a risk of missing the flutter speed and in such cases special attention is required. This kind of problem was encountered while computing the flutter speed for the phase angle $\frac{7\pi}{4}$, and the corresponding results are shown in Table 30. The root was detected by a close scanning of frequency ratios. Further it can be observed from Table 29 that the flutter speeds are not symmetric about the phase angle π. It was mentioned earlier that the aerodynamic loads on the reference blade are different when the other blade leads or lags the reference blade by the same amount. Because of this fact the flutter speeds are not symmetric about the phase angle π. So the flutter speeds computed and given in Table 29

Table 30. Flutter Results for Phase Angle $\frac{7\pi}{4}$

Rotor speed = 70.2 Rad/Sec; Damping factor = 0.0 (All the 3 modes)

Mode Number	Frequency Ratio	Frequency Rad/Sec	Rotor Speed Rad/Sec
1	0.975325	92.3677	94.7045
2	2.573295	181.3545	70.4756
2	2.557302	181.3409	70.9110
2	2.358302	180.2730	76.4419
2	2.038655	194.8187	95.5624
2	1.376477	141.0117	102.4440
2	1.048902	130.5558	124.4690
3	2.536749	227.5406	89.6977
3	2.039290	311.1087	152.5574

The lowest speed in the last entry corresponds to the flutter speed.

correspond to the chosen reference blade and the phase angles correspond to the phase lead in oscillation of the other blade. When the reference blade is fluttering the other blade may not be in a flutter condition because of the difference in air loads on the two blades.

The unsteady aerodynamic theory used in the analysis excludes the possibility of any decaying motion of the other blade as it should oscillate with the same amplitude and frequency as the reference blade. This assumption was made in the unsteady aerodynamic theory to make the mathematical analysis tractable. It is proposed that the definition of a flutter condition for a multibladed rotor be when any one of the blades experiences flutter regardless of the condition of the other blades experience. This kind of a situation is not uncommon in multibladed rotor aeroelastic instability problems. For example, in the case of flutter of a multibladed rotor in forward flight, the advancing blade might experience flutter at some azimuthal location and simultaneously the retreating blade may not be in a flutter condition. In the present analysis there are certain situations when both the blades of a two-bladed rotor experience identical air loads, i.e., when phase lead ψ_1 of the other blade is such that $e^{i\psi_1} = e^{-i\psi_1}$. In those conditions both the blades experience flutter simultaneously.

An experimental investigation for correlation of the analytical results obtained above would require that amplitude and frequency of oscillation of the reference blade be fed into the other blade to make it oscillate with the same frequency and amplitude as the reference blade. This is necessary to satisfy the assumption of the unsteady aerodynamic theory used in the analysis.

CHAPTER XI

CONCLUSIONS AND RECOMMENDATIONS

The compressible unsteady aerodynamic theory of Jones and Rao, and the transmission matrix method of obtaining natural vibration characteristics developed by Murthy were used to study the effect of phase angle on critical flutter speed of a two bladed rotor. The k-method was used to solve the flutter determinant.

Conclusions

1. The unsteady aerodynamic coefficients vary significantly with phase angle, and for a given phase angle they vary rapidly with the frequency ratio.
2. The phase angle is an important factor for critical flutter speed of a multibladed rotor.
3. The effect of phase on critical flutter speed of a two bladed rotor may not necessarily be due to the occurrence of different kinds of flutter phenomena but due to its effect on the generalized aerodynamic forces.
4. The flutter speed obtained by the equivalent single bladed rotor corresponding to zerophase angle is unconservative.

5. There is no general conclusion which phase angle leads to to critical flutter of a multibladed rotor. Each rotor system must be studied independently.

Recommendations

1. Experimental investigations are necessary for multi-bladed rotor flutter to verify the importance of the phase angle.
2. The flutter analysis should be extended to rotating, non-uniform twisted rotor blades with combined chordwise bending, flapwise bending and torsion. In the case of a multibladed rotor, the elastic and inertial couplings that exists between the blades through the root and rotor shaft should be included.
3. A parametric study is required to determine which phase angle leads to the critical flutter speed for a given two bladed rotor.
4. Further investigations are necessary for the rotors with more than two blades.
5. An obvious extension for the present study is the forward flight condition, for which the unsteady aerodynamic theories must be developed.

APPENDIX A

INTEGRATING AND DIFFERENTIATING MATRICES

Development of the Integrating Matrix

The integrating matrix is a means by which a continuous function may be integrated with the use of a finite-difference approach. This numerical method is based upon the assumption that the function f(x) may be represented by a polynomial of degree r as given in the following equation.

$$f(x) = a_o + a_1 x + a_2 x^2 + \ldots + a_r x^r \qquad \text{(A-1)}$$

Integrating matrices upto order seven are listed in Reference 9. The third order integrating matrix has been used to solve the 1) flapwise bending problem and the coupled flapwise bending and torsion vibration problems in Chapter IV. The derivation of third-order integrating matrix is given below.

The function f(x) is assumed to be approximated by a third degree polynomial as

$$f(x) = a_o + a_1 x + a_2 x^2 + a_3 x^3 \qquad \text{(A-2)}$$

Equation (A-2) may be expressed in the form of Newton's forward-difference interpolation formula as

$$f(x) = g(p) = f_o + \frac{1}{1!}\, p\, \Delta\, f_o + \frac{1}{2!}\, p(p-1)\, \Delta^2\, f_o +$$

$$\frac{1}{3!}\, p(p-1)(p-2)\, \Delta^3\, f_o \qquad \text{(A-3)}$$

where

f_i denotes the value of $f(x)$ at the station $x = x_i$,

$i = 0,1,\ldots n$

$$p = \frac{x - x_o}{h}$$

h = interval of equally spaced stations

$$\Delta^r\, f_o = (E-1)^r\, f_o$$

The shifting operator E is defined by

$$E^j\, f_i = f_{i+j}$$

Equation (A-3) leads to

$$g(p) = f_o + p(f_1 - f_o) + \frac{1}{2}(p^2 - p)(f_2 - 2f_1 + f_o)$$

$$+ \frac{1}{6}(p^3 - 3p^2 + 2p)(f_3 - 3f_2 + 3f_1 - f_o) \qquad \text{(A-4)}$$

The integration of $f(x)$ from x_i to x_j is given by

$$\int_{x_i}^{x_j} f(x)\, dx = h \int_i^j g(p)\, dp \qquad \text{(A-5)}$$

Equation (A-4) may be substituted into Equation (A-5) and integrated over each of the three intervals between x_o to x_3 to give

$$\int_{x_o}^{x_1} f(x)\ dx = \frac{h}{24}\ (9\ f_o + 19\ f_1 - 5\ f_2 + f_3) \qquad \text{(A-6)}$$

$$\int_{x_1}^{x_2} f(x)\ dx = \frac{h}{24}\ (-f_o + 13\ f_1 + 13\ f_2 - f_3) \qquad \text{(A-7)}$$

$$\int_{x_2}^{x_3} f(x)\ dx = \frac{h}{24}\ (f_o - 5\ f_1 + 19\ f_2 + 9\ f_3) \qquad \text{(A-8)}$$

The function f(x) may be integrated over a large number of equal-length intervals by repeated use of Equation (A-7). Equation (A-7) is chosen since it is applicable to the center interval and has the smallest associated error of the three equations. From Equations (A-6) to (A-8), numerical integration of f(x) over each of the n intervals x_o to x_n is given by

$$\int_{x_o}^{x_1} f(x)\,dx = \frac{h}{24}\,(9\,f_o + 19\,f_1 - 5\,f_2 + f_3)$$

$$\int_{x_1}^{x_2} f(x)\,dx = \frac{h}{24}\,(-f_o + 13\,f_1 + 13\,f_2 - f_3)$$

$$\int_{x_2}^{x_3} f(x)\,dx = \frac{h}{24}\,(-f_1 + 13\,f_2 + 13\,f_3 - f_4)$$

$$\vdots \qquad \text{(A-9)}$$

$$\int_{x_{n-2}}^{x_{n-1}} f(x)\,dx = \frac{h}{24}\,(-f_{n-3} + 13\,f_{n-2} + 13\,f_{n-1} - f_n)$$

$$\int_{x_{n-1}}^{x_n} f(x)\,dx = \frac{h}{24}\,(f_{n-3} - 5\,f_{n-2} + 19\,f_{n-1} + 9\,f_n)$$

The relations in Equations (A-9) may be expressed in matrix notation by

$$\left\{ \int_{x_{i-1}}^{x_i} f(x)\,dx \right\} = [A_3]\ \{f\} \qquad \text{(A-10)}$$

where

$$\left\{ \int_{x_{-1}}^{x_i} f(x)\, dx \right\} = \begin{Bmatrix} 0 \\ \int_{x_o}^{x_1} f(x)\, dx \\ \int_{x_1}^{x_2} f(x)\, dx \\ \vdots \\ \int_{x_{n-1}}^{x_n} f(x)\, dx \end{Bmatrix} \qquad \text{(A-11)}$$

$$\{f\} = \begin{Bmatrix} f_o \\ f_1 \\ f_2 \\ \vdots \\ f_n \end{Bmatrix} \qquad \text{(A-12)}$$

$$[A] = \frac{h}{24}\begin{bmatrix}
0 & 0 & 0 & 0 & 0 & 0 & \cdots & 0 \\
9 & 19 & -5 & 1 & 0 & 0 & & \\
-1 & 13 & 13 & -1 & 0 & 0 & & \\
0 & -1 & 13 & 13 & -1 & 0 & & \\
0 & 0 & -1 & 13 & 13 & -1 & & \\
 & & & & & & & \\
 & & & & -1 & 13 & 13 & -1 & 0 \\
 & & & & 0 & -1 & 13 & 13 & -1 \\
0 & \cdots & & & 0 & 1 & -5 & 19 & 9
\end{bmatrix}$$

(n+1) x (n+1) (A-13)

The integral of f(x) from x_o to x_i may be obtained by merely summing the integrals for each interval from x_o to x_i. That is,

$$\int_{x_o}^{x_i} f(x)\,dx = \int_{x_o}^{x_1} f(x)\,dx + \int_{x_1}^{x_2} f(x)\,dx + \ldots + \int_{x_{i-1}}^{x_i} f(x)\,dx \quad \text{(A-14)}$$

This equation is given in matrix notation for i = 0, 1,2,...n by

$$\left\{ \int_{x_o}^{x_i} f(x)\,dx \right\} = [B] \int_{x_{i-1}}^{x_i} f(x)\,dx \qquad \text{(A-15)}$$

where

$$\left\{ \int_{x_o}^{x_i} f(x)\,dx \right\} = \left\{ \begin{array}{l} 0 \\ \int_{x_o}^{x_1} f(x)\ dx \\ \int_{x_o}^{x_2} f(x)\ dx \\ \vdots \\ \int_{x_o}^{x_n} f(x)\ dx \end{array} \right\} \qquad \text{(A-16)}$$

$$[B] = \begin{bmatrix} 1 & 0 & 0 & 0 & \cdots & 0 \\ 1 & 1 & 0 & 0 & & \vdots \\ 1 & 1 & 1 & 0 & & \vdots \\ 1 & 1 & 1 & 1 & \ddots & \vdots \\ \vdots & \vdots & \vdots & \vdots & 1 & 0 \\ 1 & 1 & 1 & 1 & \cdots & 1 \end{bmatrix} \qquad \text{(A-17)}$$

$(n+1) \times (n+1)$

Substituting Equation (A-10) into Equation (A-15) gives

$$\left\{ \int_{x_o}^{x_i} f(x)\, dx \right\} = [B][A_3]\{f\} \qquad \text{(A-18)}$$

The third order integrating matrix is then defined as

$$[I] = [B]\ [A_3] \qquad \text{(A-19)}$$

Development of the Differentiating Matrix

Similar to integrating matrix, the differentiating matrix is a means by which a continuous function may be differentiated with the use of a finite-difference approach. Differentiating matrices up to order five are listed in Reference 22. A fourth-order differentiating matrix was derived in Reference 23 using Newton's forward difference interpolation formula. The fourth-order differentiating matrix has been used to solve the coupled flapwise bending and torsion vibration problem in Chapter IV. The derivation of the fourth-order differentiating matrix is given below.

Newton's fourth-order forward difference interpolation leads to a relation similar to Equation (A-4) and can be written as

$$g(p) = f_o + p(f_1 - f_o) + \frac{1}{2}(p^2 - p)(f_2 - 2f_1 + f_o)$$

$$+ \frac{1}{6}(p^3 - 3p^2 + 2p)(f_3 - 3f_2 + 3f_1 - f_o) +$$

$$\frac{1}{24}(p^4 - 6p^3 + 11p^2 - 6p)(f_4 - 4f_3 + 6f_2 - 4f_1 + f_o)$$

(A-20)

Differentiation of this function with respect to x yields the desired approximate derivative of f(x) as

$$\frac{d\ f(x)}{dx} = \frac{1}{h}\frac{d\ g(p)}{dp} \qquad \text{(A-21)}$$

and the resulting differentiating matrix for n intervals as

$$[D] = \frac{1}{12h}\begin{bmatrix} -25 & 48 & -36 & 16 & -3 & 0 & \cdots & 0 \\ -3 & -10 & 18 & -6 & 1 & 0 & & \\ 1 & -8 & 0 & 8 & -1 & 0 & & \\ 0 & & & & & & & 0 \\ & & & 0 & 1 & -8 & 0 & 8 & -1 \\ & & & 0 & -1 & 6 & -18 & 10 & 3 \\ 0 & \cdots & 0 & 3 & -16 & 36 & -48 & 25 \end{bmatrix}$$

(n+1) x (n+1)

(A-22)

APPENDIX B

ORTHOGONALITY RELATION FOR COMBINED FLAPWISE BENDING, CHORDWISE BENDING AND TORSION PROBLEM

The governing differential equations of motion for combined flapwise bending, chordwise bending and torsion described by Equations (59) to (61) can be expressed in operator notation as follows. For algebraic simplification the quantities B_1, B_2, e_A, e_o are taken as zero in Equations (59) to (61)

$$L_{11}[\phi] + L_{12}[v] + L_{13}[w] = \omega^2 m k_m^2 \phi - \omega^2 m e \sin\beta\, v + \omega^2 m e \cos\beta\, w \qquad \text{(B-1)}$$

$$L_{21}[\phi] + L_{22}[v] + L_{23}[w] = \omega^2 m w + \omega^2 m e \cos\beta\, \phi \qquad \text{(B-2)}$$

$$L_{31}[\phi] + L_{32}[v] + L_{33}[w] = \omega^2 m v - \omega^2 m e \sin\beta\, \phi \qquad \text{(B-3)}$$

where

$$L_{11} \equiv -(GJ + T k_A^2)' \frac{d}{dx} - (GJ + T k_A^2) \frac{d^2}{dx^2}$$

$$+ \Omega^2 m[(k_{m_2}^2 - k_{m_1}^2)\cos 2\beta]$$

$$L_{12} \equiv -\Omega^2 m x e \sin\beta \frac{d}{dx} + \Omega^2 m e \sin\beta$$

$$L_{13} \equiv \Omega^2 m x e \cos\beta \frac{d}{dx}$$

$$L_{21} \equiv -(\Omega^2 m x e \cos\beta)' - \Omega^2 m x e \cos\beta \frac{d}{dx}$$

$$L_{22} \equiv A'' \frac{d^2}{dx^2} + 2A' \frac{d^3}{dx^3} + A \frac{d^4}{dx^4}$$

$$L_{23} \equiv B'' \frac{d^2}{dx^2} + 2B' \frac{d^3}{dx^3} + B \frac{d^4}{dx^4} + \Omega^2 m x \frac{d}{dx} - T \frac{d^2}{dx^2}$$

$$L_{31} \equiv \Omega^2 m e \sin\beta + (\Omega^2 m x e \sin\beta)'$$

$$+ \Omega^2 m x e \sin\beta \frac{d}{dx}$$

$$L_{32} \equiv C'' \frac{d}{dx^2} + 2C' \frac{d^3}{dx^3} + C \frac{d^4}{dx^4}$$

$$+ \Omega^2 m x \frac{d}{dx} - T \frac{d^2}{dx^2} - \Omega^2 m$$

$$L_{33} \equiv L_{22}$$

$$A = (EI_2 - EI_1) \sin \beta \cos \beta$$

$$B = EI_1 \cos^2 \beta + EI_2 \sin^2 \beta$$

$$C = EI_1 \sin^2 \beta + EI_1 \cos^2 \beta$$

Let ω_r and ω_s be two distinct eigenvalues and (ϕ_r, v_r, w_r) and (ϕ_s, v_s, w_s) be the corresponding eigenfunctions resulting from the solution of the problem described by Equations (B-1) to (B-3). The eigenvalue problem can be written as

$$L_{11}[\phi_r] + L_{12}[v_r] + L_{13}[w_r]$$

$$= \omega_r^2 m k_m^2 \phi_r - \omega_r^2 m e \sin \beta v_r + \omega_r^2 m e \cos \beta w_r \qquad \text{(B-4)}$$

$$L_{21}[\phi_r] + L_{22}[v_r] + L_{23}[w_r]$$

$$= \omega_r^2 m w_r + \omega_r^2 m e \cos \beta \phi_r \qquad \text{(B-5)}$$

$$L_{31}[\phi_r] + L_{32}[v_r] + L_{33}[w_r]$$

$$= \omega_r^2 m v_r - \omega_r^2 m e \sin \beta \phi_r \qquad \text{(B-6)}$$

Similarly the following equations can be written.

$$L_{11}[\phi_s] + L_{12}[v_s] + L_{13}[w_s]$$

$$= \omega_s^2 m k_m^2 \phi_s - \omega_s^2 m e \sin \beta v_s + \omega_s^2 m e \cos \beta w_s \qquad \text{(B-7)}$$

$$L_{21}[\phi_s] + L_{22}[v_s] + L_{23}[w_s]$$

$$= \omega_s^2 \, m \, w_s + \omega_s^2 \, m \, e \cos \beta \, \phi_s \qquad \text{(B-8)}$$

$$L_{31}[\phi_s] + L_{32}[v_s] + L_{33}[w_s]$$

$$= \omega_s^2 \, m \, v_s - \omega_s^2 \, m \, e \sin \beta \, \phi_s \qquad \text{(B-9)}$$

Multiplying Equation (B-4) by ϕ_s and (B-7) by ϕ_r, subtracting one result from the other, and integrating both sides of the equation between 0 to R yields

$$\int_o^R (\phi_s \, L_{11}[\phi_r] + \phi_s \, L_{12}[v_r] + \phi_s \, L_{13}[w_r]$$

$$- \phi_r \, L_{11}[\phi_s] - \phi_r \, L_{12}[v_s] - \phi_r \, L_{13}[w_s])dx$$

$$= (\omega_r^2 - \omega_s^2) \int_o^R m \, k_m^2 \, \phi_r \, \phi_s \, dx$$

$$+ \int_o^R (-\omega_r^2 \, m \, e \sin \beta \, v_r \phi_s + \omega_r^2 \, m \, e \cos \beta \, w_r \phi_s$$

$$+ \omega_s^2 \, m \, e \sin \beta \, v_s \phi_r - \omega_s^2 \, m \, e \cos \beta \, w_s \phi_r)dx \qquad \text{(B-10)}$$

Using a similar procedure on Equations (B-5) and (B-8) and on (B-6) and (B-9) the following two equations can be obtained.

$$\int_o^R (w_s L_{21}[\phi_r] + w_s L_{22}[v_r] + w_s L_{23}[w_r]$$

$$- w_r L_{21}[\phi_s] - w_r L_{22}[v_s] - w_r L_{23}[w_s])\, dx$$

$$= (\omega_r^2 - \omega_s^2) \int_o^R m\, w_r\, w_s$$

$$+ \int_o^R \omega_r^2\, m\, e \cos\beta\, \phi_r w_s - \omega_s^2\, m\, e \cos\beta\, \phi_s w_r \qquad \text{(B-11)}$$

$$\int_o^R (v_s L_{31}[\phi_r] + v_s L_{32}[v_r] + v_s L_{33}[w_r]$$

$$- v_r L_{31}[\phi_s] - v_r L_{32}[v_s] - v_r L_{33}[w_s])\, dx$$

$$= (\omega_r^2 - \omega_s^2) \int_o^R m\, v_r v_s\, dx$$

$$+ \int_o^R (-\omega_r^2\, m\, e \sin\beta\, \phi_r v_s + \omega_s^2\, m\, e \sin\beta\, \phi_s v_r)\, dx \qquad \text{(B-12)}$$

Adding Equations (B-10), (B-11) and (B-12) yields

$$\int_o^R (\phi_s L_{11}[\phi_r] + \phi_s L_{12}[v_r] + \phi_s L_{13}[w_r]$$

$$- \phi_r L_{11}[\phi_s] - \phi_r L_{12}[v_s] - \phi_r L_{13}[w_s]$$

$$+ w_s L_{21}[\phi_r] + w_s L_{22}[v_r] + w_s L_{23}[w_r]$$

$$- w_r L_{21}[\phi_s] - w_r L_{22}[v_s] - w_r L_{23}[w_s]$$

$$+ v_s L_{31}[\phi_r] + v_s L_{32}[v_r] + v_s L_{33}[w_r]$$

$$- v_r L_{31}[\phi_s] - v_r L_{32}[v_s] - v_r L_{33}[w_s])\, dx$$

$$= (\omega_r^2 - \omega_s^2) \int_o^R m \{k_m^2 \phi_r\phi_s + w_r w_s + v_r v_s$$

$$- e \sin \beta \ (\phi_r v_s + \phi_s v_r)$$

$$+ e \cos \beta \ (\phi_r w_s + \phi_s w_r)\} \, dx \qquad \text{(B-13)}$$

Integrating by parts the integrals on the left-hand side and simplifying, the following relations can be obtained.

$$\int_o^R (\phi_s L_{11}[\phi_r] - \phi_r L_{11}[\phi_s]) \, dx$$

$$= \{\phi_s'(GJ + T k_A^2)\phi_r\}_o^R - \{\phi_r' \ (GJ + T k_A^2)\phi_s\}_o^R \qquad \text{(B-14a)}$$

$$\int_o^R (\phi_s L_{12}[v_r] - \phi_r L_{12}[v_s] + v_s L_{31}[\phi_r] - v_r L_{31}[\phi_s]) \, dx$$

$$= -\{\Omega^2 \, m \, x \, e \sin \beta \ \phi_s v_r\}_o^R$$

$$+\{\Omega^2 \, m \, x \, e \sin \beta \ \phi_r v_s\}_o^R \qquad \text{(B-14b)}$$

$$\int_o^R (\phi_s L_{13}[w_r] - \phi_r L_{13}[w_s] + w_s L_{21}[\phi_r] - w_r L_{21}[\phi_s]) \, dx$$

$$= (\phi_s \ \Omega^2 \, m \, x \, e \cos \beta \ w_r)_o^R - (\phi_r \ \Omega^2 \, m \, x \, e \cos \beta \ w_s)_o^R$$

$$\text{(B-14c)}$$

$$\int_o^R (w_s L_{22}[v_r] - w_r L_{22}[v_s] + v_s L_{33}[w_r] - v_r L_{33}[w_s])\, dx$$

$$= (A' w_s v_r'' + A\, w_s v_r''' - A\, w_s' v_r'' - A' w_r v_s''$$

$$- A\, w_r v_s''' + A\, w_r' v_s'' + A'\, v_s w_r'' + A\, v_s w_r'''$$

$$- A\, v_s' w_r'' - A' v_r w_s'' - A\, v_r w_s''' + A\, v_r' w_s'')_o^R \qquad \text{(B-14d)}$$

$$\int_o^R (w_s L_{23}[w_r] - w_r L_{23}[w_s])\, dx$$

$$= (B'\, w_s w_r'' + B\, w_s w_r''' - B\, w_s' w_r''$$

$$- B'\, w_r w_s'' - B\, w_r w_s''' + B\, w_r' w_s'')_o^R \qquad \text{(B-14e)}$$

$$\int_o^R (v_s L_{32}[v_r] - v_r L_{32}[w_s])\, dx$$

$$= (C'\, v_s v_r'' + C\, v_s v_r''' - C\, v_s' v_r''$$

$$- C'\, v_r v_s'' - C\, v_r v_s''' + C\, v_r'\, v_s'')_o^R \qquad \text{(B-14f)}$$

Substituting the relations given by Equations (B-14) into Equation (B-13) and rearranging yields

$$(\omega_r^2 - \omega_s^2) \int_o^R m\{k_m^2 \phi_r\phi_s + w_r w_s + v_r v_s - e \sin\beta(\phi_r v_s + \phi_s v_r)$$

$$+ e \cos\beta(\phi_r w_s + \phi_s w_r)\}\, dx =$$

$$\{(GJ + T k_A^2)(\phi_s' \phi_r - \phi_r' \phi_s)\}_o^R +$$

$$\{-v_r(A w_s''' + A' w_s'' + C v_s''' + C' v_s'' + \Omega^2 m x e \sin\beta\, \phi_s)\}_o^R$$

$$+ \{-w_r(B w_s''' + B' w_s'' + A v_s''' + A' v_s'' - \Omega^2 m x e \cos\beta\, \phi_s)\}_o^R$$

$$+ \{v_r'(A w_s'' + C v_s'')\}_o^R + \{w_r'(B w_s'' + A v_s'')\}_o^R$$

$$+ \{v_s(A w_r''' + A' w_r'' + C v_r''' + C' v_r'' + \Omega^2 m x e \sin\beta\, \phi_r)\}_o^R$$

$$+ \{w_s(B w_r''' + B' w_r'' + A v_r''' + A' v_r'' - \Omega^2 m x e \cos\beta\, \phi_r)\}_o^R$$

$$+ \{-w_s'(B w_r'' + A v_r'')\}_o^R + \{-v_s'(A w_r'' + C v_r'')\}_o^R \qquad \text{(B-15)}$$

If the boundary conditions of the system are such that the right-hand side of Equation (B-15) is zero, then the differential eigenvalue problem as defined by Equations (B-1) to (B-3) is said to be a self-adjoint differential eigenvalue problem. The boundary conditions corresponding to Fixed, Hinge and Free ends etc., make the differential eigenvalue problem of Equations (B-1) to (B-3) self-adjoint and the following orthogonality relationship can be identified.

The eigenfunctions (ϕ_r, v_r, w_r) and (ϕ_s, v_s, w_s) correspond to the distinct eigenvalues ω_r and ω_s respectively and are orthogonal in the following fashion.

$$\int_o^R m \{k_m^2 \phi_r \phi_s + w_r w_s + v_r v_s - e \sin \beta(\phi_r v_s + \phi_s v_r) + e \cos \beta(\phi_r w_s + \phi_s w_r)\} dx = 0 \qquad \text{(B-16)}$$

The vanishing of the right-hand side of Equation (B-15) can be demonstrated, for example, by considering fixed-free boundary conditions. The boundary conditions given by Equation (76) can be expressed in terms of deflections as shown below.

$$\text{Fixed:} \quad w = v = w' = v' = \phi = 0 \quad (\text{at } x = 0) \qquad \text{(B-17)}$$

$$\text{Free:} \quad \begin{aligned} M_x &= (GJ + T k_A^2)' = 0 \\ M_y &= B w'' + A v'' = 0 \\ M_z &= A w'' + C v'' = 0 \end{aligned} \quad (\text{at } x = R)$$

$$-V_y = A w''' + A' w'' + C v'' + C' v'' + \Omega^2 m e x \sin \beta \phi = 0$$

$$-V_z = B w''' + B' w'' + A v''' + A' v'' - \Omega^2 m e x \cos \beta \phi = 0 \qquad \text{(B-18)}$$

By substituting Equations (B-17) and (B-18) into the R.H.S. of (B-15), it is obvious that it vanishes by the fact that the eigenfunctions satisfy all the boundary conditions.

Subcases of the orthogonality relation given by Equation (B-16) can be written as follows.

1. Combined flapwise bending and chordwise bending

$$\int_o^R m \{w_r w_s + v_r v_s\} dx = 0 \qquad \text{(B-19)}$$

2. Combined flapwise bending and torsion

$$\int_o^R m \{k_m^2 \phi_r \phi_s + w_r w_s + e(\phi_r w_s + \phi_s w_r)\} dx = 0 \qquad \text{(B-20)}$$

3. Flapwise bending

$$\int_o^R m w_r w_s = 0 \qquad \text{(B-21)}$$

4. Pure torsion

$$\int_o^R m k_m^2 \phi_r \phi_s = 0 \qquad \text{(B-22)}$$

REFERENCES

1. Lagrange, J. L., Mechanique Analytique (1788).

2. Strutt, J. W., and Rayleigh, B., The Theory of Sound, Volume I, Dover Publications, New York, 1945.

3. Myklestad, N. O., "A New Method of Calculating Normal Modes of Uncoupled Bending Vibration of Airplane Wings and Other Types of Beams", Journal of Aeronautical Sciences, 11, 153-162 (1944).

4. Molloy, C. T., "Four Pole Parameters in Vibration Analysis", Colloguim on Mechanical Impedance Methods for Mechanical Vibrations, Edited by R. Plunket, Applied Mechanics Division, A.S.M.E., (Shock and Vibration Committee), (1958), pp 43-68.

5. Pestel, E. C., and Leckie, F. A., Matrix Methods in Elastomechanics, McGraw-Hill Book Company, Inc., New York (1963).

6. Rubin, S., "Transmission Matrices for Vibration and Their Relation to Admittance and Impedance", Journal of Engineering of Industry, Trans. A.S.M.E., Volume 86 (1964) Series B, No. 1, pp 9-21.

7. Murthy, V. R., and Nigam, N. C., "Dynamic Characteristics of Stiffened Rings by Transfer Matrix Approach", to appear in Journal of Sound and Vibration.

8. Rubin, S., "Unpublished Notes on Transmission Matrices".

9. Hunter, William F., "The Integrating Matrix Method for Determining the Natural Vibration Characteristics of Propeller Blades", NASA TN D-6064, Dec., 1970.

10. Francis, J. G. F., "The QR-Transformation - A Unitary Analogue to the LR-Transformation", Comput.J. Vol. 4, Pt. 1, October 1961, pp 265-271, Pt. 2, October 1962, pp 332-345.

11. Rubin, S., "Review of Mechanical Immittance and Transmission Matrix Concepts", Journal of Acoustical Society of America, Volume 41, No. 5, May 67, pp 1171-79.

12. Rocke Richard Dale, "Transmission Matrices and Lumped Parameter Models for Continuous Systems", Doctoral Thesis, California Institute of Technology, Pasadena, California, 1966.

13. Murthy, V. R., "Application of Frequency Response Technique to Vibration of Cyclic Structures", M. Tech. Thesis, Indian Institute of Technology, Kanpur.

14. Lin, Y. K., Probabilistic Theory of Structural Dynamics, McGraw-Hill Book Company, 1967.

15. McDaniel Thomas J., "Dynamics of Circular Periodic Structures", J. Aircraft, March 1971, pp 143-149, Vol. 8, No. 3.

16. Hubolt, John C., and Brooks, G. W., "Differential Equations of Motion for Combined Flapwise Bending, Chordwise Bending, and Torsion of Twisted Non-uniform Rotor Blades", NACA Report 1346, 1958.

17. Wilkinson, J. H., The Algebraic Eigenvalue Problem, Clarendon Press (Oxford) 1965.

18. Hurty, W. H., and Rubinstein, M. S., Dynamics of Structures, Prentice Hall Inc., 1964.

19. Bisplinghoff, R. L., Ashley, H., and Halfman, R. L., Aeroelasticity, Addison-Wesley Publishing Company Inc., Reading, Massachusetts, 1957.

20. Wadsworth, M., and Wilde, E., "Differential Eigenvalue Problems with Particular Reference to Rotor Blade Bending", Aeronautical Quarterly, May 1968, pp 192-204.

21. Timoshenko, S., Vibration Problems in Engineering, D. Van Nostrand Company, Inc., 1955.

22. Abramowitz, M., and Segun, I. A., Handbook of Mathematical Functions, Dover Publications, Inc., New York, 1965.

23. White, William Felton Jr., "Effect of Compressibility on Three-Dimensional Helicopter Rotor Blade Flutter", Doctoral Thesis, Georgia Institute of Technology, 1973.

24. Loewy, R. G., "A Two Dimensional Approximation to the Unsteady Aerodynamics of Rotary Wings", Journal of Aerospace Sciences, Volume 24, No. 2, Feb., 1957, pp 81-92, 144.

25. Jones, J. P., "The Influence of Wake on the Flutter and Vibration of Rotor Blades", Aeronautical Quarterly, Volume IX, pp 258-286 (1958).

26. Timman, R., and Van de Vooren, A. I., "Flutter of Helicopter Rotor Rotating in its Wake", Journal of Aerospace Sciences, Volume 24, No. 9, pp 694-704, Sep., 1957.

27. Jones, W. P., and Rao, B. M., "Compressibility Effects on Oscillating Rotor Blades in Hovering Flight", AIAA Journal, Volume 8, No. 2, pp 321-329, Feb., 1970.

28. Hammond, C. E., and Pierce, G. A., "A Compressible Unsteady Aerodynamic Theory for Helicopter Rotors", presented at the AGARD Specialists Meeting on the Aerodynamics of Rotary Wings, Marseville, France, Sep. 13-15, 1972.

29. Viswanathan, S. P., Ph.D. Thesis, to be submitted, Georgia Institute of Technology.

30. Murthy, V. R., "Dynamics of Rotating and Non-Rotating Beams", AE 604, Special Problem, School of Aerospace Engineering, Georgia Institute of Technology, Sep., 1972.

31. Jones, W. P., "The Oscillating Aerofoil in Subsonic Flow", Reports and Memoranda No. 2921, Feb., 1953.

32. Smilg, B., and Wasserman, L. S., "Application of Three-Dimensional Flutter Theory to Aircraft Structures", AF Technical Report 4798, July 1942.

33. Desmarais, R. N., and Bennet, R. M., "An Automated Procedure for Computing Flutter Eigenvalues", Journal of Aircraft, Volume 11, No. 2, Feb., 1974, pp 75-80.

VITA

Vadrevu Ramachandra Murthy was born to Seeta Rama Lakshmi and Venkata Veera Raghava Chakravarty on May 21, 1943, in Kanavaram, Andhra Pradesh, India. After attending secondary schools in Rajahmundry viz., V. T. High School (1951-53), Town Middle School (1953-54), and Municipal High School (1954-57), he joined the Government Arts College (1957-1961) and received Bachelor of Science with first class in April 1961. Till August 1965 he served in Life Insurance Corporation of India and enrolled at the Andhra University Engineering College (1965-68) and received Bachelor of Civil Engineering with distinction and university first rank, in April 1968. Subsequently he pursued the study of Aeronautical Engineering at Indian Institute of Science, Bangalore (1968) and Indian Institute of Technology, Kanpur (1969-71). He received Master of Technology in Aeronautical Engineering from I.I.T., Kanpur in August 1971. Then he prosecuted further studies at Georgia Institute of Technology, Atlanta (1971-74). He received M.S. in Aerospace Engineering in August 1972 and completed all the requirements for Ph.D. in November 1974. Presently he is employed by Iowa State University in the department of Aerospace Engineering as Visiting Assistant Professor.